Università degli Studi di Roma “La Sapienza”

PhD in Chemical Sciences
XXIV cycle
Curriculum: *Synthesis and Reactivity*

ANION RECOGNITION IN WATER:

COMPLEXATION BY URANYL SALOPHEN DERIVATIVES AND A GLIMPSE OF STOCHASTIC SENSING

Supervisor:
Prof. Antonella Dalla Cort

Candidate:
Gianpiero Forte

Co-supervisor:
Prof. Luigi Mandolini

Table of Contents

Chapter 1. ***Anion binding and sensing.*** **4**

1.1 The quest for anion receptors. *4*

1.2 Sensing the recognition event. *8*

1.3 Anion receptors in aqueous solutions. *11*

1.4 Metal salophen complexes as anion receptors. *18*

1.5 References. *23*

Chapter 2. ***Synthesis of water-soluble uranyl salophen complexes.*** **28**

2.1 Uranyl-salophen complexes. *28*

2.2 Uranyl-salophen complexes as anion receptors. *31*

2.3 Recognition of anions in aqueous solutions. *36*

2.4 Strategies to achieve higher solubility in water. *43*

2.5 Conclusions and future perspectives. *50*

2.6 Experimental section. *50*

2.7 References. *57*

Chapter 3. ***Anion binding properties of the water-soluble uranyl salophen derivative.*** **62**

3.1 The spectrophotometric study of the binding constants. *62*

3.2 Optical properties of 3/1 and the study of the association with anions. *65*

3.3 Conclusions and future directions. *76*

3.4 Experimental section. *77*

Table of Contents

3.5 References *78*

Chapter 4. *Single-molecule experiments:* *construction of rotaxanes to monitor the polymerase activity.* **80**

4.1 Stochastic sensing of molecules using nanopore devices. *80*

4.2 Lipid bilayers. Folding method and issues. *84*

4.3 Alpha-hemolysin as a suitable and versatile pore for the stochastic sensing of molecules. *87*

4.4 Results and discussion. *93*

4.5 Conclusions. *95*

4.6 Experimental section. *95*

4.7 References. *98*

CHAPTER 1

Anion binding and sensing.

This chapter is intended to cover the main features of anion binding in both organic and aqueous solutions. It is not meant to be a comprehensive digest about anion recognition, but it rather aims at giving an overview of the general principles that are at the basis of this process. In the first part, the most important characteristics of the receptors are presented together with interactions generally used to achieve recognition and sensing in organic solvents. A second part is meant to stress the problems related to anion binding in aqueous solutions. Examples are reported to highlight particular aspects of the recognition phenomenon. The last part of the chapter focuses on the characteristics of metal-salophen complexes and on their anion binding properties.

1.1 The quest for anion receptors.

Supramolecular recognition of anionic species is nowadays an extremely active subject of research, as witnessed by the quite large number of reviews and a monograph published over the last years.[1] The interest towards the recognition of ionic species arose in the late 1960s, soon after the publication of Pedersen's work on the recognition of alkali metal ions performed by crown ethers.[2] In spite of the incredible occurrence of anions both in biochemical and industrial processes, the attention of supramolecular chemistry was, at the beginning, mainly directed to the development of receptors for cations. Drawing inspiration from natural systems (Fig 1.1) the recognition of metal ions from the groups I and II, as well as of ammonium ions, has been

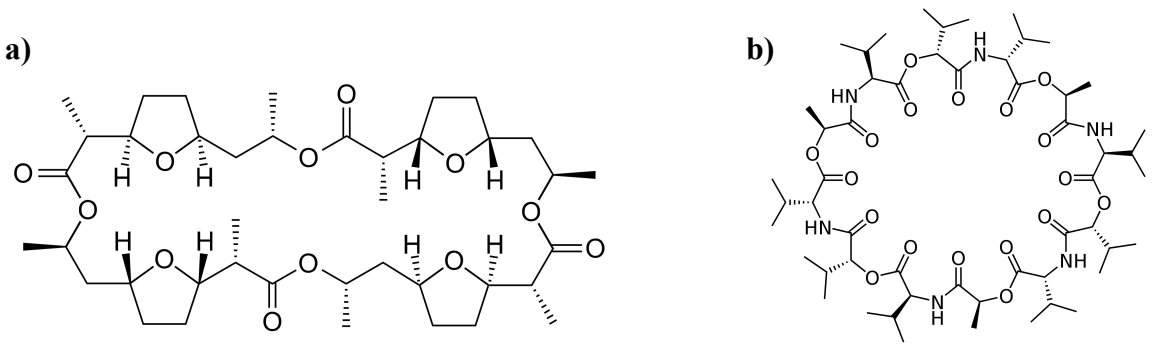

Figure 1.1 Examples of natural antibiotics that bind to cations: (*a*) nonactin[3] (*b*) valinomycin.[4]

widely investigated. Instead, the anion recognition field had a quite slow start and, except for few noteworthy examples, it actually developed only in the last two decades. Therefore, this is a relatively young field in supramolecular chemistry and, as a consequence, still appealing.

The reasons for a such late development in this area reside in some intrinsic characteristics of the anions which make them more difficult to bind than cations. Anions are larger than isoelectronic cations (table 1),[5] having a smaller charge-over-size ratio which causes the electrostatic interactions with the receptors to be less effective than those occurring with the smaller cations.

Cation	*r*[Å]	Anion	*r*[Å]
Na^+	1.16	F^-	1.19
K^+	1.52	Cl^-	1.67
Rb^+	1.66	Br^-	1.82
Cs^+	1.81	I^-	2.06

Table 1 Comparison of the radii r of isoelectronic cations and anions in octahedral environments.

Anions may also be involved in protonation equilibria and they come with a wide range of geometries such as spherical, linear, trigonal planar, tetrahedral and octahedral. In addition, large organic anions display even more complex structures (Fig. 1.2).

Hydrophobicity also play an important role in their binding since, according to the Hofmeister series,[6] lipophilic anions show a tendency to bind more strongly to hydrophobic binding sites.

Thus, while metal cations have a quite simple spherical geometry and their selective recognition is largely related to the size of the host cavity, a high degree of design of the receptors and often additional structural motifs are required to selectively bind to anionic species. The squaramide based macrocycle **1/1** reported by Costa and co-workers, for example, can bind to tetrahedral anions, sulfate in particular, and the selectivity is imposed by the two ammonium groups and the structural constraints of the hydrogen bond donor array of the squaramide unit.[7]

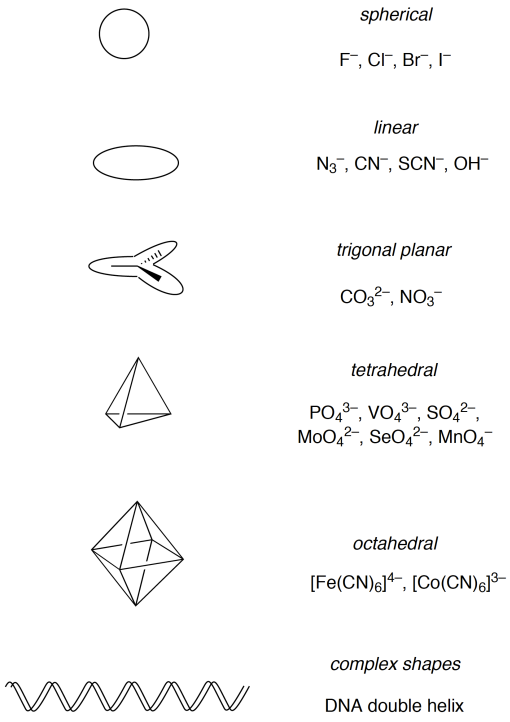

Figure 1.2 Structural geometries of anions.

The first report of a synthetic receptor for anions dates back to 1968, when Park and Simmons reported that the cavity of *in*,*in*-1,(k+2)-diazabicyclo

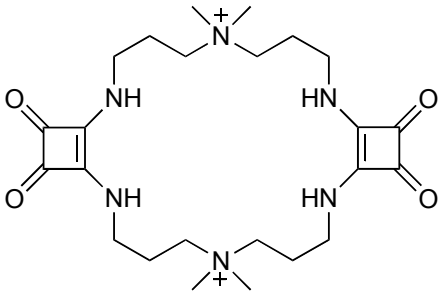

1/1

[k.l.m]alkane-ammonium ions **1/2**[i] is suitable for hosting halide anions.[8] ^{1}H NMR spectroscopy revealed that the i^+,i^+-[9.9.9] cage easily forms a katapinate[ii] with chloride in aqueous acidic media, while the interaction with bromide is less favorable and that with iodide is negligible. The authors suggest that the anion is likely involved in two hydrogen bonds inside the cage, [$^+$N–H···Cl$^-$···H–N$^+$], rather than interacting with a single ammonium group, [$^+$N–H···Cl$^-$ H–N$^+$]. The driving force for the katapinosis process is the formation of hydrogen bonds inside the cavity, whereas the selectivity is imposed by the size of the cage. Indeed, while the i^+,i^+-[9.9.9] include bromide less favorably than chloride and does not interact with iodide, the receptor i^+,i^+-[10.10.10] readily forms katapinates with all the three halide ions.[iii]

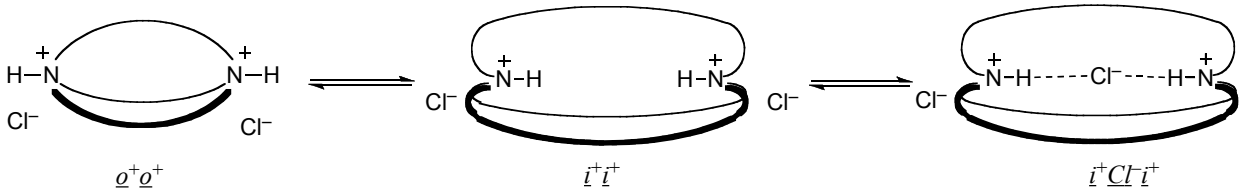

Figure 1.3 Equilibrium between the forms o^+,o^+ and $i^+,i^+$of compound **1/2**.

The synthesis of cyclic receptors and cages is quite a common feature to introduce selectivity both in cation and anion recognition. These structures provide a close environment and a tunable stiffness which allow discrimination based on the size and shape of the guest.[9] Such tridimensional structures provide the correct topology of the binding sites, in order to meet precise geometrical requirements. Cram first pointed out that, compared to analogous acyclic compounds, the pre-organization of the anchor groups in these receptors[10] generally increases the affinity towards the targeted substrate. This feature is especially relevant when highly directional interactions are involved in the binding process. Among these, hydrogen bonding is

[i] k = l = m ≥ 9

[ii] The authors define katapinosis as "diffusion of molecules into a larger molecule with a sensible cavity to give a discrete molecular species".

[iii] The kinetics of the inclusion process with compound [10.10.10] is much faster than the one observed for [9.9.9]. This is probably due to the favorable equilibrium constant between the forms o^+,o^+ and i^+,i^+ of the [10.10.10] (K = 3.3).

unquestionably one of the most exploited to achieve anion coordination in organic solvents.

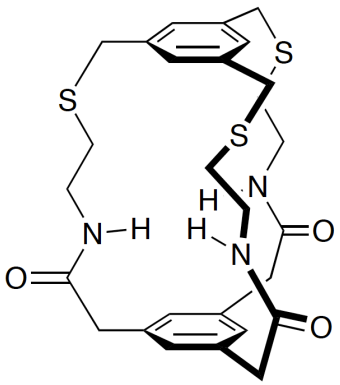

1/3

In 1986 Pascal and co-workers described the first cyclophane receptor **1/3**, purely based on amide groups, able to recognize fluoride in DMSO by a hydrogen bonding array.[11] The awareness of the potentialities of hydrogen bonding in the anion recognition field gave rise to the development of a plethora of receptors bearing hydrogen bond donor groups. These include indole, pyrrole, hydroxyl group, urea, and thiourea. Also, the positively charged guanidinium and imidazolium moieties, like ammonium group, coordinate anionic species through charge assisted hydrogen bondings.

Besides hydrogen bonding, the binding of anions to electron-deficient centers has been widely explored. Receptor containing Lewis-acidic atoms, for example boron[12] and silicon[13] have been described hitherto. The use of transition metals is particularly appealing because many of these complexes show fluorescence emission. Zinc is the second most abundant transition metal in living organisms after iron and forms many fluorescent coordination compounds able to recognize phosphate species.[14]

Gunnlaugsson and co-workers reported that highly designed receptors, bearing transition metal centers, bind to anions with different stoichiometries. Terbium(III) complex **1/4**, for instance, recognize multiple phosphate species in acetonitrile *via* hydrogen bonding and metal coordination, resulting in fluorescence quenching or enhancement depending on the anion concentration.[15]

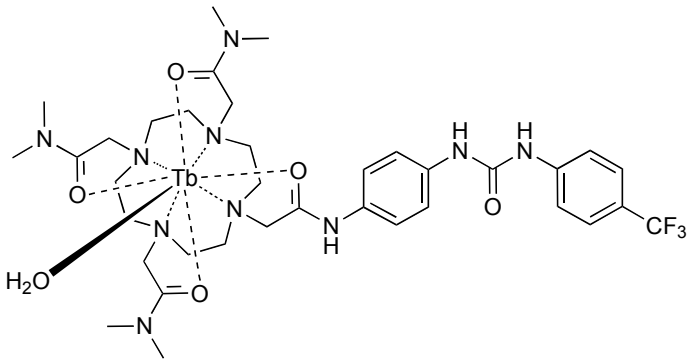

1/4

It should be stressed that a sharp classification of receptors, based on the main interaction exploited, is somewhat reductive since, in many cases, anchor sites of different nature cooperate

to effectively bind to the guest. Furthermore, some functional groups in the receptors play fundamental structural roles, although they are not directly involved in the recognition process. For example, Gale and co-workers reported that the nitrogen atom of the pyridine moiety in compound **1/5** coordinates the amide hydrogen atoms, stabilizing the structure of the receptor and inducing the correct topology to selectively bind carboxylates. Compound **1/6**, on the other hand, not only is less selective in anion binding, but it rapidly undergoes hydrolysis in the presence of water.[1b,iv]

NMR spectrometry and UV-Vis spectroscopy are the most commonly used techniques to study the binding phenomenon in solution. Indeed, a quantitative relation exists between the binding affinity and the changes in the chemical shift or in the light absorption of the host-guest systems. Although less accessible than other techniques, Isothermal Titration Calorimetry (ITC) can provide the values of the affinity constant and the thermodynamic parameters for a complexation reaction with a single experiment. X-rays diffraction analysis of a single crystal of the complexes, compared with data obtained in solution, may confirm structural features of the system, such as the binding mode and the occurrence of secondary interactions.

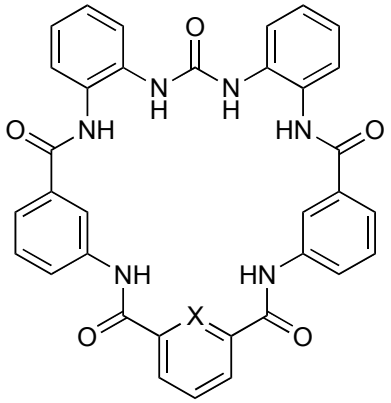

1/5, X = N
1/6, X = CH

Nowadays great attention is directed to those receptors able to associate an easily detectable output signal to the binding event. Such devices, i.e. sensors, allow to determine chemical species in solution both qualitatively and quantitatively.

1.2 Sensing the recognition event.

As previously mentioned, the field of sensing is presently gaining great attention in supramolecular recognition. *Chemosensors* are those devices in which the binding event causes a measurable change of physical properties such as color, light emission or reduction potential (Fig. 1.4).[16]

[iv] In DMSO/0.5% water, hydrolysis takes place within 1 h.

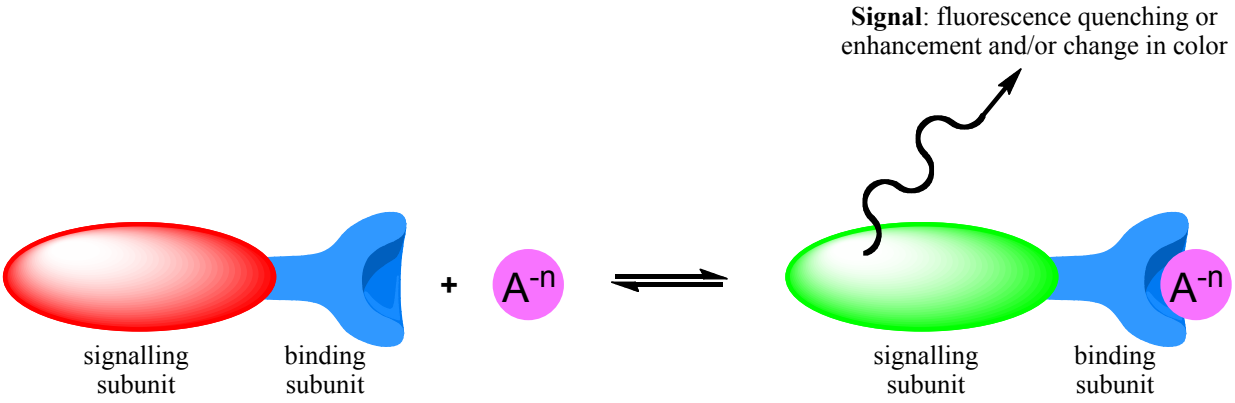

Figure 1.4 General scheme of a chemosensor.

The enormous interest towards fluorescence emission is largely due to the high sensitivity of the technique and also to the qualitative response provided upon UV light irradiation of the sample.

Luminescent groups have been covalently attached to the receptors in the proximity of the anchor sites and the complexation of the anions causes the quenching or the enhancement of their fluorescence emission. The tris(2,2'-bipyridyl)ruthenium(II) complex has been the most extensively investigated because of its physical properties.[17] An example of how this luminophore has been incorporated into anion receptors is provided by compound **1/7**, reported by Gale and co-workers, which binds to chloride in dimethyl sulfoxide (Fig. 1.5).[18] More complex sensors that rely on luminescence have also been reported. Some of them undergo conformational changes upon anion binding and, as a consequence, the formation of luminescent

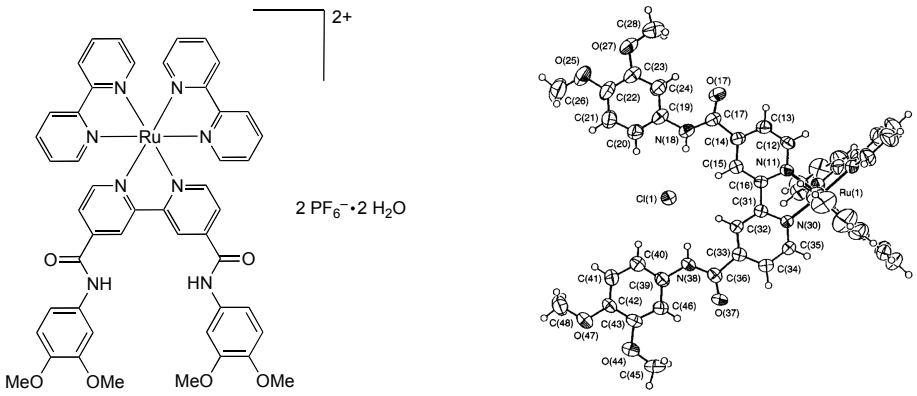

Figure 1.5 Compound **1/7** (*left*) and the structure of its complex with chloride (*right*).

excimer is made possible.[19] In some other cases a multicomponent system is employed to produce a displacement-assay-type chemosensor. The binding to the receptor causes the displacement of a luminescent compound previously coordinated and the restoration of its fluorescence, which was quenched while the luminophore was bound.[20]

Colorimetric sensors probably represent the state of the art in this field. They are receptors able to transduce anion complexation into a color change that allows a naked eye detection of the binding event. It is worth noting that the substituted 1,8-naphthalimide moiety has been largely employed to design this type of sensors since it shows suitable photophysical properties that can be tuned through a proper structural design.[21] Colorimetric sensing can be achieved not only through the weak interactions previously described, but also through a wider range of features. These include the basicity of anions[22] and the formation of stable bonds, such as covalent bonds[23] (Fig. 1.6) or the fluorine-silicon bond[24] (Fig. 1.7).

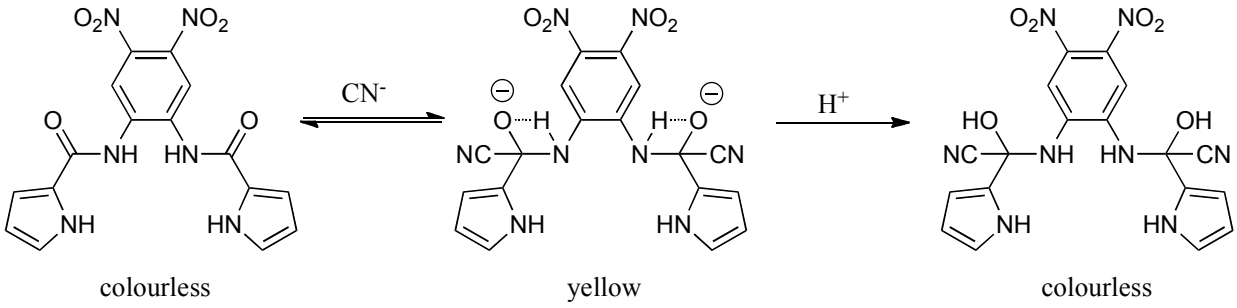

Figure 1.6 Recognition of cyanide by covalent bond formation.

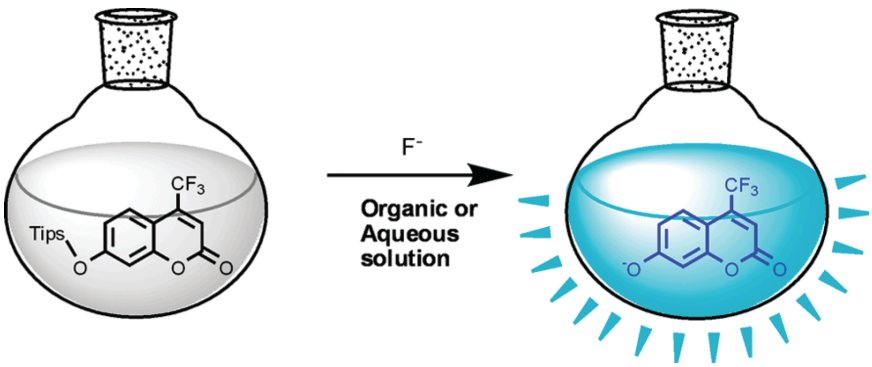

Figure 1.7 Pictorial representation of fluoride sensing by a TIPS (triisopropylsilyl) protected coumarin derivative. The removal of the sylil group in the presence of fluoride causes the fluorescence to turn on.

Since colorimetric receptors are extremely promising devices in the qualitative sensing of anions in solution, an important feature is clearly the detection limit that they can provide, namely, the lowest analyte concentration that gives rise to an appreciable change in color. Yen and co-workers, in this regard, reported the synthesis of the colorimetric sensor **1/8** (Fig. 1.8) able to recognize and discriminate maleate from fumarate at part per million concentration.[25]

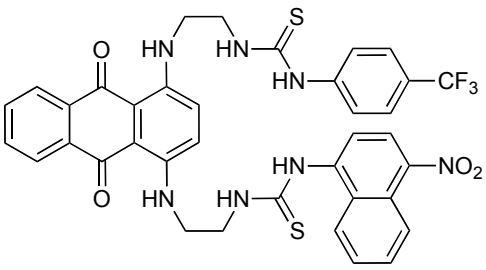

1/8

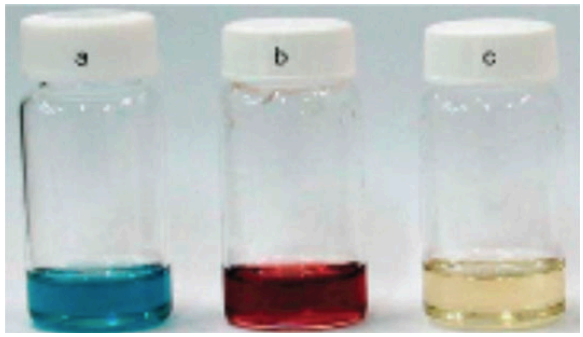

Figure 1.8 Compound **1/8** (*left*). Color changes of **1/8** upon addition of various anions in DMSO: (*a*) **1/8** only; (*b*) **1/8** + 2.0 equivalents of maleate; (*c*) **1/8** + 2.0 equivalents of fumarate (*right*).

Furthermore, a naked eye detection can be achieved through physical state changes. The pyromellitamide **1/9** forms a self-assembled gel that dissociates upon anion binding.[26] The gelation process is driven by the onset of a hydrogen bonding network provided by the amide groups, the same involved in the recognition process, and the dissociation process takes place in a period of time that is proportional to the strength of the association.

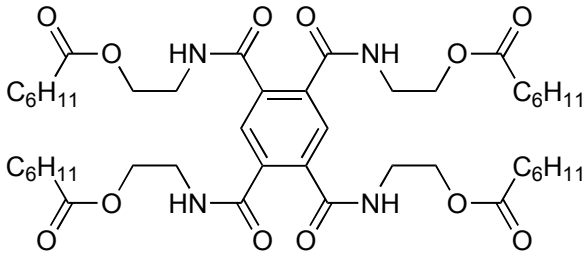

1/9

1.3 Anion receptors in aqueous solutions.

The endeavor to create synthetic systems able to bind and sense anionic species in organic solvents is justified by the potential application that they have. Indeed, they can be used as ion-selective electrodes, phase transfer catalysts (PTC) or for the active transport across membranes, thus having a biomedical interest.

However most effort is nowadays addressed to those receptors able to achieve anion recognition in aqueous solutions. Anions play a crucial role in biology. For instance, the genomic material in living systems (i.e. DNA and RNA) has a polyanionic chain backbone and the processes at the basis of life basically require the handling of anionic species. As they are involved in many biochemical processes, the presence of anions inside the human body is strictly related to the health and they may serve as markers for the onset of particular pathologies. Clearly the early diagnosis of such diseases also depends on the development of biosensors able to detect and quantify the concentration of specific anions in human tissues and body fluids. Anomalously high level of pyrophosphates in the synovial fluid, for example, can be related to *chondrocalcinosis*, namely, the formation of calcium pyrophosphate crystals in the connective tissues, which causes a rheumatologic disorder also known as CPPD (calcium pyrophosphate dihydrate disease).[27] On the other hand fluoride, once thought to be very useful in dental care, administered to children and added in toothpastes, is now believed to have adverse health effects and the advisability of processes as water fluoridation are currently controversial subjects.[28] Other anions, instead, are effectively harmful to animals. Despite its extremely high toxicity, connected to the inhibition of cytochrome c oxidase activity,[29] cyanide is still largely used in many industrial processes. Accidents involving its release in the environment have occurred also in recent years.[30]

Anions represent indeed one of the major anthropogenic pollutants of waste and groundwater. Phosphates are largely used as additives in detergents, leavening agents and, together with nitrates, are employed as components in fertilizers. Both of them account for water eutrophication, the excessively high presence of nutrients in the sea, rivers and lakes, which lead to the abnormal growth of aquatic plants. The resulting lack of oxygen availability in water, i.e. hypoxia, causes the death of animal aquatic species and the subsequent derangement of the ecosystems (Fig. 1.9).

Figure 1.9 The eutrophication of the Potomac River is evident from its bright green water, caused by a dense bloom of cyanobacteria.

Thus, it comes naturally that the development of devices able to bind and sense[v] negatively charged species in aqueous solutions is an important target that links analytical, medicinal and

[v] Receptors able to work in biological environments are named *biosensors.*

supramolecular chemistry. It is worth pointing out that, if the recognition of anions in organic solvents is quite difficult to achieve, their binding in aqueous solutions is an even more challenging task. In water, anions can be involved in protonation equilibria and some of them exist only in a narrow range of pH, where they are not fully protonated. Furthermore, they are effectively solvated and their hydration free energies are generally higher with respect to cations, even if they have the same absolute charge and comparable size.

Water is a solvent with unique properties.[31] Being at the same time both hydrogen bond donor and acceptor, the solvent competes in the recognition process. Besides water displays a very high dielectric constant (table 2), which lowers the strength of electrostatic interactions between charged species (i.e. between the anion and a positively charged receptor). On the basis of these considerations, higher design complexity of the receptors is required to supply host-guest interactions able to survive in such medium.

The solubility of receptors in water is a major issue to take into account. Systems, whose capability in binding anions have been assessed in organic solvents, are generally insoluble in water. An inspection of the literature demonstrates that, in many cases, a certain amount of organic solvent is required both to assure the proper solubility of receptors and to increase the strength of the interactions which would not be detectable in pure water. The water content of the solvent mixture can be increased as far as the host molecules do not aggregate and their affinity towards the anions can be measured. Even though the hydrophilicity degree of the receptors can be increased by the introduction of polar substituents, yet in some cases a small percentage of an organic solvent is still required. To date very few receptors both soluble in pure water and with a sufficiently high affinity towards anionic guests have been reported.

Solvent	ε [F mol^{-1}]	Solubility in water
water	78	
methanol	33	miscible
dimethyl sulfoxide	47	miscible
acetonitrile	37	miscible

Table 2 Dielectric constants of various solvents.

Kubik divided receptors soluble in aqueous solutions into three different classes.[32]

1) receptors tolerating no more than 30% water in the solvent mixture display a well-organized hydrogen bonding array which tightly bind the anions;

2) receptors allowing the water content to be greater than 30% generally show a good affinity towards anions but however are not soluble in pure water;
3) receptors that are soluble in 100% water and efficiently bind to anions.

Summarizing, the recognition and sensing of anions in water require two major problems to be solved: *a.* the choice of a weak interaction to achieve recognition and that is able to survive in the aqueous medium; *b.* a strategy to synthesize receptors soluble in water.

At the beginning, and for a long time, it was believed that only the presence of positive charges on the receptors or the coordination to a metal ion could provide an interaction strong enough to compete with anion solvation. However, today it has been demonstrated that properly designed electro-neutral receptors can satisfactorily bind to anions in aqueous solutions with sufficiently high water content. These receptors often combine different types of weak interactions that work cooperatively to overcome the strong water contribution in stabilizing anions. This is what Timmerman and co-workers referred to as the "Gulliver-effect".[33]

Macrocyclic polyamines and their bicyclic analogues, such as **1/10** and **1/11**,[34] bind to anions in aqueous solutions. These receptors are protonated to a significant extend even in neutral environment and hence are particularly suitable to interact with anionic guests *via* hydrogen bonding. Quantitative measurement of the association strength may be difficult in these cationic species due to the competition with the counterions and to the occurrence of several acid-base equilibria, resulting in the simultaneous presence of multiple host species which interact with anions with different strength. Generally high protonation degree corresponds to a stronger interaction with anions. The pH at which a full protonation is achieved depends on the structure of the receptor. For instance, two amino groups close to each other will be difficult to protonate because of the unfavorable positive charge accumulation. However the binding properties of these receptors depends not only on the protonation degree, but also on the position where first protonation occurs. Compared to secondary amines, tertiary amines require lower pH values to be protonated. Therefore, they can be introduced in specific positions on the receptor to control the protonation pattern and the selectivity. This can be furthermore tuned by varying the size of the

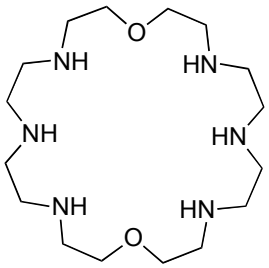

1/10

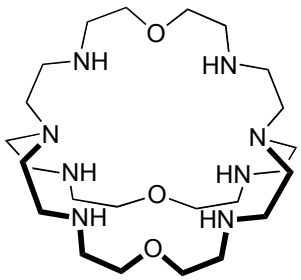

1/11

cavity and the rigidity of the receptor. The latter is influenced by the protonation degree, as the structure tends to maximize the distance between ammonium groups. It is also possible to use rigid linkers or the quaternization of the nitrogen atoms, as in **1/12**. This introduces a positive charge that is independent of the pH, but involves the loss of hydrogen bonding.

As previously mentioned, anions play a crucial role in many biological processes. Through evolution, nature has created systems able to bind to anions with high affinity and selectivity in aqueous solutions. This is made possible because binding sites in the proteins and active sites in the enzymes display a pre-organized array of the anchor groups, which tightly bind to anions in cooperative manner. Moreover natural systems provide an environment than less polar the bulk solvent and anions may experience stronger electrostatic interactions than in water. Proteins and enzymes largely exploit favorable hydrophobic interactions to bind to those anionic species who hardly tolerate a polar environment such as the one provided by water. For example, hydrophobic pockets can accommodate lipophilic side chains of amino acids, helping to increase the affinity towards the substrate. Hydrophobic interactions have been successfully employed in the inclusion of naphthalenesufonates by β-cyclodextrin in water[35] or of chloride inside a metal coordinated calixarene[36].

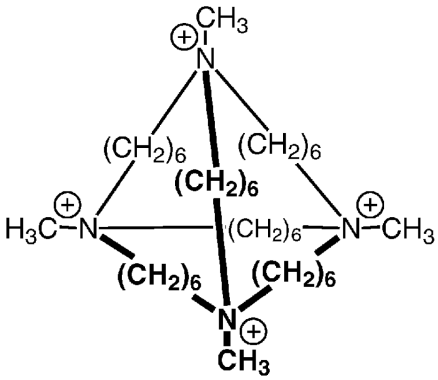

1/12

Amino acids are the building blocks for proteins and enzymes. Although less than half out of the 20 natural amino acids bears groups able to bind anions, on the side chain, proteins such as PBP (phosphate binding protein), SBP (sulfate binding proteins) or the chloride channels in some bacteria bind to their substrates with incredible affinity and selectivity. It comes natural that amino acid based receptors can be used for the recognition of anions in aqueous solutions.[37] As an example, Kubik reported that the oyster-like bis(cyclopeptides) **1/13 a-d** are able to bind to sulfate and iodide in water-methanol and water-acetonitrile solutions.

The high affinity towards the substrate is due not only to the interactions between the receptor and the anion, but also to the favorable interactions between the two cyclopeptide subunits induced by conformational changes upon the binding event.[38]

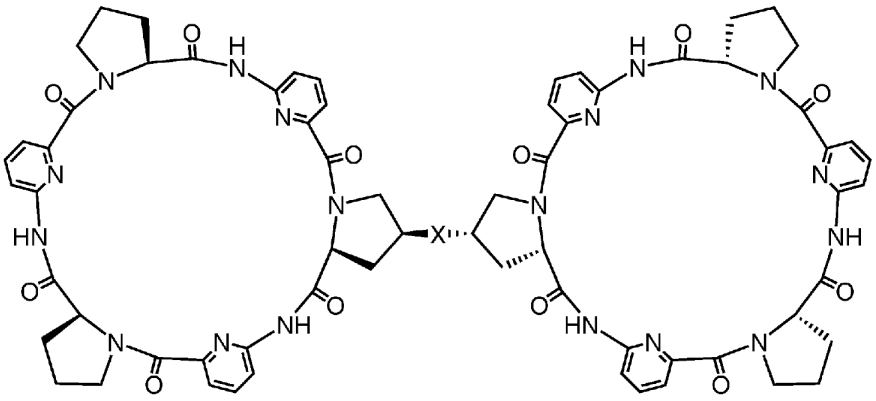

1/13

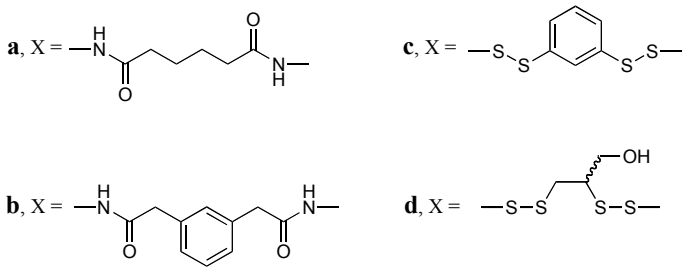

Guanidinium based receptors such as **1/14** have a more disperse positive charge than ammonium based ones and thus the interactions with anions are less intense. However, they have the advantage to be useful over a wide range of pH. Also non-cyclic hosts containing guanidinium moieties have been reported to interact with anions in water. Schmidtchen pioneered this field, in the early 1994, reporting the ability of receptors **1/15** and **1/16** to bind to biologically relevant phosphate species in water (Fig. 1.10).[39]

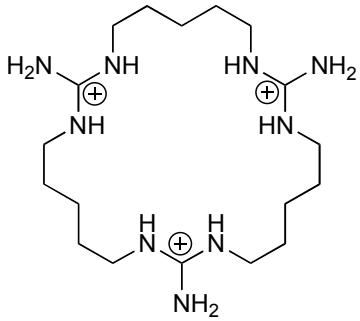

1/14

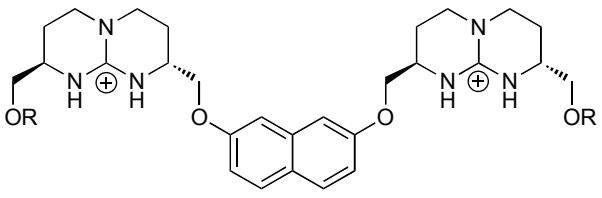

1/15, R = Si(Ph)$_2$*t*-Bu
1/16, R = H

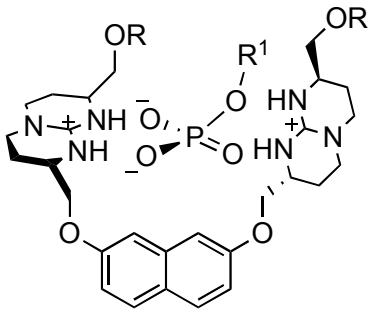

Figure 1.10 Compounds **1/15** and **1/16** (*left*) and the proposed interaction with phosphate species (*right*).

Lewis acid containing receptors have been widely used in anion recognition chemistry also in water. The presence of an electron deficient center, immobilized in an organic frame, permit to achieve a foreseeable directionality of the binding interaction. Boron containing compounds such as boronic acids can coordinate and sense[40] anions even in water. Compound **1/17**, made soluble in water using two sulfonium groups, can bind L-dopa under physiological pH conditions.[41]

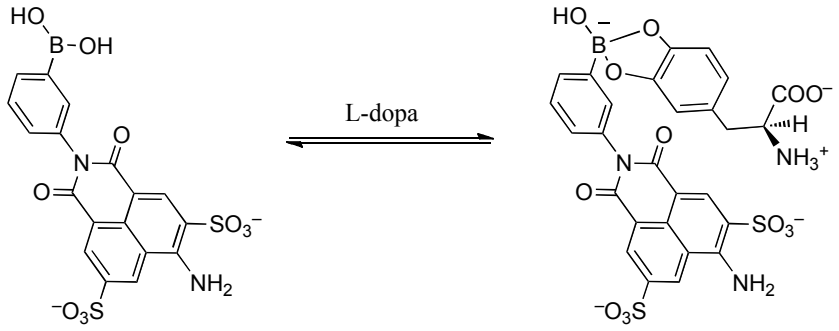

1/17

Of course, metal complexes must have a free binding site available for further coordination with anions. In the absence of donor guests, this site can be for example occupied by a molecule of solvent.[42] In the years, Copper(II) and Zinc(II) have revealed to be the most suitable metals to be used. Copper (II) complexes undergo a drastic absorption change upon anion binding while Zinc(II), being diamagnetic, allows NMR spectroscopy investigation of the binding phenomenon. Some organic receptors bearing two metal centers have been designed in order to preferably bind anions which can bridge the two metal cations.[vi] Fabbrizzi and co-workers reported that receptor **1/18** can bind to a series of inorganic anions showing color shift from blue to green, thus providing a naked eye evidence of the phenomenon.[43]

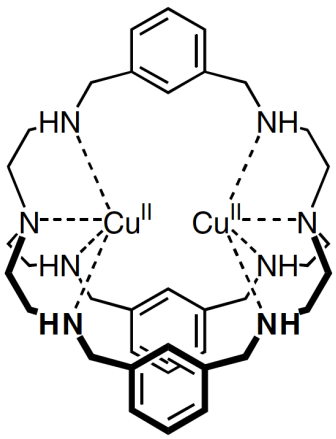

1/18

Analogous complexes have been designed by covalently linking the Zn(II)cyclen [1,4,7,10-tetraazadodecane] moiety to an organic scaffold. Concerning this, Kimura and co-workers studied the behavior of metal receptors **1/19** and **1/20** in binding phosphate dianions in water,[44] which mimic the binding mode of enzymes such as alkaline phosphatase.

[vi] The bridged double metal complexes are called *cascade complexes.*

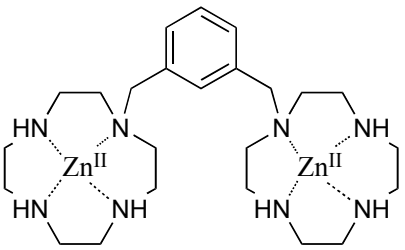

1/19

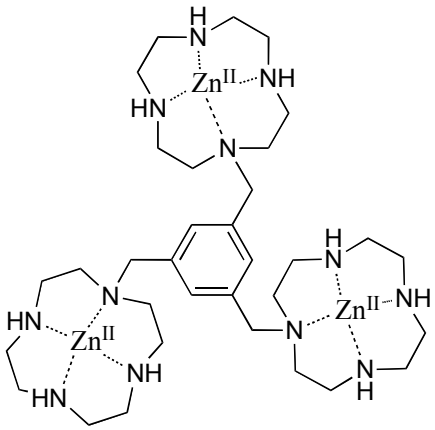

1/20

Similarly fluorescent Zn(II)homo-dinuclear bis-dipicolylamine complexes **1/21** and **1/22** have been employed as non-covalent tags for phosphorylated proteins,[45] while the compound **1/23** has found application as fluorescent biosensor to monitor the protein kinase catalyzed phosphorylation.[46]

The study on organic compounds containing transition metals continues to be a very rich area of interest. Nowadays many efforts are made to modify the organic frameworks in order to achieve high degree of selectivity and/or affinity towards targeted anionic species. The design of easily synthesizable complexes is still a target to pursue.

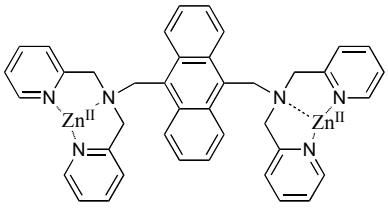

1/21

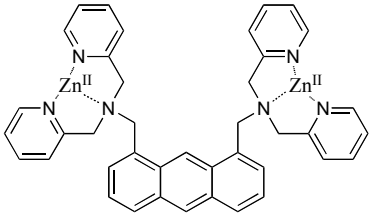

1/22

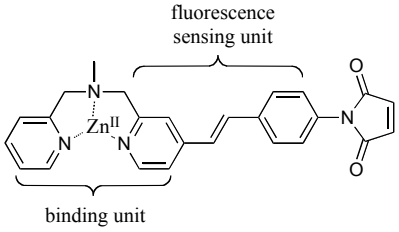

1/23

1.4 Metal salophen complexes as anion receptors.

Schiff base ligands are the most versatile compounds in coordination chemistry[47] and they can accommodate and stabilize different metal in various oxidation states, thus controlling their

properties in catalysis and molecular recognition. For this reason such structures have been referred to as "priviledged ligands".[48,vii]

Salen ligands are tetradentate Schiff bases which were first described in 1933 (Fig. 1.11).[49] They derive from the condensation of an aliphatic diamine with two equivalents of salicylaldehyde and they gain much attention in 1990s when Jacobsen[50] and Katsuki[51] reported that chiral Mn-salen derivatives (Fig. 1.11a) could perform enantioselective epoxidations on unsubstituted alkenes.

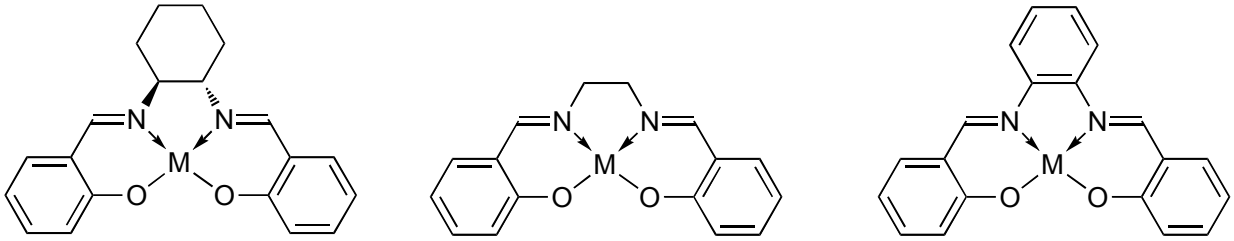

Figure 1.11 Chemical structures of cyclohexyl-metal-salen (*a*), metal-salen (*b*) and metal-salophen (*c*).

Salophens are very closely related to salen ligand, but the diamine used is an aromatic one (Fig. 1.12). In their dianionic form, both salen and salophen ligands provide four binding sites, two covalent and two coordinative, arranged in a planar array. This setting allows an equatorial

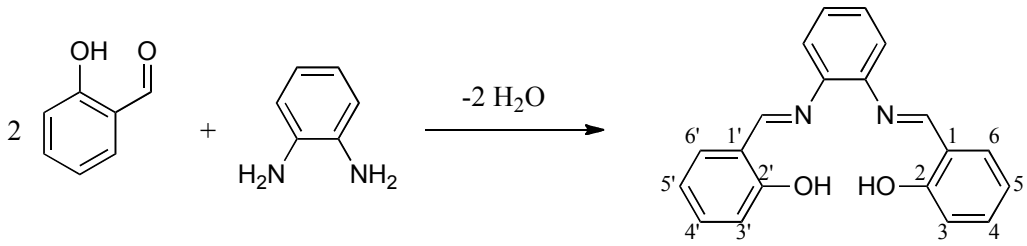

Figure 1.12 Synthesis of the salophen ligand. The conventional numbering of the carbon atoms is reported.

coordination to the metal, which keep the two apical positions available for the coordination to a further ligand. Metal-salophen complexes are planar structures thoroughly conjugated, which recall the metal coordination of porphyrins and are much easier to synthesize.[52] The synthetic accessibility of metal-salophen derivatives is actually one of the main features of these compounds. They indeed allow for a modular synthetic approach thanks to the possibility to

[vii] Ligands whose metal derivatives are active over a wide range of chemical processes, affording transformation with high yield and selectivity.

independently modify their building blocks. The great number of synthetic routes to substituted 1,2-diaminobenzene and substituted phenols, and thus salicylaldehyes, points up the versatility of these structures.

The properties of salen and salophen complexes primarily rely on the coordinated metal, but a critical role is played by its coordination geometry. As outlined above, these ligands display a prominent disposition to a square-planar coordination arrangement, which implies the metal to lie in the plane formed by the N_2O_2-donor array. Yet few cases of slightly distorted coordination geometry towards a tetrahedral one have been reported.[53] In the square-planar coordination arrangement, the metal can further interact with an ancillary ligand by using one of the axial positions or an equatorial one, if present.

In metal coordination chemistry, the recognition of chemical species, operated by a metal organic complex, has been regarded as a reverse of the coordination process. This goes back to the birth of supramolecular chemistry, when the first accounts reported that the *s*-block metal ions were recognized by the crown ethers. What sets the difference between coordination and supramolecular chemistry, a thoroughly debated issue, is that, in metal receptors, organic ligands forms kinetically inert and stable complexes with the metal cation, whereas the supramolecular host-guest recognition is often characterized by a fast ligand exchange.

According to Steed,[54] anion receptors containing a metal center can be classified, according to its role, as follows:

i) those in which the metal plays a structural role and supports the organization of the host establishing non-labile interactions with the organic ligands;
ii) those in which it provides the primary binding site for anions;
iii) those where it is part of the sensing unit;
iv) self-assembled coordination complexes which involve anion templation;
v) solid-state polymer networks which bind anions.

Metal-salophen based receptors mostly belong to the second group since, apart from additional binding motifs, they essentially employ the free binding site of the metal to interact with the guest. The anion binding properties of various metal salophen complexes are well established and documented.[55]

Iron(III) salen and salophen complexes were first described in 1938.[56] They have been reported to form μ-oxo-bridged dimers of formula [{Fe(salen)}$_2$O] and [{Fe(saloph)}$_2$O],[57]

analogous to structures found in several met-forms[viii] of the invertebrate oxygen binding protein hemerythrin (Hr).[58] Iron(III) Schiff bases form bridged complexes of formula [{Fe(ligand)}$_2$X], [{Fe(ligand)}$_3$X], in which Y is a di- or tricarboxylate anion[59] and [Fe(ligand)Y]$_2$,where Y is a carboxylate monoanion or a phenolate.[60] Moreover iron salophen complexes have been recently inserted on the active site of apo-myoglobin (apo-Mb)[61] and heme-oxygenase (HO)[62] in order to create artificial metallo-proteins.

A number of salophen and salen complexes carrying different transition metal cations have been successfully employed to dope polymeric membranes to be used as ion selective electrodes (ISEs). Complexes bearing zirconium(IV),[63] cadmium(II),[64] vanadyl (VO^{2+}),[65] gallium(III),[66] aluminium(III) and tin(IV)[67] cations, supported on plasticizers such as PVC give a selective response upon anion recognition. In many of these cases, the selectivity is independent of the Hofmeister series, thus indicating that the metal-anion affinity directly governs the process.

Zinc is the only metal cation present in all classes of enzymes. It has a flexible coordination geometry which allows proteins to rapidly undergo conformational changes when performing biological reactions.[68] Zinc complexes display fluorescence properties that are influenced by the anion binding and are particularly appealing as sensors.[69] Interesting informations regarding the anion binding properties of Zn-salophen derivatives have been reported by Kleij and co-workers.[70] The association between the complex **1/24** and a series of tetrabutylammonium salts was rationalized by proton NMR spectroscopy. Anions such as chloride, bromide, iodide, acetate and phenoxyde induce an upfield shift of imine and aryl protons of the receptor, while the non-coordinating anions PF_6^- and ClO_4^- lead to negligible changes in the spectrum. Notably the complex shows a tendency to form a 2:1 complex in the presence of low concentrations of acetate, as confirmed in the solid state by the X-rays diffraction analysis of the complex crystal (see Fig. 1.13). Instead, receptor **1/25** display a less strong tendency to form 2:1 complexes because of the steric hindrance provided by the additional *tert*-butyl groups.

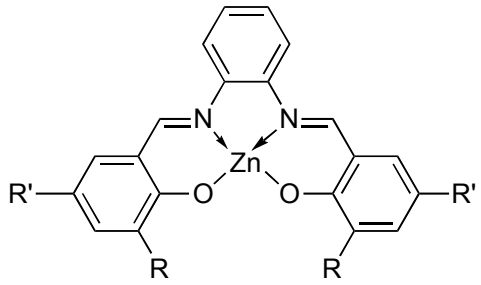

1/24; R = *t*-Bu, R' = H
1/25; R, R' = *t*-Bu

[viii] *Met* denotes an oxidized, functionally inactive state of the oxygen binding proteins hemoglobin, hemocyanin and hemerythrin.

Figure 1.13 Structure of the complex between **1/24** and acetate, showing the 2:1 association with the anion bridging the two metal receptors.

Recently the Zinc- and Copper-salophen complexes **1/26**, bearing two ammonium groups, have been reported to interact with DNA in water.[71] Our group reported the synthesis of the neutral Zn-salophen complex **1/27**, able to bind to carboxylates in pure water.[72] Unexpectedly it operates an enantioselective recognition of amino acids through multiple binding interactions.

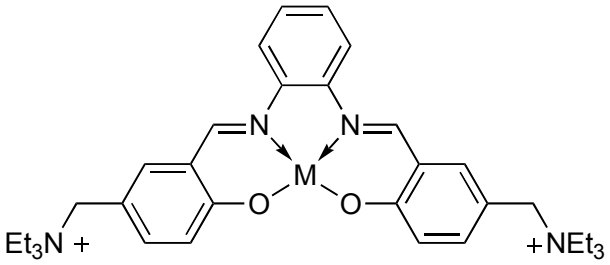

1/26; M = Zn(II), Cu(II)

Unquestionably, among the great number of metal-salophen complexes, uranyl derivatives are those most extensively surveyed in the anion recognition field. Owed to their peculiar geometry, these complexes allow for the introduction of additional binding motifs that can directly interact with the anions, located on the fifth equatorial binding site of the metal, enhancing the affinity and/or the selectivity. Uranyl-salophen derivatives are neutral receptors and allow the study of the binding phenomena without the interference of electrostatic interactions. Since the work presented is mainly focused on these complexes, their properties will be discussed in detail in the following chapter.

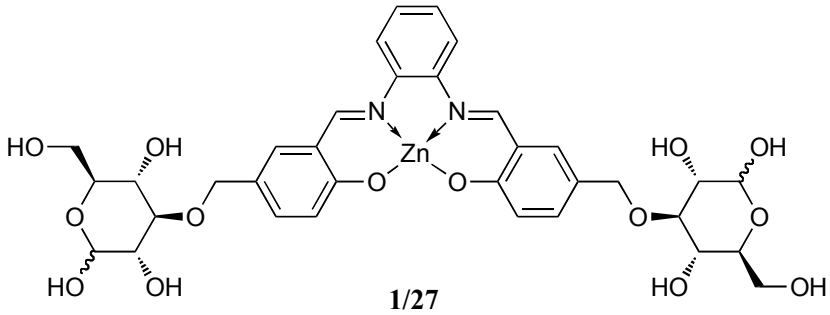

1/27

1.5 References.

[1] (a) F. P. Schmidtchen, M. Berger, *Chem. Rev.*, **1997**, *97*, 1609-1646. (b) *Supramolecular Chemistry of Anions*, ed. A. Bianchi, K. Bowman-James, E. Garcia-España, Wiley-VCH, New York, 1997. (c) G. Antonisse, D. N. Reinhoudt, *Chem. Commun.*, **1998**, 443-448. (d) P. A. Gale, *Coord. Chem. Rev.*, **2000**, *199*, 181-233. (e) P. D. Beer, P. A. Gale, *Angew. Chem. Int. Ed.*, **2001**, *40*, 486-516. (f) P. A. Gale, *Coord. Chem. Rev.*, **2001**, *213*, 79-128. (g) Special issues on anion coordination chemistry in *Coord. Chem. Rev.*, **2003**, *240* and **2006**, *250*. (h) S. Kubik, C. Reyheller, S. Stüwe, *J. Inclusion Phenom. Macrocyclic Chem.*, **2005**, *52*, 137-187. (i) C. Caltagirone, P. A. Gale, *Chem. Soc. Rev.*, **2009**, *38*, 520-563. (j) Themed issue: *Chem. Soc. Rev.* **2010**, *39*, 3581-4008.

[2] C. J. Pedersen, *J. Am. Chem. Soc.*, **1967**, *89*, 7017-7036.

[3] B. T. Kilbourn, J. D. Dunits, L. A. R. Pioda, W. Simon, *J. Mol. Biol.*, **1967**, *30*, 559-563.

[4] M. Pinkerton, L. K. Steinrauf, P. Dawkins, *Biochem. Bioph. Res. Co.*, **1969**, *35*, 512-518.

[5] R. D. Shannon, *Acta Crystallogr. Sect. A*, **1976**, *32*, 751-767.

[6] F. Hofmeister, *Arch. Exp. Pathol. Pharmakol.*, **1888**, *24*, 247-260.

[7] R. Prohens, G. Martorell, P. Ballester, A. Costa, *Chem. Commun.*, **2001**, 1456-1457.

[8] C. H. Park, H. E. Simmons, *J. Am. Chem. Soc.*, **1968**, *90*, 2431-2432.

[9] (a) E. A. Katayev, J. L. Sessler, V. N. Khrustalev, Y. A. Ustynyuk, *J. Org. Chem.*, **2007**, *72*, 7244-7252. (b) N. K. Kim, K. -J. Chang, D. Moon, M. S. Lah, K. -S. Jeong, *Chem. Commun.*, **2007**, 3401-3403.

[10] Cram, D. J. *Angew. Chem. Int. Ed.*, **1988**, *27*, 1009-1020.

[11] R. A. Pascal, J. Spergel, D. V. Engbersen, *Tetrahedron Lett.*, **1986**, *27*, 4099-4102.

[12] (a) H. E. Katz, *J. Am. Chem. Soc.*, **1985**, *107*, 1420-1421. (b) H. E. Katz, *Organometallics*, **1987**, *6*, 1134-1136.

[13] K. Tamao, T. Hayashi, Y. Ito, *J. Organomet. Chem.*, **1996**, *506*, 85-91.

[14] P. Jiang, Z. Guo, *Coord. Chem. Rev.*, **2004**, *248*, 205-229.

[15] C. M. Gomes dos Santos, T, Gunnlaugsson, *Dalton Trans.*, **2009**, 4712-4721.

[16] P. D. Beer, A. D. Keefe, *J. Organomet. Chem.*, **1989**, *375*, C40-C42.

[17] (a) V. Balzani, F. Barigeletti, L. De Cola, *Top. Curr. Chem.*, **1990**, *158*, 31-71. (b) A. Juris, V. Balzani, F. Barigeletti, S. Campagna, P. Belser, A.von Zelewsky, *Coord. Chem. Rev.*, **1988**, *84*, 85-277

[18] (a) F. Szemes, D. Hesek, Z. Chen, S. W. Dent, M. G. B. Drew, A. J. Goulden, A. R. Graydon, A. Grieve, R. J. Mortimer, T. Wear, J. S. Weightman, P. D. Beer, *Inorg. Chem.*, **1996**, *35*, 5868-5879. (b) P. D. Beer, S. W. Dent, T. Wear, *J. Chem. Soc. Dalton Trans.*, **1996**, 2341-2346. (c) P. D. Beer, *Acc. Chem. Res.*, **1998**, *31*, 71-80.

[19] (a) S. K. Kim, J. H. Bok, R. A. Bartsch, J. Y. Lee, J. S. Kim, *Org. Lett.*, **2005**, *7*, 4839-4842. (b) J. K. Choi, S. H. Kim, J. Yoon, K. H. Lee, R. A Bartsch, J. S. Kim, *J. Org. Chem.*, **2006**, *71*, 8011-8015. (c) J. K. Choi, K. No, E.-H. Lee, S.-G. Kwon, K.-W. Kim, J. S. Kim, *Supramol. Chem.*, **2007**, *19*, 283-286.

[20] (a) A. Metzger, V. M. Lynch, E. V. Anslyn, *Angew. Chem. Int. Ed.*, **1997**, *36*, 862-865. (b) A. Metzger, E. V. Anslyn, *Angew. Chem. Int. Ed.*, **1998**, *37*, 649-652.

[21] for a recent review: R. M. Duke, E. B. Veale, F. M. Pfeffer, P. E. Kruger, T. Gunnlaugsson, *Chem. Soc. Rev.*, **2010**, *39*, 3936-3953 and the references therein

[22] (a) T. Gunnlaugsson, P. E. Kruger, P. Jensen, F. M. Pfeffer, G. M. Hussey, *Tetrahedron Lett.*, **2003**, *44*, 8909-8913. (b) D. Esteban-Gomez, L. Fabbrizzi, M. Liechelli, *J. Org. Chem.*, **2005**, *70*, 5717-5720. (c) J. V. Ros-Lin, R. Martinez-Máñez, F. Sancenón, J. Soto, K. Rurak, H. Weißhoff, *Eur. J. Org. Chem.*, **2007**, 2449-2458. (d) F. Han, Y. Bao, Z. Yang, T. M. Fyles, J. Zhao, X. Peng, J. Fan, Y. Wu, S. Sun, *Chem. Eur. J.*, **2007**, 2880-2892.

[23] D.-G. Cho, J. L. Sessler, *Chem. Soc. Rev.*, **2009**, *38*, 1647-1642 and the references therein.

[24] P. Sokkalingam, C.-H. Lee, *J. Org. Chem.*, **2011**, *76*, 3820-3828.

[25] Y.-P. Tseng, G.-M. Tu, C.-H. Lin, C.-T. Chang, C.-Y. Lin, Y.-P. Yen, *Org. Biomol. Chem.*, **2007**, *5*, 3592-3598.

[26] J. E. A. Webb, M. J. Crossley, P. Turner, P. Thordarson, *J. Am. Chem. Soc.*, **2007**, *129*, 7155-7162.

[27] (a) M. Doherty, C. Belcher, M. Regan, A. Jones, J. Ledingham, *J. Ann. Rheum. Dis.*, **1996**, *55*, 432-436. (b) A. E. Timms, Y. Zhang, R. G. Russell, M. A. Brown, *Rheumatology*, **2002**, *41*, 725-729.

[28] R. J. Carton, *Fluoride*, **2006**, *39*, 163-172.

[29] A. Touceda-Varela, E. I. Stevenson, J. A. Galve-Gasión, D. T. F. Dryden, J. C. Mareque-Rivas, *Chem. Commun.*, **2008**, 1998-2000.

[30] O. A. E. Abdalla, F. O. Suliman, H. Al-Ajmi, T. Al-Hosni, H. Rollinson, *Environ. Earth Sci.*, **2010**, *60*, 885-892.

[31] P. Ball, *H_2O: A Biography of Water*, Phoenix Press, London, **2000**. (b) G. V. Oshovsky, D. N. Reinhoudt, W. Verboom, *Angew. Chem. Int. Ed.*, **2007**, *46*, 2366-2393.

[32] S. Kubik, *Chem. Soc. Rev.*, **2010**, *39*, 3648-3663.

[33] L. J. Prins, D. N. Reinhoudt, P. Timmerman, *Angew. Chem., Int. Ed.*, **2001**, *40*, 2382-2426.

[34] E. García-España, P. Díaz, J. M. Llinares, A. Bianchi, *Coord. Chem. Rev.*, **2006**, *250*, 2952-2986.

[35] Y. Inoue, T. Hakushi, Y. Liu, L.-H. Tong, B.-J. Shen, D.-S. Jin, *J. Am. Chem. Soc.*, **1993**, *115*, 475-481.

[36] M. Staffilani, K. S. B. Hancock, J. W. Steed, K. T. Holman, J. L. Atwood, R. K. Juneja, R. S. Burkhalter, *J. Am. Chem. Soc.*, **1997**, *119*, 6324-6335.

[37] S. Kubik, *Chem. Soc. Rev.*, **2009**, *38*, 585-605.

[38] (a) S. Kubik, R. Kirchner, D. Nolting, J. Seidel, *J. Am. Chem. Soc.*, **2002**, *124*, 12752-12760. (b) S. Otto, S. Kubik, *J. Am. Chem. Soc.*, **2003**, *125*, 7804-7805. (c) C. Reyheller, B. P. Hay, S. Kubik, *New J. Chem.*, **2007**, *31*, 2095-2102.

[39] P. Schiessl, F. P. Schmidtchen, *J. Org. Chem.*, **1994**, *59*, 509-511.

[40] T. W. Hudnall, F. P. Gabbai, *J. Am. Chem. Soc.*, **2007**, *129*, 11978-11986.

[41] S. Atilgan, E. U. Akkaya, *Tetrahedron Lett.*, **2004**, *45*, 9269-9271

[42] J. Pérez, L. Riera, *Chem. Soc. Rev.*, **2008**, *37*, 2658-2667.

[43] L. Fabbrizzi, P. Pallavicini, L. Parodi, A. Taglietti, *Inorg. Chim. Acta*, **1995**, *238*, 5-8.

[44] E. Kimura, S. Aoki, T. Koike, M. Shiro, *J. Am. Chem .Soc.*, **1997**, *119*, 3068-3076.

[45] T. Sakamoto, A Ojida, I. Hamachi, *Chem. Commun.*, **2009**, 141-152.

[46] T. Anai, E. Nakata, Y. Koshi, A. Ojida, I. Hamachi, *J. Am. Chem. Soc.*, **2007**, *129*, 6232-6239.

[47] P. A. Vigato and S. Tamburini, *Coord. Chem. Rev.*, **2004**, *248*, 1717-2128.

[48] T. P. Yoon, E. N. Jacobsen, *Science*, **2003**, *299*, 1691-1693.

[49] P. Pfeiffer, E. Breith, E. Lübbe and T. Tsumaki, *Justus Liebigs Ann. Chem.*, **1933**, *503*, 84-130.

[50] W. Zhang, J. L. Loebach, S. R. Wilson, E. N. Jacobsen, *J. Am. Chem. Soc.*, **1990**, *112*, 2801-2803.

[51] R. Irie, K. Noda, Y. Ito, N. Matsumoto, T. Katsuki, *Tetrahedron Lett.*, **1990**, *31*, 7345-7348.

[52] P. G. Cozzi, *Chem. Soc. Rev.* **2004**, *33*, 410-421.

[53] (a) A. D. Garnovskii, A. L. Nivorozhkin, V. I. Minkin, *Coord. Chem. Rev.*, **1993**, *126*, 1-69. (b) F. Thomas, O. Jarjayes, C. Duboc, C. Philouze, E. Saint-Aman, J.-L. Pierre, *Dalton Trans.*, **2004**, 2662-2669.

[54] J. W. Steed, *Chem. Soc. Rev.*, **2009**, *38*, 506-519.

[55] A. Dalla Cort, P. De Bernardin, G. Forte, F. Yafteh Mihan, *Chem. Soc. Rev.*, **2010**, *39*, 3863-3874.

[56] P. Pfeiffer, W. Christeleit, T. Hesse, H. Pfitzinger, H. Thielert, *J. Prakt. Chem.*, **1938**, *150*, 261-316.

[57] (a) J. R. Dorfman, J. J. Girerd, E. D. Simhon, T. D. P. Stack, R. H. Holm, *Inorg. Chem.*, **1984**, *23*, 4407-4412. (b) F. M. Ashmawy, A. R. Ujaimi, *Inorg. Chim. Acta*, **1991**, *187*, 155-158.

[58] (a) R. E. Stenkamp; L. H. Jensen, *Adv. Inorg. Biochem.* **1979**, *1*, 219-233. (b) I. M. Klotz, D. M. Jr. Kurtz, *Acc. Chem. Res.,* **1984**, *17*, 16-22.

[59] P. Kopel, Z. Sindelar, R. Klicka, *Transition Met. Chem.*, **1998**, *23*, 139-142.

[60] R. G. Wollmann, D. N. Hendrickson, *Inorg. Chem.*, **1978**, *17*, 926-930.

[61] (a) M. Ohashi, T. Koshiyama, T. Ueno, M. Yanase, H. Fujii, Y. Watanabe, *Angew. Chem. Int. Ed.*, **2003**, *42*, 1005-1008. (b) T. Ueno, M. Ohashi, M. Kono, K. Kondo, A. Suzuki, T. Yamane, Y. Watanabe, *Inorg. Chem.*, **2004**, *43*, 2852-2858. (c) T. Ueno, T. Koshiyama, M. Ohashi, K. Kondo, M. Kono, A. Suzuki, T. Yamane, Y. Watanabe, *J. Am. Chem. Soc.*, **2005**, *127*, 6556-6562. (d) T. Ueno, T. Koshiyama, S. Abe, N. Yokoi, M. Ohashi, Y. Satake, H. Nakajima, Y. Watanabe, *J. Organomet. Chem.*, **2007**, *692*, 142-147. (e) S. Abe, T. Ueno, P. A. N. Reddy, S. Okazaki, T. Hikage, A. Suzuki, T. Yamane, H. Nakajima, Y. Watanabe, *Inorg. Chem.*, **2007**, *46*, 5137-5139.

[62] T. Ueno, N. Yokoi, M. Unno, T. Matsui, Y. Tokita, M. Yamada, M. Ikeda-Saito, H. Nakajima, Y. Watanabe, *Proc. Natl. Acad. Sci. USA.*, **2006**, *103*, 9416-9421.

[63] Ł. Górski, A. Saniewska, P. Parzuchowski, M. E. Meyerhoff, E. Malinowska, *Anal. Chim. Acta*, **2005**, *551*, 37-44.

[64] A. K. Singh, S. Mehtab, *Talanta*, **2008**, *74*, 806-814.

[65] M. R. Ganjali, F. Mizani, M. Salavati-Niasari, *Anal. Chim. Acta*, **2003**, *481*, 85-90.

[66] J. T. Mitchell-Koch, E. Malinowska, M. E. Meyerhoff, *Electroanalysis*, **2005**, *17*, 1347-1353.

[67] S. Shahrokhian, M. K. Amini, R. Kia, S. Tangestaninejad, *Anal. Chem.*, **2000**, *72*, 956-962.

[68] B. L. Vallee, D. S. Auld, *Biochemistry*, **1990**, *29*, 5647-5659.

[69] (a) A. Dalla Cort, L. Mandolini, C. Pasquini, K. Rissanen, L. Russo, L. Schiaffino, *New J. Chem.*, **2007**, *31*, 1633-1638. (b) M. E. Germain, T. R. Vargo, B. A. McClure, J. J. Rack, P. G. Van Patten, M. Odoi, M. J. Knapp, *Inorg. Chem.*, **2008**, *47*, 6203-6211.

[70] S. J. Wezenberg, E. C. Escudero-Adán, J. Benet-Buchholz, A. W. Kleij, *Chem.–Eur. J.*, **2009**, *15*, 5695-5700.

[71] A. Silvestri, G. Barone, G. Ruisi, D. Anselmo, S. Riela, V. T. Liveri, *J. Inorg. Biochem.*, **2007**, *101*, 841-848.

[72] A. Dalla Cort, P. De Bernardin, L. Schiaffino, *Chirality*, **2009**, *21*, 104-109.

CHAPTER 2

Synthesis of water-soluble uranyl salophen complexes.

The general characteristics of the uranyl-salophen complexes are presented in this chapter. The first part provides a general overview of their structural features and their properties as anion receptors, both in organic solvents and in aqueous solutions. Thereafter, the first water soluble uranyl salophen derivative and the issues pertaining its synthesis are reported here, together with the attempts made so far to increase the solubility in water of metal-salophen complexes.

2.1 Uranyl-salophen complexes.

Uranium mainly occurs in nature as uranyl cation, UO_2^{2+}, in which the metal is in the highest oxidation state and bound to two oxygen ("yl") atoms. These *oxo* ligands are in the *trans* arrangement and the robustness of the uranium-oxygen bond can be ascribed to its covalent character.[1] The two U=O bonds are therefore kinetically and thermodynamically stable, and the reactions primarily occur on the equatorial binding sites present on the metal. It is well known that the uranyl cation forms stable complexes with the salophen ligand and the deprotonation of the two phenolic groups, upon the coordination, leads to neutral metallo-oraganic complexes.[2] Though very few cases of hexagonal bipyramidal coordination geometry have been reported for the uranyl cation,[3] its salophen complexes display a well-defined preference for a pentagonal bipyramidal coordination geometry. In this arrangement, the four equatorial binding site on the metal center are occupied by the donor atoms of the ligand and the fifth one generally accommodates a solvent molecule, such as water or methanol, in the absence of other guests.[4] The uranyl salophen complex can be regarded as a hard Lewis acid immobilized in an organic framework, thus it displays the properties of the uranyl cation and preferably interacts with hard Lewis bases.[5] Being the radius of the uranyl cation (r = 1.38 Å) too large to fit the cavity of the ligand, the coordination causes a distortion of the salophen structure and the resulting complex has a "bird-like" shape rather than a planar one, with the aromatic rings lying outside the N_2O_2 plane. Non-symmetrical substituted complexes are inherently chiral[6] and a number of configurationally stable derivatives are under investigation as potential asymmetric supramolecular catalysts.[7] Uranyl-salophen complexes, indeed, proved to interact with anionic species and carbonyl compounds,[8] thus behaving as receptors, carriers[9] and supramolecular

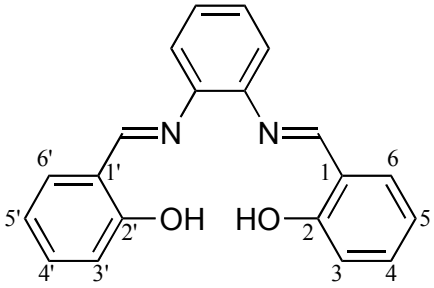

Figure 2.1 Structure of the salophen ligand with the numbering of the salicylaldehyde aromatic rings.

catalysts.[10] The positions 3 and 3' of the ligand (fig 2.1) are the closest to the binding site of uranyl salophen complexes and through a proper decoration of the receptors in these positions with designed pendant arms it is possible to achieve an enhancement of affinity and selectivity. Notably the macrocyclic compound **2/1**, reported by Reinhoudt and co-workers,[11] binds to urea in a supramolecular fashion with an extremely high affinity (K_{ass} is estimated to be higher than 10^8 M^{-1}), mimicking the binding site of the enzyme urease. As confirmed by solid state analysis,

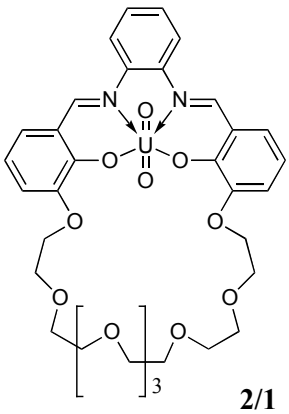

2/1

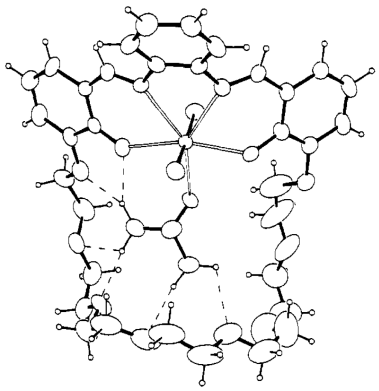

Figure 2.2 Compound **2/1** (*left*). X-ray structure of compound **2/1** coordinating a urea molecule (*right*) Both the interaction with the metal center and the hydrogen bonds with the crown ether are shown.

the recognition combines the primary Lewis acid-base interaction to the metal with the hydrogen bonding between the amido groups and the oxygen atoms of the crown ether (Fig 2.2). Compound **2/2**, instead, exploits van der Waals π-π stacking interactions to increase the affinity towards ketones with an extended aromatic surface, such as perynaphtenone (K_{ass}: 8000 M^{-1}). As far as supramolecular catalysis is concerned, the coordination to uranyl-salophen derivatives proved to activate the carbonyl group towards nucleophilic attack and stabilize the transition

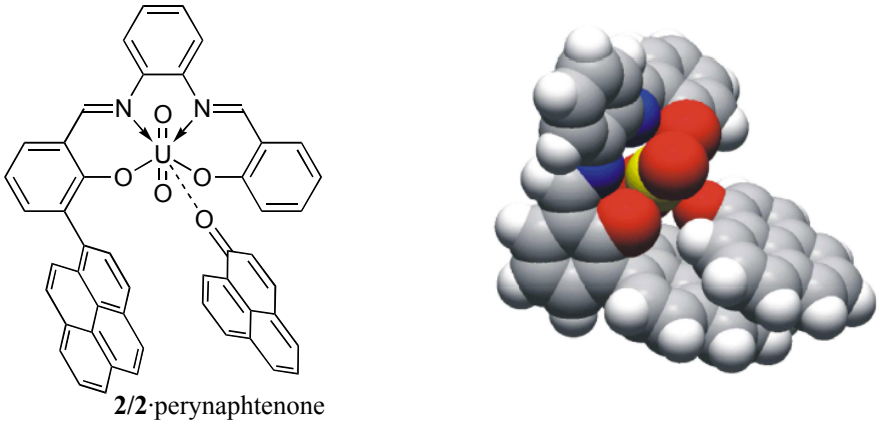

Figure 2.3 Computer drawn CPK model (*right*) of the complex between compoud **2/2** and perynaphtenone (*left*).

state of addition reactions. Examples are the Diels-Alder cycloaddition between benzoquinone and 1,3-cyclohexadiene, performed by derivative **2/3**[ix] (Fig. 2.4a),[12] the Michael-type conjugate addition of thiophenol to 2-cyclopenten-1-one performed by compound **2/4** (Fig. 2.4b)[13] and the phenyl acetate ester bond cleavage in the macrocyclic derivative **2/5** (Chart 1).[14]

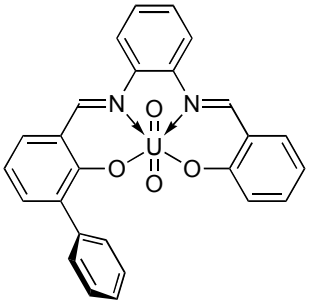

2/3

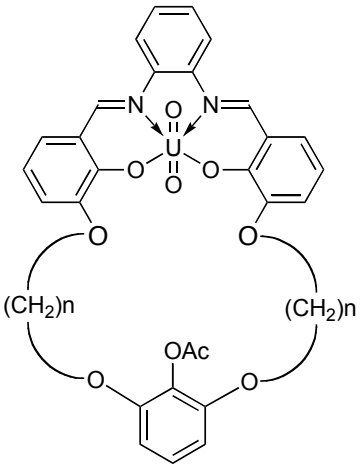

2/5, n=2-4

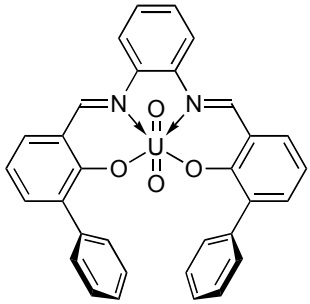

2/4

Chart 1.

[ix] Only the *endo* product is afforded in detectable yield.

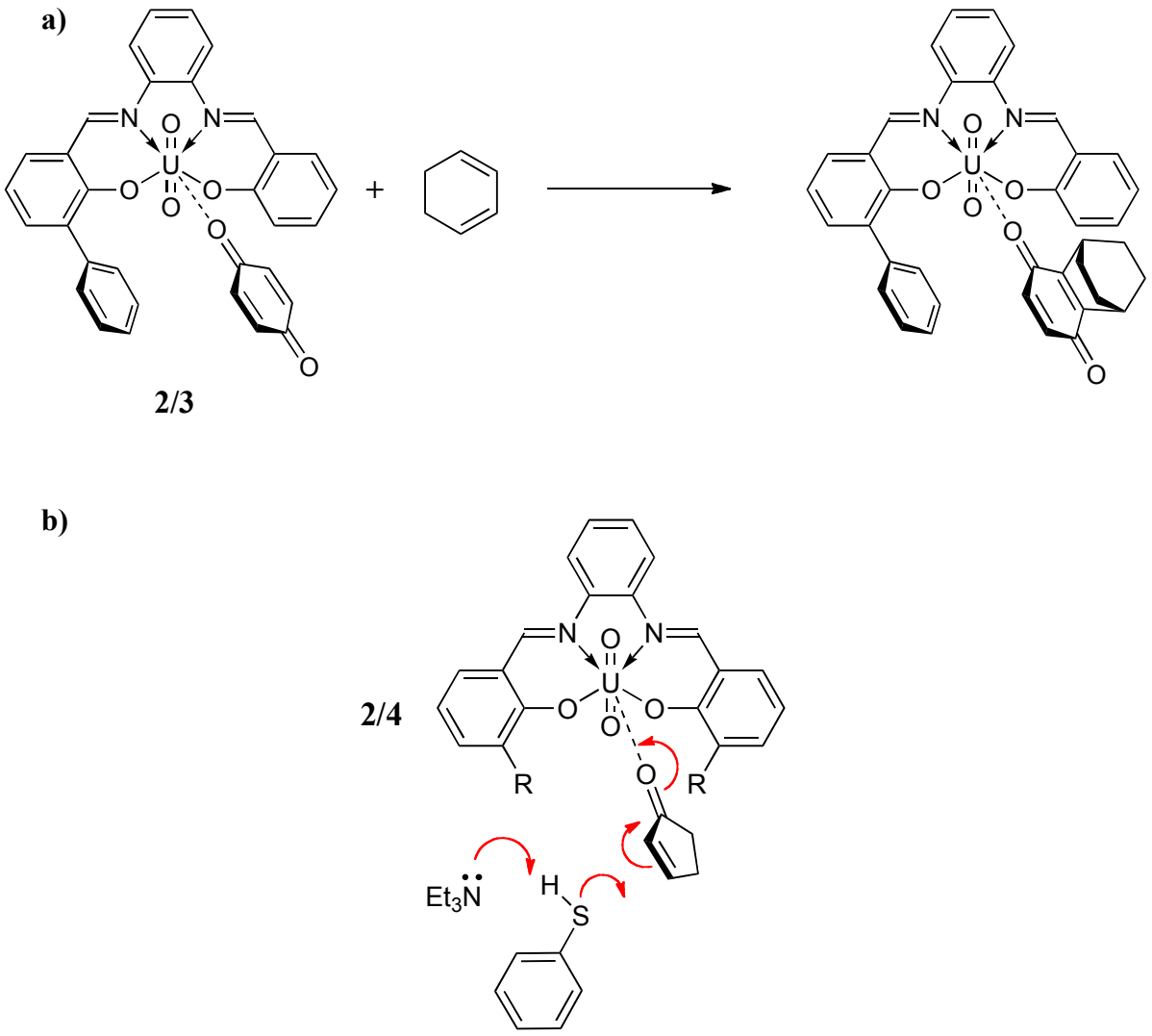

Figure 2.4 Uranyl-salophen derivatives as catalysts. (*a*) Diels-Alder cycloaddition performed by derivative **2/3** and (*b*) representation of the transition state for the Michael-type addition of thiophenol to 2-cyclopenten-1-one.

2.2 Uranyl-salophen complexes as anion receptors.

As already mentioned, uranyl-salophen derivatives are hard Lewis acids and can form complexes with anions. Pointless to state that the harder the character of the anion, the stronger the interaction will be. In a work dating back to the early nineties, Reinhoudt and co-workers shed some light on the ability of these metal complexes to bind to anionic species.[15] They reported the X-ray structure of the complex between receptor **2/6** and tetraethylammonium

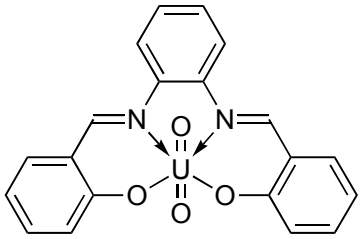

2/6

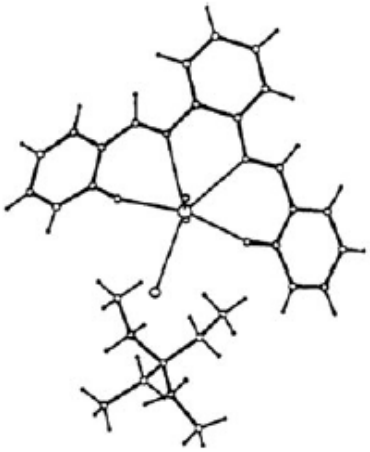

Figure 2.5 X-ray structure of compound **2/6** (*left*) coordinating tetramethylammonium chloride (*right*).

chloride, thus confirming both the bent structure and the coordination geometry of the uranyl center in such compounds (Fig. 2.5). Again, higher affinity and selectivity can be achieved by decorating the 3 position on the salicylaldehyde precursor. The receptor **2/7** bears two amido groups and binds to dihydrogen phosphate anion in a competitive solvent such as DMSO (K_{ass} = $1.5 \cdot 10^3$ M^{-1}), while no complexation was observed with Cl^-, HSO_4^-, SCN^- and ClO_4^-. The interaction between the phosphate and **2/7** is only three times stronger than that observed for receptor **2/8** (K_{ass} = $5.1 \cdot 10^2$ M^{-1}) and this is a clear evidence that the driving force in the

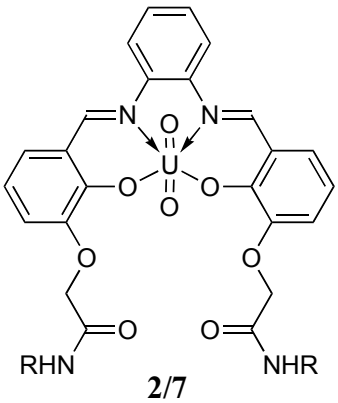

2/7

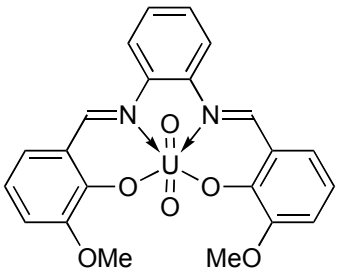

2/8

R = 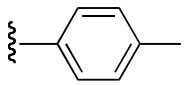

recognition process is the acid-base interaction and that the additional hydrogen bonding interactions from the -(C=O)NH- groups provide an extra stabilization of the complex. The involvement of the amido groups is highlighted by the downfield shift of the NH protons, in the

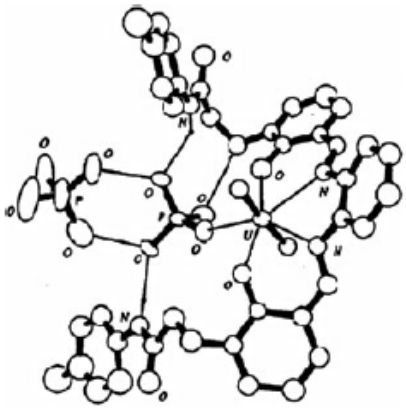

Figure 2.6 Structure of the complex **2/7**·$2H_2PO_4^-$. TBA fragments and solvent molecules are omitted for clarity. The crystal was obtained by slow diffusion of diisopropyl ether into a MeCN solution of **2/7** and two-fold excess of the $Bu_4N^+ H_2PO_4^-$.

NMR spectrum, upon phosphate complexation and this coordination arrangement is also featured in the solid state. X-ray analysis indeed shows that a $H_2PO_4^-$ anion interacts with the metal center and forms hydrogen bonds with the pendant arms of the ligand. Interestingly a second phosphate anion remains bound to the first one through hydrogen bonding, although it does not interact directly with any part of the receptor (Fig. 2.6).[16]

High affinity towards fluoride anion is a common feature in uranyl-salophen derivatives.[17] The simplest complex **2/6**, indeed, binds tightly to F^- in DMSO (K_{ass} = $2.51 \cdot 10^6$ M^{-1}) while showing negligible affinity towards the other halides and the less basic anions ClO_4^- and SO_4^{2-}. Nevertheless, species such as AcO^-, CN^- and $H_2PO_4^-$, that form less stable complexes than fluoride, still compete with it to bind to receptor **2/6** (table 1).

Anion	K (M^{-1})
AcO^-	2570
$H_2PO_4^-$	$1 \cdot 10^4$
CN^-	230
F^-	$> 10^6$

Table 1 Binding constant values for the association of the receptor **2/6** with various anions in DMSO at 25 °C.

In order to increase the selectivity for the fluoride recognition, an approach based on the host sterical demand can be employed.[18] Receptor **2/9**, bearing two *tert*-butyl groups on the

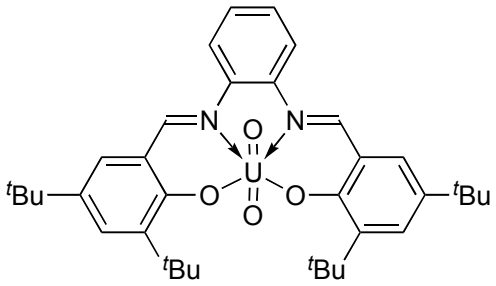

2/9

positions closest to the binding site, while showing a 50-fold decrease in the binding affinity towards phosphate, still binds effectively the other two competitive anions. Thus a more sterically demanding macrocyclic host was thought to be able to discriminate fluoride over all the other anions. Nevertheless, as a consequence of the rigidity of the *o*-phenilenediamine linker, it was not possible to obtain a suitable cyclic salophen based receptor and hence the more flexible salen derivative **2/10** was synthesized. The affinity of cyclophane **2/10** towards fluoride is still comparable to that showed by the other uranyl-salophen receptors, but its selectivity turns out to be at least 10^5 higher. Indeed, no considerable changes in the UV-vis absorption spectrum of a **2/10** solution were detected upon the addition of solutions of acetate, cyanide or phosphate tetraalkylammonium salts.[17]

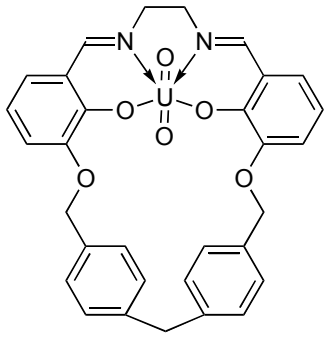

2/10

Furthermore our group reported that uranyl-salophen derivatives can coordinate ion pairs both in solution and in the solid state. Given that the recognition of the ion pairs is generally favored with respect to the single ion binding in organic solvents,[19] receptors **2/11** and **2/12**,

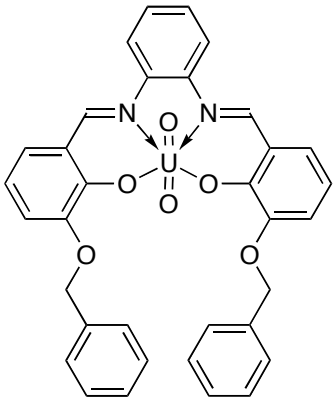

2/11

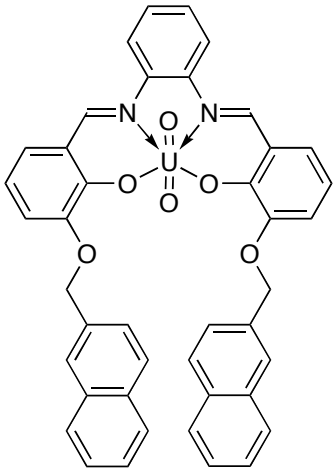

2/12

endowed with aromatic pendant arms, demonstrated to strongly bind to alkali metal[20] and ammonium[21] halides. Proton NMR and X-ray analysis highlighted that the halide anion binds to the free coordination site on the uranium, while the ammonium cation lies on the aromatic

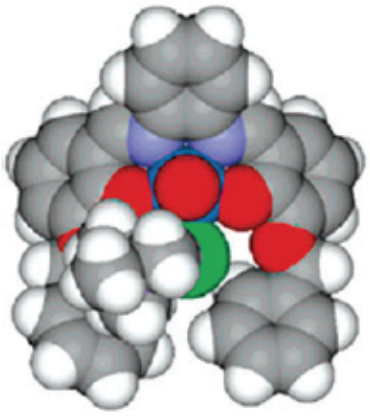

Figure 2.7 VdW presentation of the structure of the complex between receptor **2/11** and TMACl.

surface of the two side arms, establishing π-cation interaction (Fig. 2.7). More complex supramolecular architectures appear, instead, in the coordination of alkali metal halides. A dimeric assembly forms around a $(MX)_2$ core when, for example, cesium chloride binds to receptor **2/11** (Fig 2.8).

Undoubtedly, uranyl-salophen complexes are highly versatile receptors in organic solvents and, under proper conditions, they maintain the affinity towards anions even in aqueous solutions.

Anion sensitive membranes display a selectivity governed by the lipophilicity of the ions, according to the previously mentioned Hofmeister series. This selectivity can be altered with the use of a receptor which has high affinity towards the targeted anion and which is able to overcome the energy required to extract it from the aqueous solution. Reinhoudt and co-workers outlined the practical applications of the uranyl-salophen recognition properties in the anion transport field.[22] A number of differently 5'-substituted complexes was synthesized and their ability in selective anion transport across membranes was found to be significantly dependent on the nature of the substituents. In particular 5,5'-dinitro derivative doped membranes (PVC based) revealed to work as selective electrodes for the nitrite anion. Ion selective electrodes (ISEs) and chemical field-effect transistors (CHEMFETs)[x] are devices in which the ion-receptor interaction is converted into an electric signal.[23] They are sensors largely used to monitor the concentration of a targeted ion in water environment, especially in biological essays.[24] Uranyl-salophen complexes bearing long alkyl chains on the phenylenediamine ring have been used as ionophores to create selective electrodes. In particular derivatives **2/13**-**2/15** have been employed

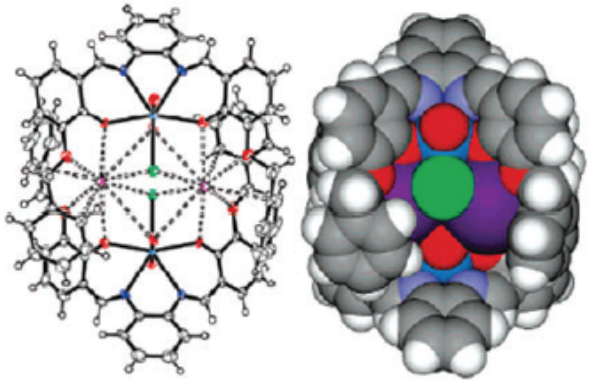

Figure 2.8 X-ray structure of the dimeric assembly between CsCl and complex **2/11**.

[x] CHEMFETs are silicon-based microsensors that can transduce the membrane potential of an ion selective membrane deposited on top of the semiconductor into an electronic signal.

to create phosphate-selective electrodes,[25] while derivatives **2/13**, **2/16-2/18** to build fluoride-selective ones.[26]

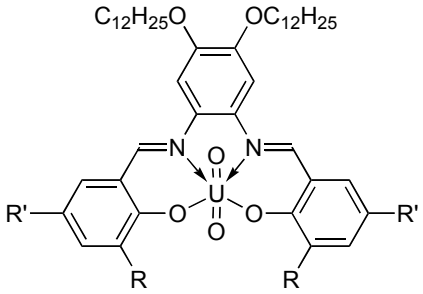

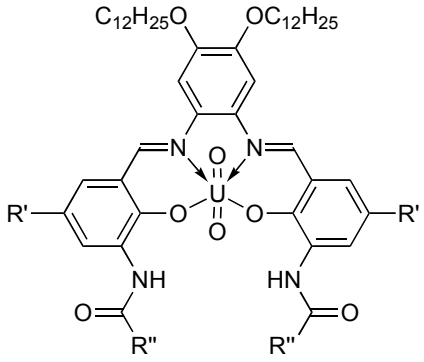

2/13: R, R' = H
2/14: R = OCH_3, R' = H
2/15: R = H, R' = OCH_3

2/16: R' = H, R" = C_7H_{15}
2/17: R' = *t*-Bu, R" = C_7H_{15}
2/18: R' = H, R" = CH_3

2.3 Recognition of anions in aqueous solutions.

Given that uranyl-salophen receptors, when embedded in a polymeric membrane, seem to be able to pay off the dehydration energy of the anions, it comes naturally to direct the attention to a more extensive investigation of their properties in the aqueous medium. Receptor **2/6** is completely insoluble in water and different strategies can be adopted to bring it in aqueous environment. Our group, in collaboration with that of Prof. Bartik (Université Libre de Bruxelles), proposed the inclusion of receptor **2/6** into cetyltrimehylammonium bromide (CTABr) micelles. In 50 mM solution of the surfactant, **2/6** becomes soluble up to millimolar concentrations and binds to fluoride with the highest affinity so far reported for a neutral receptor in water (K_{ass} = 10800 ± 800 M^{-1}).[27] Given that the affinity of the same receptor towards fluoride drops far down in methanol (K_{ass} = 360 ± 20 M^{-1}), when compared with that shown in DMSO (see table 1), it is clear that the role of the CTABr is not that of a simple carrier, since it provides a less competitive environment around the binding site, as proteins and enzymes do. NOE and PRE experiments, indeed, demonstrate that **2/6** is located in the outer part of the micelle, with the protons H3 and H4 (see Fig. 2.1) pointing towards the bulk solution (Fig. 2.9).

This approach has the clear advantage that no chemical modifications are required, but it has to be stressed that the location and the stability of the uranyl-salophen complexes heavily

depend on their structure. Therefore this cannot be considered a general method. Moreover, even if in this case the system benefits by the supramolecular contribution of the surfactant, it should be noted that the binding between the anion and the receptor is further influenced by the electrostatic attraction exerted by the cationic heads of CTABr and by the competition with the counterions.

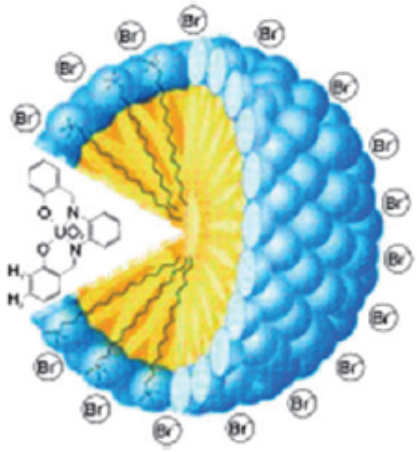

Figure 2.9 Pictorial representation of receptor **2/6** inside the CTABr micelle.

The approach we present in this work is quite different and aims at the introduction of hydrophilic groups on the salophen ligand in order to make the uranyl-complex soluble in water. The choice was whether to introduce charged or neutral moieties. The presence of negatively charged groups may lead to a decrease of the binding constants due to repulsive interactions with the anions, whereas positively charged moieties would lead, in principle, to the same issues of the presence of cationic surfactants. This means that the binding process does not involve a clean anion to metal association, but more likely it would be the result of different interactions, comprising the competition with the counterion for the binding site and the electrostatic interaction with the cationic group. Our investigation was first meant to the evaluation of the pure Lewis acid-base interaction in water, instead. On these premises we introduced neutral hydrophilic groups using a strategy previously reported by our group.[28] One of the major detoxification processes that occur in the liver of animals consists in the conjugation of xenobiotic substances with a sugar moiety. Drawing inspiration from the nature, we planned to introduce a glucose pendant on the salicylaldehyde. Therefore receptor **2/23**, bearing two D-glucose units, was synthesized according to the scheme reported in figure 2.10.

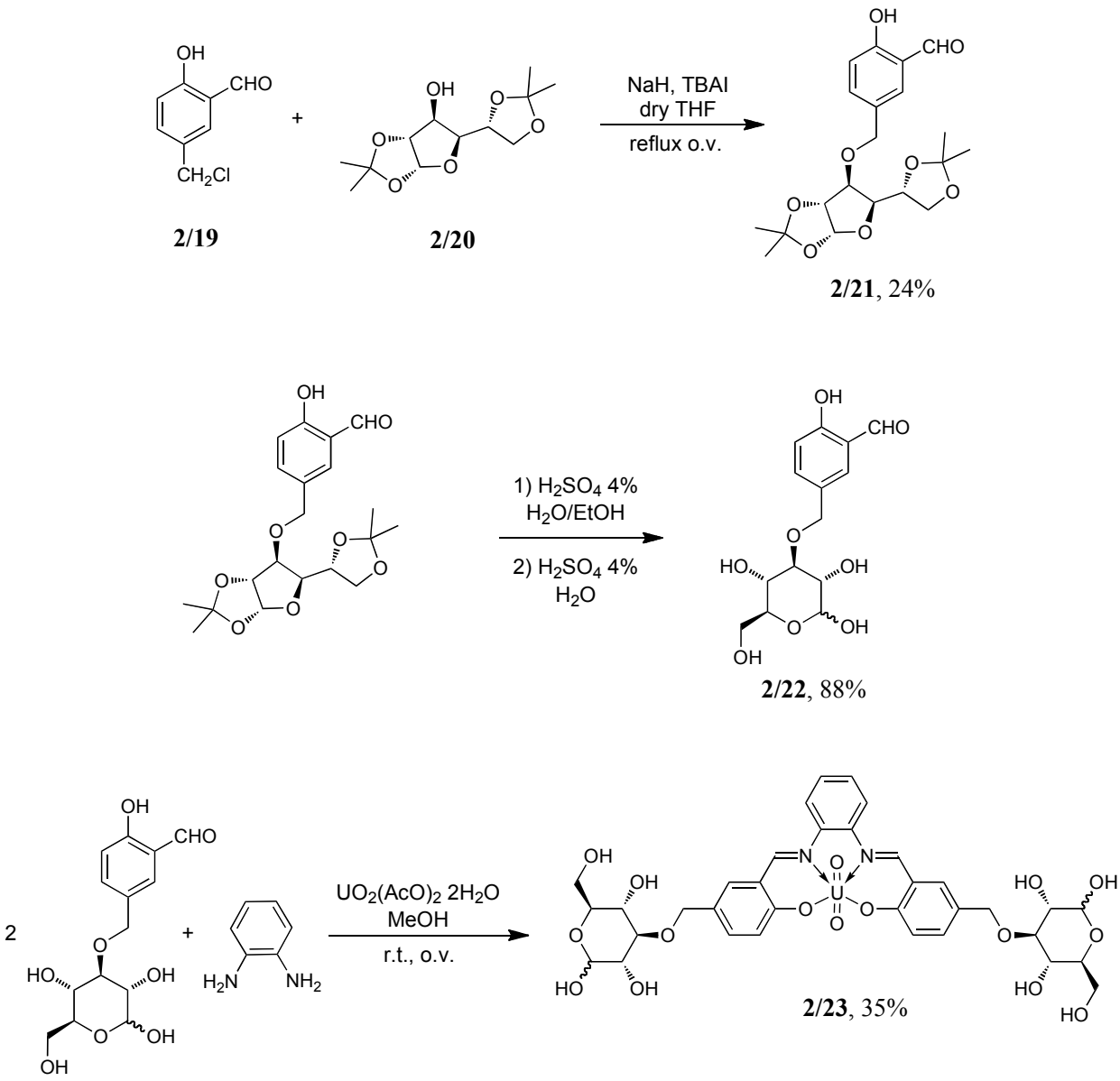

Figure 2.10 Synthetic pathway to complex **2/23**.

The synthetic pathway consists of three main steps. The chloromethyl salicylaldehyde **2/19** was reacted with the commercially available protected glucose **2/20** in the presence of an excess sodium hydride as base. Subsequent removal of the protecting groups with sulfuric acid afforded aldehyde **2/22**. The reaction was actually carried out in two steps because different conditions are required to remove the two acetonide moieties. The final metal assisted condensation of *ortho*-phenylenediamine with two equivalents of **2/22** in methanol afforded the desired product, which was recovered through precipitation with diethyl ether. With respect to the reported synthesis of the Zn coordinated **2/23** analogue, few procedures have been optimized. In particular the solvents for the chromatographic purification have been replaced to achieve a better separation

of the crude reaction products. In addition, refluxing the mixture for one hour did not afford the compound **2/23** and consequently the solution was stirred overnight at room temperature, instead. The complex displays a fair solubility in pure water, sufficiently high to carry out the spectophotometric experiments that will be presented in the next chapter.

The removal of the two acetone molecules to afford **2/22**, although achieved with more than satisfactory yield, requires different solvent conditions to gain completion. In order to perform a one-pot removal of both the two acetonide moieties, we tested different conditions, such as increasing concentration of sulfuric acid, TFA, and acidic resins. We found that the Amberlyst 15 (H^+ form) resin affords the deprotected product in a single step, nevertheless the yield was significantly lower than the classic two-step removal, which still remains the best procedure.

A drawback in the synthesis of aldehyde **2/22** is the poor yield of the first step, which is around 25%. We tried to increase it by changing different parameters in the reaction conditions and in the work-up protocol, but to no avail. We speculated that the deprotonated chloromethyl salicylaldehyde may undergo an elimination process, leading to the formation of the semi-quinone species **2/24** (Fig. 2.11).[29] Being much more reactive than the parent salicyladehyde, this species can yield the byproducts found in the crude reaction mixture.

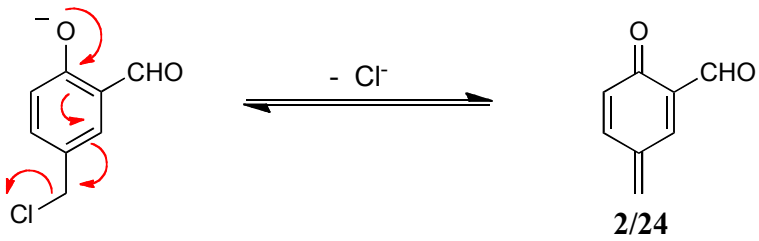

2/24

Figure 2.11 Proposed mechanism for the formation of the species **2/24**.

Nonetheless the low yield of the reaction still represents a weakness of the synthetic pathways. We reasoned that the problem could be solved through the design of a different way to link the sugar moiety to the aldehyde unit. The route to compound **2/26** contemplates the Lewis acid assisted substitution to the activated anomeric carbon of the glucose, followed by the introduction of a formyl group on the phenyl moiety, the removal of the acetyl groups with sodium methoxide and the eventual hydrolysis of the methoxy group with lithium chloride in dry DMF (Fig. 2.12).[30] Accordingly to a reported procedure,[31] α-D-glucose pentaacetate was reacted

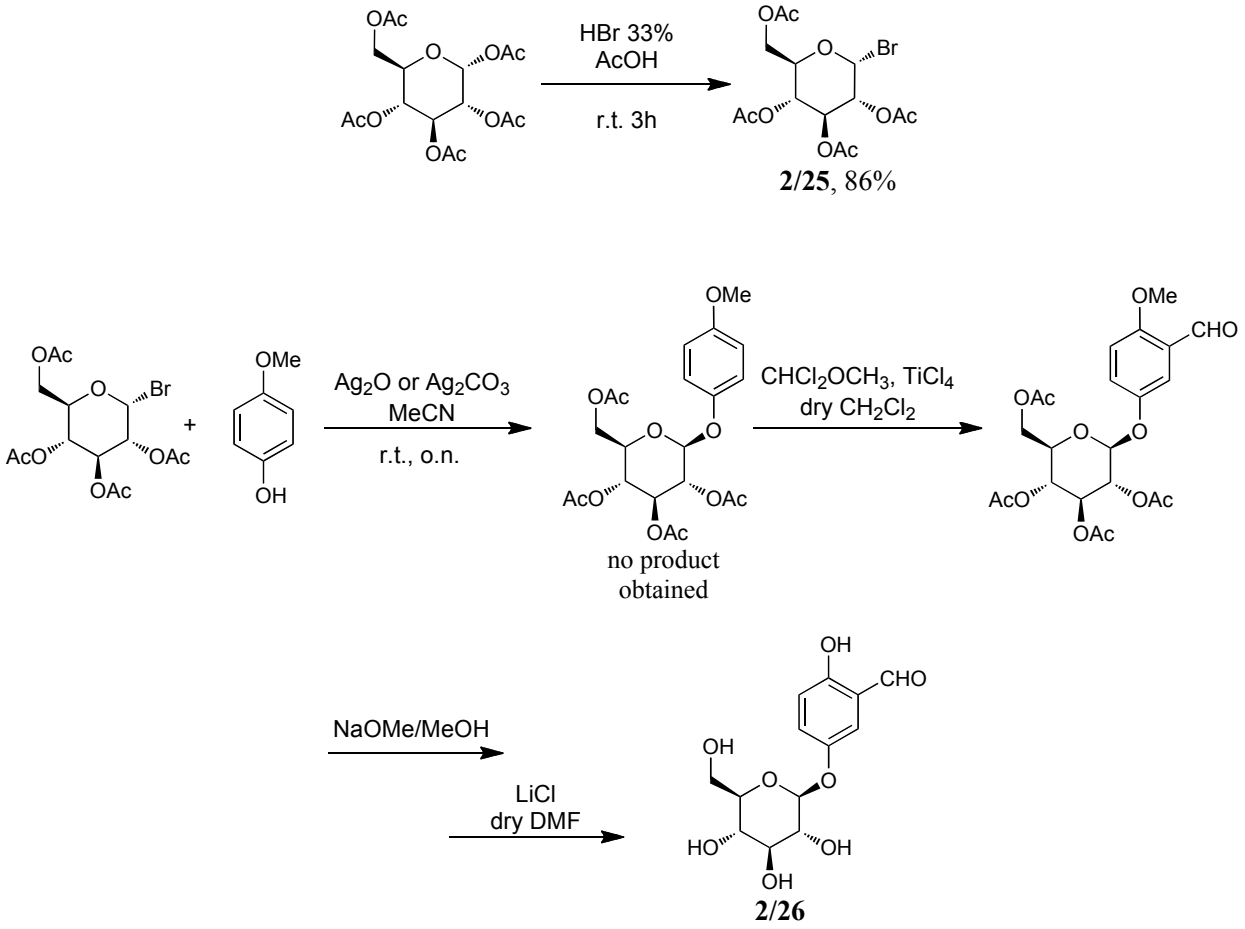

Figure 2.12 Proposed route to compound **2/26**.

with hydrogen bromide in acetic acid to activate the C1 position. Unfortunately any attempt to further react the bromide **2/25** with 4-methoxyphenol with silver oxide or silver carbonate in acetonitrile failed to afford the product.

The copper catalyzed Huisgen 1,3-dipolar cycloaddition between alkynes and azides (CuAAC) is nowadays largely used in organic and bioorganic synthesis.[32] Alkynes and azides, although displaying a mutual reactivity, are compatible with many organic functional groups, especially those present in biomolecules. For the wide applicability, the CuAAC has been used in many different fields ranging from the biomolecule tagging[33] to the covalent coverage of surfaces[34] and it was defined as the "cream of the crop" of the click-chemistry.[35] An interesting characteristic of the CuAAC is that, unlike the non-catalyzed reaction, it is 100% regioselective and affords the *anti* isomer as the only product (Fig. 2.13).[36] We envisaged that the triazole

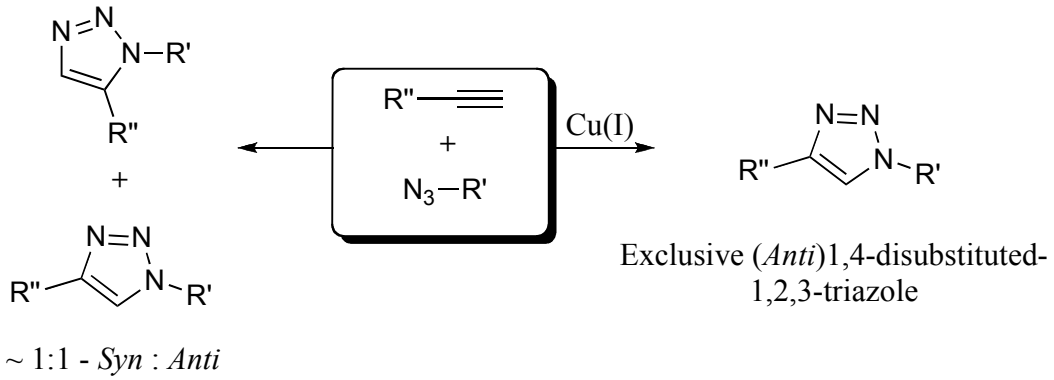

Figure 2.13 Product distribution pattern for the Cu(I) catalyzed (*right*) and the spontaneous (*left*) Huisgen-1,3-dipolar cycloaddition of an azide to an alkyne.

formation could be a viable way to successfully connect the sugar moiety to the salicylaldehyde and thus we planned a synthetic strategy which makes use of the CuAAc reaction (scheme in Fig. 2.14).

The 5-azidomethyl salicylaldehyde can be easily obtained from the corresponding benzyl chloride in almost quantitative yield, while the protected propargyl glucofuranose **2/29** can be synthesized by reacting the corresponding alcohol (**2/20**) with propargyl bromide in the presence of a base. The reaction was performed using sodium hydroxide as base and TBAI as phase transfer catalyst,[37] and afforded the product with a yield higher than 90% after chromatographic purification. The following triazole formation was carried out in the classic conditions reported for the Huisgen CuAAC, using ascorbic acid as reducing agent to generate Cu(I) *in situ*. The aldehyde **2/31** was thus obtained after the removal of the acetonide groups using sulfuric acid as previously described. Eventually, complex **2/32** was obtained and fully characterized through two dimensional COSY spectroscopy. Noteworthy the aldehyde **2/31** was obtained from the 5-chloromethyl salicyaldehyde and **2/20** with 50% overall yield, while the aldehyde **2/22** in 22% yield starting from the same reagents. Thus, despite this new pathway requires a greater number of steps with respect to the synthesis of **2/22**, it allows to obtain a glucose appended salicylaldehyde in higher yields than the previous one. The leading idea of this new synthetic route was that the presence of the triazole moiety would have increased the solubility in water of the final complex, as well as providing a versatile method to afford a library of suitable precursors for water soluble metal-salophen complexes. Considering the results we were dealing with, this approach seemed to be very promising, but unfortunately the final complex **2/32** displays a poor solubility in pure water, lower than that of **2/23**.

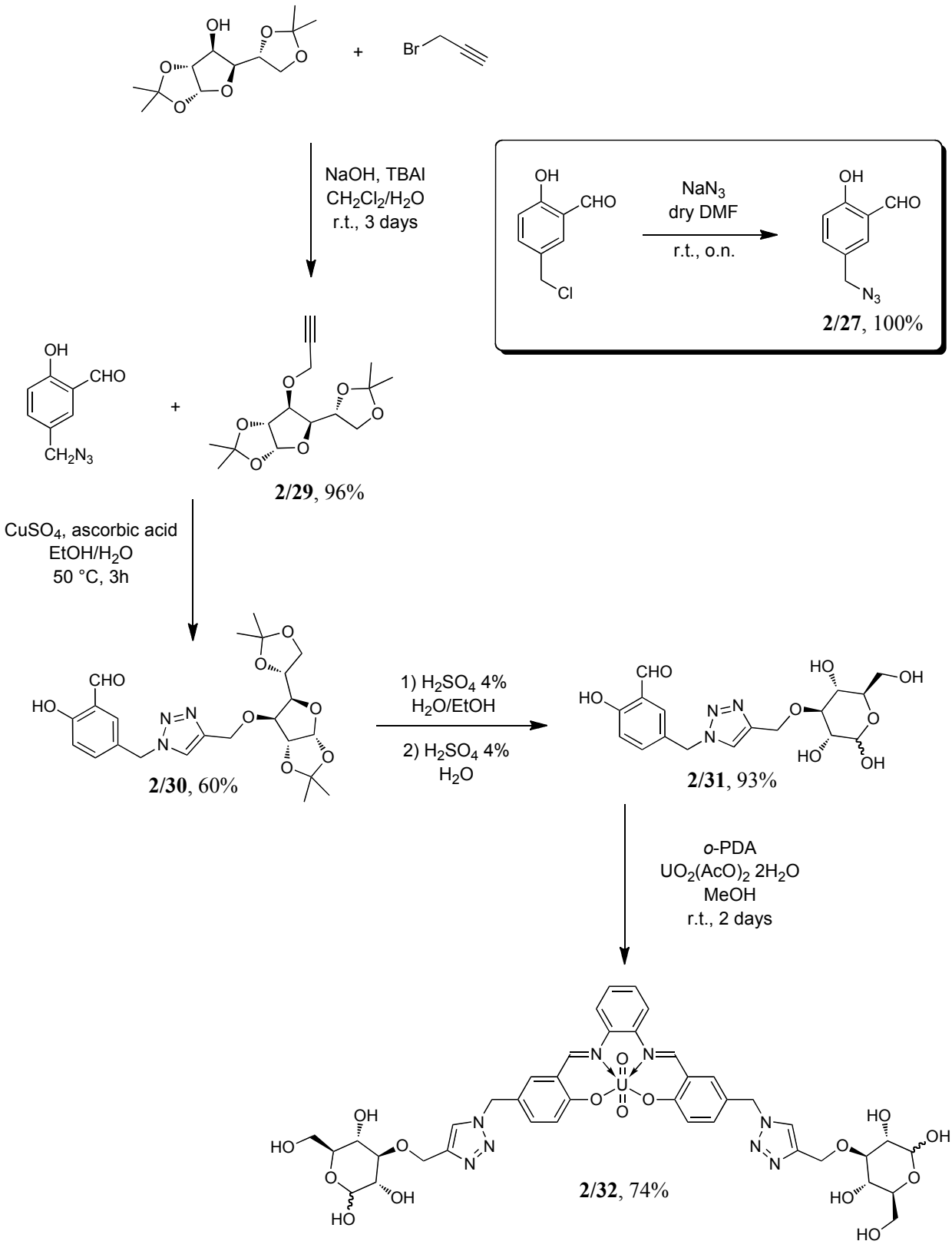

Figure 2.14 Synthetic route to complex **2/32**.

2.4 Strategies to achieve higher solubility in water.

As mentioned, complex **2/23** has an acceptable, yet low, solubility in water. It is able to bind to some inorganic and organic anions in water and its binding properties will be discussed in detail in the following chapter. Nevertheless the quite low solubility precludes any technique, other than the UV-vis light absorption spectroscopy, to be used to investigate its binding properties in solution. NMR spectroscopy, for example, is ineligible because the solutions of **2/23** cannot reach concentrations high enough to fulfill its sensitivity. The NMR characterization was indeed made in polar organic solvent such as methanol or, even better, dimethyl sulfoxide. Moreover the presence of the two glucose moieties does not allow any additional lipophilic substituent to be present on the ligand skeleton since this causes a dramatic solubility drop. This is witnessed by the fact that phenyl decorated complex **2/33**, previously synthesized, is completely insoluble in water, and slightly soluble in the majority of the organic polar solvents such as methanol and dimethyl formamide. Our initial goal was, once established their binding properties, the study of the catalytic behavior of the uranyl-salophen derivatives in water. In the recent years much the reaction that proceed in water have gained an increasing attention.[38] With respect to the organic solvents, water offers unquestionably many advantages, not least the fact that it is a cheap, non toxic, largely available solvent and thus an appealing medium for organic reactions. Since 1980, when Rideout and Breslow reported the hydrophobic acceleration of the Diels-Alder reaction in the presence of water,[39] it was clear that the aqueous environment plays a sort of catalytic role. The so-called "on water" catalysis[40] is however not to be ascribable completely to hydrophobic effects since, in some cases, the enhancement of the reaction rate may be also recorded with respect to solvent-free conditions. Given that the role of water is far from being fully understood and that its catalytic activity varies according to a number of parameters, the recurring *on water*, *in the presence of water* and *on water* definitions are to date interchangeably used to describe reactions that proceed under very different conditions.[38] Although organic reactions benefit from the rate enhancement provided by the aqueous solutions, water does not meet requirements, such as stereoselectivity, generally fulfilled by the catalysts especially when

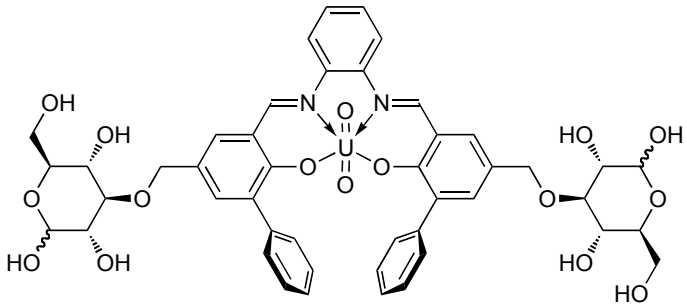

2/33

the synthesis of natural active products is involved. As the use of water as solvent (or co-solvent) for organic reactions is becoming more and more widespread, the quest for water soluble catalysts able to perform ever more demanding transformations turns to be of great interest in organic chemistry. Consequently we strived to find a suitable way to synthesize ligands with high solubility in water to form hydrophilic metal-salophen complexes. The synthesis of aldehyde **2/31** was in part conceived with this purpose. Even though modified *ortho*-phenilenediamines with appended sugar moieties have been reported,[41] their synthesis involves air sensitive intermediates that require extremely careful handling. Hence our choice to focus on the aldehydic precursor of the salophen ligand as junction site for an hydrophilic pendant.

Naringin, **2/34**, is a naturally occurring flavanone glycoside. It is the major flavonoid in grapefruit, responsible for its bitter taste, and exerts a variety of beneficial pharmacological effects.[42] The molecule consists of a rhamnosyl-glucosyl disaccharide moiety connected to the naringenin flavanone structure, which theoretically should be suitable to form salophen-like structures (Fig 2.15). Thus naringin can be regarded as a potentially ready-to-use precursor for the synthesis of a water soluble salophen-type ligands **2/35**. Nevertheless, to date, any attempt to react naringin with 1,2-diaminobenzene, including the metal template one-pot synthesis of the complex, failed to afford the desired product.

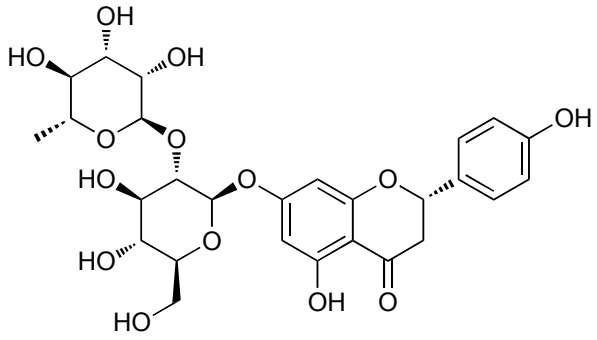

2/34

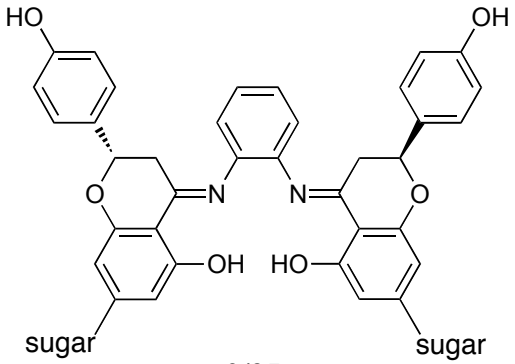

2/35

The idea of having a disaccharide unit on the salicylaldehyde, instead of the glucose moiety, seems a viable way to reach a higher solubility in water. The chemistry of carbohydrates is fascinatingly wide and offers a broad range of protocols that allows to achieve the selective

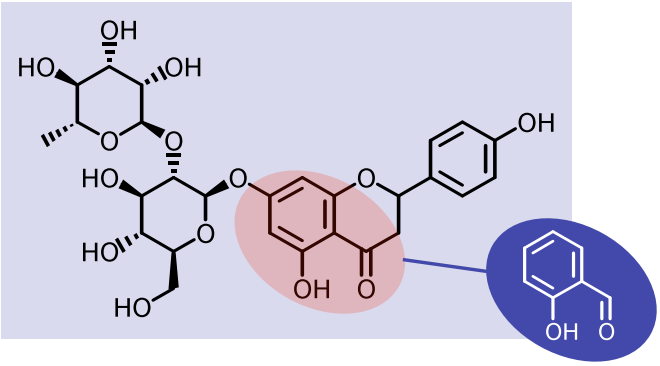

Figure 2.15 Structural relations between the flavanone moiety and the salicylaldehyde.

reactivity of the single hydroxy groups of the sugars.[43] The reaction between the β-methyl lactoside **2/39** (LacβOMe) and benzyl bromide in the presence of dibutyltin oxide is described in the literature.[44] The dibutyltin oxide is known to form cyclic dibutylstannylene acetals with sugars, preferably with *cis* diol arrays,[45] which show an enhanced nucleophilicity of the equatorial oxygen atom.[46] With the methyl lactoside **2/39** the reaction proceeds *via* a 5-membered stannylene intermediate, which spans the oxygen atoms in the positions 3 and 4 of the galactopyranoside unit, and affords exclusively the 3'-benzyl derivative of LacβOMe, **2/40**, with complete regioselectivity (Fig. 2.16). Accordingly we

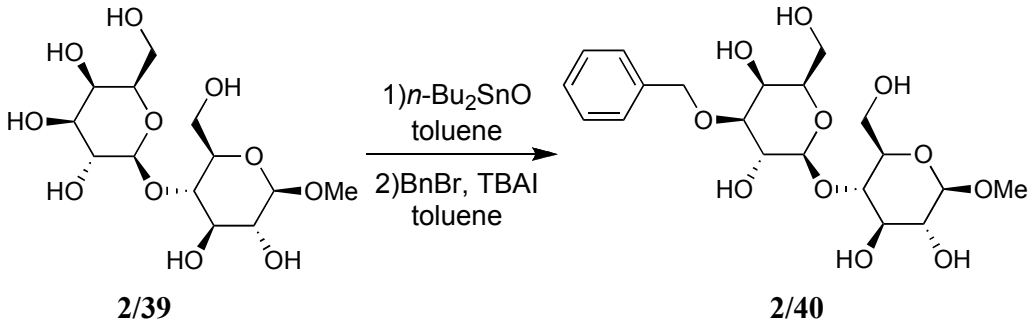

Figure 2.16 Regioselective benzyl protection of the 3'-hydroxy group of the LacβOMe

prepared the β-methyl lactoside (scheme in Fig. 2.17) and tried to react it with 5-chloromethyl salicylaldeyde using the dibutyltin oxide. However the starting material was always recovered unreacted. Since the coupling reaction is reported with benzyl bromide and not chloride we thought that the problem could be the scarce reactivity of the benzyl halide. Thus we synthesized the 5-bromomethyl salicylaldeyde, but we were not able to obtain the coupling product.

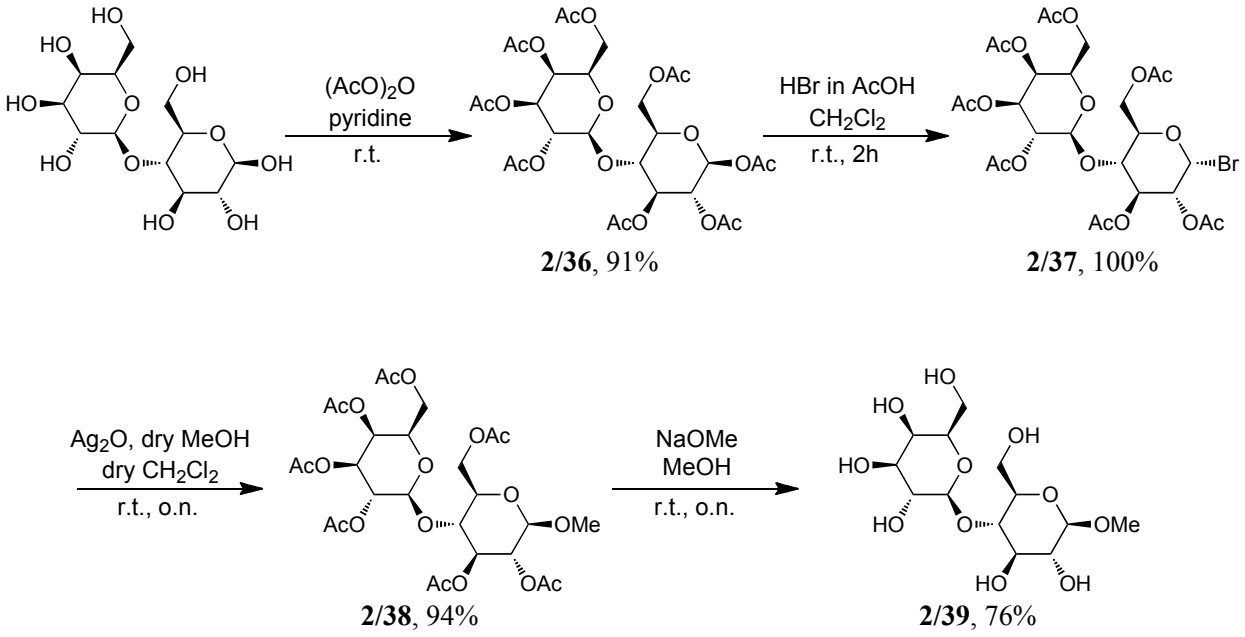

Figure 2.17 Synthetic route to LacβOMe **2/39**.

Due to our limited experience in the field of sugar chemistry, we started a collaboration with Dr. Emiliano Bedini (University of Naples). The proposed synthetic pathway leads to the saccharide-salicylaldehyde derivative in four steps, starting from the per-*O*-acetylated sugars.[47] The reaction exploits the 5-chloromethyl salicylaldeyde S-alkylation of glycosyl isothiouronium salts, readily available from acetylated saccharides through glycosyl iodides (Fig. 2.18).[48] The

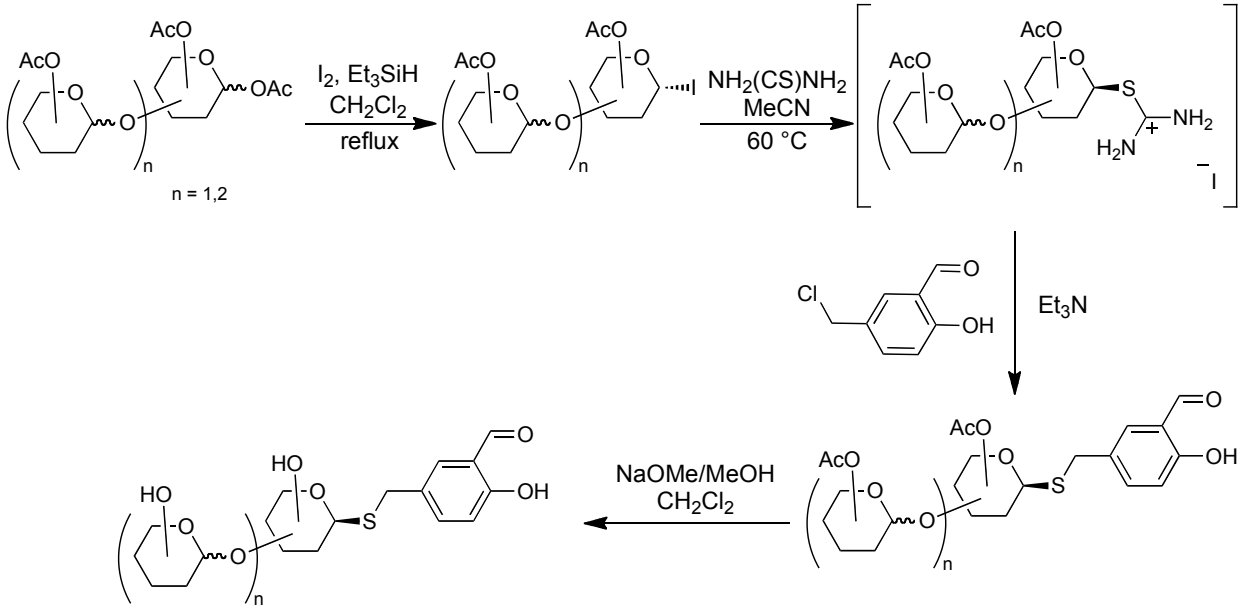

Figure 2.18 General synthetic route to oligosaccharide-salicylaldehyde thioglycolide derivatives.

procedure is highly stereoselectivity[xi], and extremely versatile since α and β as well as 1→4 and 1→6 linkages are all stable to reaction conditions.Therefore this can be a viable approach to guarantee a good solubility in water whatsoever substituents are present on the salicylaldeyde.

To date a series of oligosaccharides have been successfully coupled with the 5-chloromethyl salicylaldeyde, including di- and trisaccharides. With the lactose derived product **2/41** we were able to synthesize the corresponding uranyl-salophen complex **2/42**, using the classic metal template conditions (Fig. 2.19). Although its solubility is still not quite satisfactory, this new approach offers a plethora of options to connect different types of sugar to the salophen

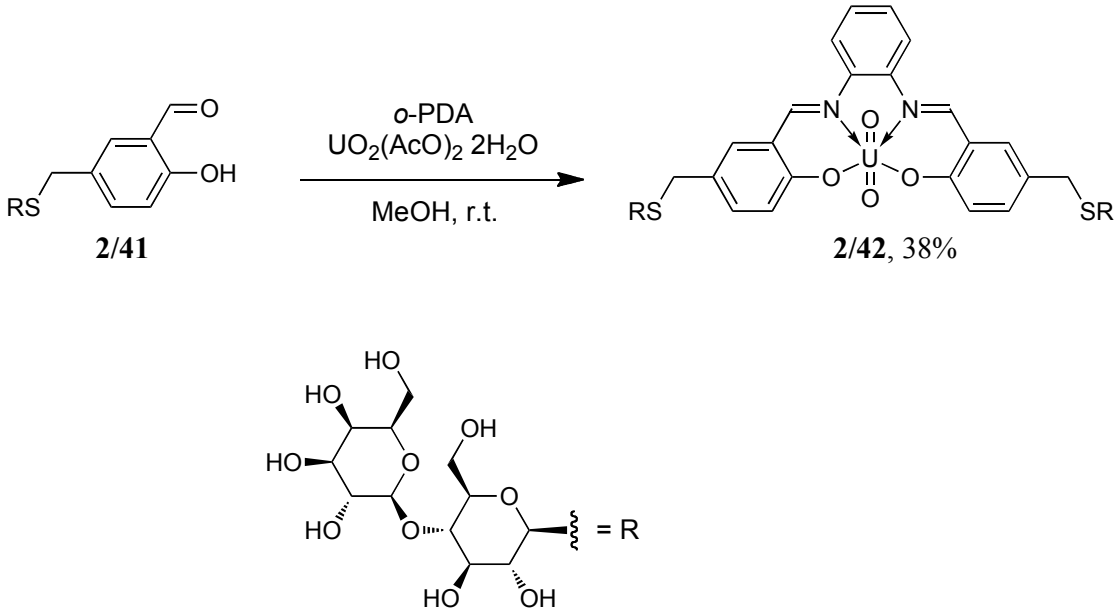

Figure 2.19 Synthesis of the thiolactoside appended complex **2/42**.

skeleton, thus increasing the hydrophilic portion of the ligand. Furthermore saccharide appended small organic compounds may undergo a gelation process in aqueous solutions and are known to be part of the *low-molecular-weight hydrogelators* (LMWHs) pool.[49] As outlined in the previous chapter, gels may act as sensors because the sol-gel transition can be influenced by other non covalent processes which induce or inhibit the gel formation. The versatility of this new synthetic approach will lead to the creation of a library of metal-salophen derivatives with different oligosaccharides appended, whose properties in aqueous solutions can be studied. We consider to investigate their behavior in such media and evaluate their eligibility to form anion-responsive gels.

[xi] The 1,2-*trans* thioglycoside largely predominates, regardless of the sugar nature.

All the synthetic approaches here reported clearly contemplate a step which leads to a highly polar product. This is, of course, a common feature and one of the major drawbacks in the synthesis of water soluble organic compounds. As pointed out by Reinhoudt, Verboom and co-workers, "ideally the water solubility should not be introduced until the last step of the synthesis",[50] since the classic purification methods, such as flash chromatography, cannot be always used.

In order to make the synthesis of water soluble metal salophen-type receptors simpler and much more elegant, we searched an alternative strategy to achieve such receptors. We came up with the idea that the supramolecular inclusion of the adamatane derived compounds into the cavity of the β-cyclodextrin could be suitably employed to bring the complexes in water.

Cyclodextrins **2/43** (Fig. 2.20)[51] are known to form 1:1 inclusion complexes in aqueous solutions, exploiting the hydrophobic interactions between the guest and the lipophilic cavity of the host.[52] In particular the adamantyl moiety (AD) perfectly fits the cavity of the β-cyclodextrin (β-CD) and the strength of such interaction in water typically ranges between 10^3 and 10^5 M^{-1},

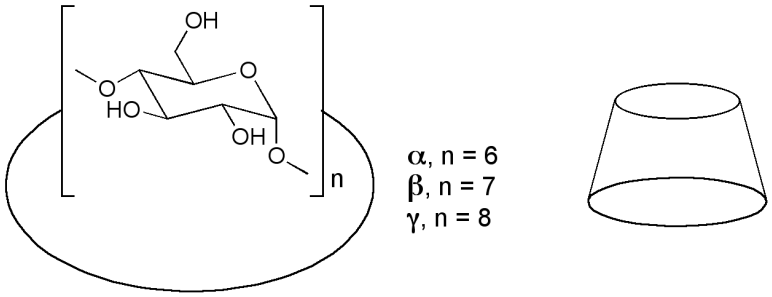

2/43

Figure 2.20 Structure of the naturally occurring cyclodextrins **2/43** (*left*) and their schematic representation as a truncated cone (*right*).

depending on the structure of both the host and the guest (Fig. 2.21).[53] Due to the unique property of enhancing the solubility in water of organic solutes, the non covalent interaction between β-CD and AD has been successfully exploited to achieve solubility of dendrimeric structures,[54] self-assembly of porphyrin nanowires in water,[55] hydrophilic supramolecular co-polymers[56] and to enhance the affinity of single-walled carbon nanotube (SWCNT) based biosensors, as a better alternative to the avidin-biotin interaction.[57]

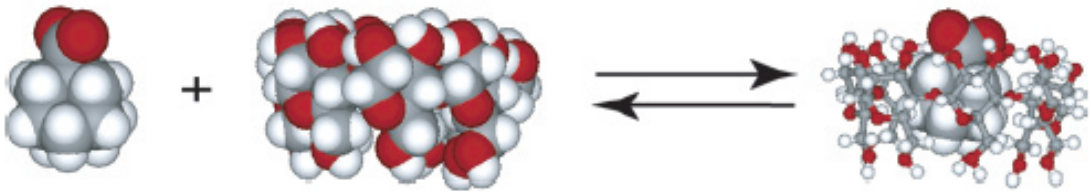

Figure 2.21 Schematic representation of the complexation equilibrium between adamantane carboxylate and β-cyclodextrin showing the close fit of AD to the β-CD cavity.

Accordingly we synthesized the aldehyde **2/46**, endowed with an adamantyl group directly linked to the aromatic ring. The synthetic route to complex **2/47** is reported in Fig. 2.22 and contemplates the electrophilic aromatic substitution of the adamantyl carbocation on the phenol, followed by the introduction of the formyl group and the condensation with 1,2-diaminobenzene in the classic conditions described above for the other uranyl-salophen derivatives.

We isolated the complex **2/47** and we are currently studying its behavior in aqueous solutions of β-CD to find the best solubility conditions. The UV-vis light absorption and the two-dimensional ROESY characterization of the **2/47**-β-CD aggregate will be carried out soon.

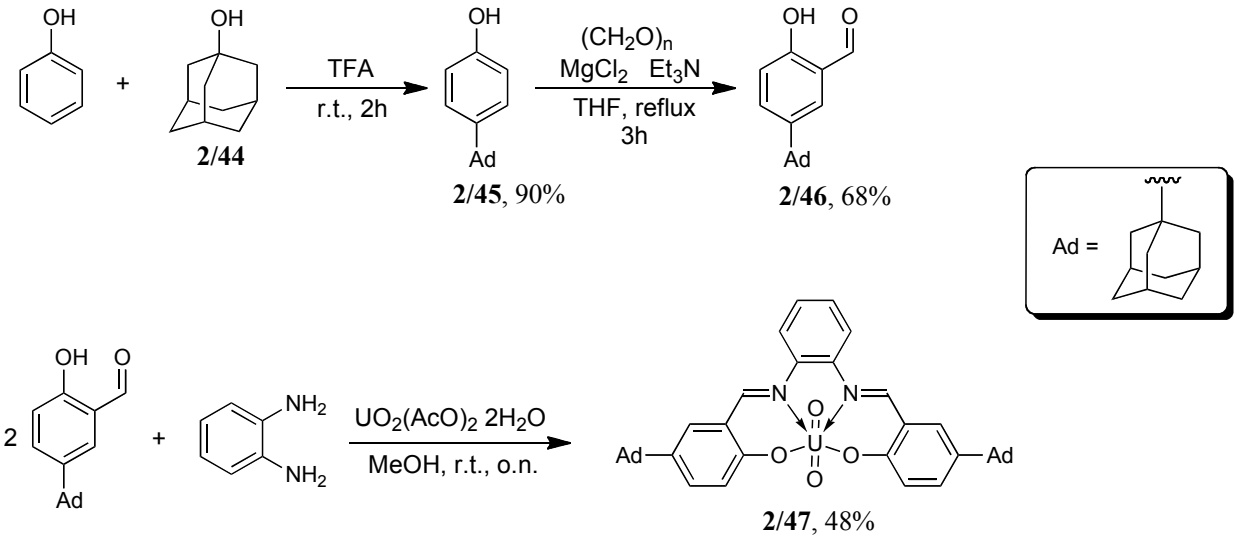

Figure 2.22 Synthetic route to adamantyl decorated complex **2/47**.

2.5 Conclusions and future perspectives.

In this chapter the synthesis of the water soluble uranyl-salophen complex **2/23** has been described. At the moment the quite low solubility of **2/23** is the aspect we are mostly focused on. Among all the attempts made so far to overcome this limit, the conjugation between the glycosyl isothiouronium salts and the 5-chloromethyl salicylaldehyde seems to be the only viable solution. As mentioned, we are currently working on the synthesis of several oligosaccharide appended salophen ligands since the presence of the sugar moieties may have more interesting implications than the mere increase of the metal complex solubility.

Furthermore a novel approach to make metal-salophen complexes soluble in water, based on the inclusion into cyclodextrins of the adamantyl moieties present on the receptor, is here reported. The absence of highly polar groups on the ligand skeleton represents the major synthetic advantage of this strategy.

2.6 Experimental section.

5-chloromethyl-2-hydroxybenzaldehyde (2/19).[58]

2-hydroxybenzaldehyde (5 ml, 47.7 mmol) and formaldehyde 37% solution in water (3.6 ml, 48.3 mmol) were mixed in concentrated hydrogen chloride (48 ml) and the mixture was stirred overnight at room temperature. The white solid formed was filter off, washed with water and redissolved in diethyl ether. The organic solution was dried over anhydrous sodium sulphate and the solvent removed under vacuum to afford a pinkish solid. After recrystallization from *n*-hexane, the product was isolated as white solid (5.661 g, yield = 48%).

^{1}H NMR (200 MHz, $CDCl_3$) δ (ppm) = 11.05 (s, 1H), 9.88 (s, 1H), 7.58-7.52 (m, 2H), 6.98 (d, 1H, *J* = 8.46 Hz), 4.58 (s, 2H).

1,2:5,6-Di-*O*-isopropylidene-3-O-(3-formyl-4-hydroxybenzyl)-α-D-glucofuranose (2/21).[28]

Sodium hydride 60% dispersion in mineral oil (1.0 g, 25 mmol) was placed under argon atmosphere in a dry flask, washed three times with *n*-hexane, and suspended in anhydrous THF (10 ml). At 0 °C, a solution of 1,2:5,6-di-*O*-isopropylidene-α-D-glucofuranose **2/20** (0.802 g, 3.08 mmol) in anhydrous THF (5 ml) was slowly added. After the evolution of hydrogen had ceased, the resulting solution was stirred for 20 min at room temperature. A solution of 5-

chloromethyl-2-hydroxybenzaldehyde **2/19** (0.503 g, 2.95 mmol) in anhydrous THF (5 ml) was slowly added, followed by tetrabutylammonium iodide (0.029 g, 0.079 mmol), and the resulting yellow solution was refluxed overnight. After cooling, the mixture was poured onto crushed ice, neutralized with hydrogen chloride and extracted three times with chloroform. The combined organic layers were washed with brine and dried over anhydrous sodium sulphate. Chromatographic treatment of the crude product (silica gel, chloroform:ethyl acetate 95:5) afforded 0.279 g of the product as a colorless oil (yield = 24%).

^{1}H NMR (200 MHz, $CDCl_3$) δ (ppm) = 11.00 (s, 1H), 9.88 (s, 1H), 7.55–7.48 (m, 2H), 6.97 (d, 1H, *J* = 8.54 Hz), 5.89 (d, 1H, *J* = 3.66 Hz), 4.70–4.55 (m, 3H), 4.41–4.29 (m, 1H), 4.15–3.96 (m, 4H), 1.49 (s, 3H), 1.41 (s, 3H), 1.36 (s, 3H), 1.31 (s, 3H). **^{13}C NMR** (50 MHz, $CDCl_3$) δ (ppm) = 5 196.6, 161.5, 136.9, 133.0, 129.4, 120.5, 118.0, 112.1, 109.3, 105.4, 82.8, 81.7, 81.4, 72.5, 71.4, 67.7, 27.0, 26.9, 26.4, 25.7. **ESI-MS**: m/z = 395.1 $[M+H]^+$, 417.4 $[M+Na]^+$.

3-*O*-(3-formyl-4-hydroxybenzyl)-D-glucose (2/22).[28]

1,2:5,6-Di-*O*-isopropylidene-3-*O*-(3-formyl-4-hydroxy-benzyl)-α-D-glucofuranose **2/21** (0.270 g, 0.68 mmol) was dissolved in 9 ml of 4% H_2SO_4 in water/ethanol 1:1 and the solution was stirred overnight at room temperature. The reaction mixture was neutralized with $CaCO_3$ and filtered. The solid was washed with methanol and the hydroalcoholic solution was concentrated under vacuum to obtain a syrupy oil that was dissolved in 4% H_2SO_4 in water (9 ml) and stirred overnight. Neutralization with $CaCO_3$ followed by filtration and solvent removal under vacuum afforded 0.188 g of the desired product, a 1:1 mixture of the α and β anomers, as a colorless syrupy oil (yield = 88%).

^{1}H NMR (200 MHz, methanol-d_4) δ (ppm) = 10.00 (s, 1H), 7.78 (s, 1H), 7.65 (d, 1H, *J* = 8.57 Hz), 6.93 (d, 1H, *J* = 8.53 Hz), 5.13 (d, 0.5H, *J* = 3.73 Hz), 4.53 (d, 0.5H, *J* = 7.20 Hz), 3.91–3.60 (m, 3H), 3.55–3.24 (m, overlapped with isotopic impurity of the solvent). **^{13}C NMR** (50 MHz, methanol-d_4) δ (ppm) = 197.3, 162.2, 138.1, 133.6, 132.2, 132.0, 122.2, 118.0, 98.2, 94.1, 86.2, 83.4, 81.1, 77.9, 76.4, 75.0, 74.8, 73.9, 73.0, 72.9, 71.6, 71.5. **ESI-MS**: m/z = 315.2 $[M+H]^+$, 337.1 $[M+Na]^+$

Complex 2/23.[59]

A solution of 3-*O*-(3-formyl-4-hydroxybenzyl)-D-glucose **2/22** (0.073 g, 0.232 mmol), 1,2-diaminobenzene (0.013 g, 0.117 mmol), and $UO_2(OAc)_2$ 2 H_2O (0.051 g, 0.12 mmol) in MeOH (8 ml) was stirred for 16 h. The complex was precipitated by slow addition of excess diethyl

ether to the reaction mixture. After filtration, compound **2/23** was isolated as a red-orange solid (0.078 g, yield 35%).

^{1}H NMR (300 MHz, methanol-d_4) δ (ppm) = 9.54 (s, 2H), 7.82␣7.52 (m, 2H), 7.07 (d, 2H, J = 8.41 Hz), 5.07 (d, 0.5H, J = 3.73 Hz), 4.46 (d, 0.5H, J = 7.79 Hz), 3.84␣3.59 (m, 6H), 3.47␣3.30 (m, overlapped with the solvent signal). **^{13}C NMR** (75 MHz, methanol-d_4) δ (ppm) = 167.6, 164.6, 145.3, 135.0, 133.6, 127.3, 127.1, 126.9, 122.1, 118.7, 117.9, 95.3, 91.1, 83.1, 80.3, 75.0, 73.5, 72.9, 72.5, 72.3, 71.0, 70.1, 68.7, 68.6, 59.8, 59.7. **HRMS (ESI-TOF)**: m/z calculated for $C_{34}H_{38}N_2O_{16}NaU^+$ 991.2627, found 991.2643. The elemental analysis was not satisfactory even though NMR spectra and HPLC analysis confirmed purity. The formation of stable metal carbides might be the reason for the poor analysis.[28,41]

2,3,4,6-Tetra-*O*-acetyl-α-bromo-D-glucopyranose (2/25).[31]

To neat α-D-glucose pentaacetate (1.242 g, 3.18 mmol) 33% HBr solution in acetic acid was added. The resulting solution was stirred at room temperature. When tlc analysis (cyclohexane:ethyl acetate, 1:1) showed complete conversion of the starting material to one single product (about 3h), the crude reaction was transferred into a separatory funnel and dichloromethane was added. The organic layer was extracted with portions of water, until the acid was washed away, and dried over anhydrous sodium sulfate. Evaporation of the solvent under vacuum afforded 1.127 g of the product as a white solid (Rf = 0.5; yield = 86%).

^{1}H NMR (200 MHz, $CDCl_3$) δ (ppm) = 6.61 (d, 1H, J = 3.98 Hz), 5.61-5.52 (m, 1H), 5.21-5.12 (m, 1H), 4.88-4.81 (m, 1H), 4.36-4.30 (m, 2H), 4.16-4.10 (m, 1H), 2.10-2.04 (m, 12H).

5-azidomethyl-2-hydroxybenzaldehyde (2/27).[60]

5-chloromethyl-2-hydroxybenzaldehyde **2/19** (0.503 g, 2.95 mmol) and sodium azide (0.202 g, 3.11 mmol) were mixed in anhydrous DMF and stirred overnight under argon atmosphere. The solution was diluted with ethyl acetate (20 ml) and washed several times with water. The organic layer was dried over anhydrous sodium sulfate and the solvent removed under vacuum to afford 0.446 g of the product as an orangish oil (yield = 85 %).

^{1}H NMR (200 MHz, $CDCl_3$) δ (ppm) = 11.08 (s, 1H), 9.91 (s, 1H), 7.60-7.54 (m, 2H), 6.99 (d, 1H, J = 8.46 Hz), 2.67 (s, 2H). **GC-MS (+)**: m/z = 177 $[M]^+$, 100%

1,2:5,6-Di-*O*-isopropylidene-3-*O*-propynyl-α-D-glucofuranose (2/29).

Propargyl bromide 80% wt in toluene (1 ml, 11.2 mmol) and 1,2:5,6-di-*O*-isopropylidene-a-D-glucofuranose **2/20** (2.115 g, 8.13 mmol) were combined in dichloromethane (20 ml). A 50% wt NaOH solution in water (10 ml) was added, followed by tetrabutylammonium iodide (1.556 g, 4.21 mmol), and mixture was vigorously stirred for 3 days. The mixture was transferred in a separatory funnel and the aqueous layer was exctracted with CH_2Cl_2. The combined organic portions were dried over anhydrous sodium sulfate and the solvent was removed under vacuum. After chromatographic treatment of the crude reaction (silica gel; ethyl acetate:*n*-hexane, 8:2) the product was recovered as a colorless oil (2.323 g, yield = 96%).

^{1}H NMR (300 MHz, $CDCl_3$) δ (ppm) = 5.95 (d, 1H, *J* = 3.60 Hz), 4.70-4.68 (m, 1H), 4.35-4.30 (m, 3H), 4.22-4.03 (m, 4H), 2.54 (t, 1H, *J* = 2.40 Hz) 1.56 (s, 3H), 1.49 (s, 3H), 1.41 (s, 3H), 1.38 (s, 3H). **GC-MS (+)**: m/z = 283 $[M - CH_3\cdot]^+$, 100%

1,2:5,6-Di-*O*-isopropylidene-3-*O*-[4-(3-formyl-4hydroxybenzyl)-triazol-1-yl]methyl-α-D-glucofuranose (2/30).

5-azidomethyl-2-hydroxybenzaldehyde **2/27** (0.446 g, 2.52 mmol), 1,2:5,6-Di-*O*-isopropylidene-3-*O*-propargyl-α-D-glucofuranose **2/29** (0.835 g, 2.80 mmol), ascorbic acid (0.218 g, 1.24 mmol) and copper(II) sulfate (0.085 g, 0.53 mmol) were combined in ethanol/ water, 1:1 (170 ml). The solution was stirred at 50 °C for 3h and then allowed to cool down to room temperature. The greenish-yellow solution was extracted three times with dichloromethane. The combined organic layers were washed with brine, dried over anhydrous sodium sulfate and the solvent was removed under vacuum. Chromatographic treatment of the crude reaction (silica gel; ethyl acetate:chloroform, 1:1) afforded 0.713 g of the product as a colorless waxy solid (yield = 60 %, non optimized).

^{1}H NMR (300 MHz, $CDCl_3$) δ (ppm) = 11.06 (s, 1H), 9.87 (s, 1H), 7.56-7.44 (m, 3H), 7.03-7.00 (m, 1H), 5.85 (d, 1H, *J* = 3.60 Hz), 5.50 (s, 2H), 4.80-4.78 (m, 2H), 4.59-4.57 (m, 1H), 4.26-3.97 (m, 5H), 1.48 (s, 3H), 1.37 (s, 3H), 1.30 (s, 6H).

3-*O*-[4-(3-formyl-4hydroxybenzyl)-triazol-1-yl]methyl-D-glucopyranose (2/31).

1,2:5,6-Di-*O*-isopropylidene-3-*O*-[4-(3-formyl-4hydroxybenzyl)-triazol-1-yl]methyl-α-D-glucofuranose **2/30** (0.605 g, 1.27 mmol) was dissolved in 4% H_2SO_4 in water/ethanol 1:1 (20 ml) and the solution was stirred overnight at room temperature. The reaction mixture was neutralized with $CaCO_3$ and filtered. The solid was washed with methanol and the

hydroalcoholic solution was concentrated under vacuum to obtain a syrupy yellow oil that was dissolved in 4% H_2SO_4 in water (10 ml) and stirred overnight. Neutralization with $CaCO_3$ followed by filtration and solvent removal under vacuum afforded 0.467 g of the desired product as an off-white solid (yield = 93%).

^{1}H NMR (200 MHz, methanol-*d*$_4$) δ (ppm) = 10.00 (s, 1H), 7.94 (s, 1H), 7.67 (d, 1H J_{meta} = 2.08 Hz), 7.50 (dd, 1H, J_{meta} = 2.22 Hz, J_{ortho} = 8.58 Hz), 6.92 (d, 1H, J_{ortho} = 8.58 Hz), 5.53 (s, 2H), 5.04 (d, 0.5H, *J* = 3.56 Hz), 4.44 (s, 0.5H, *J* = 7.4 Hz), 3.82-3.55 (m, 3H), 3.44-3.17 (m, overlapped with the solvent signal). **HRMS (ESI-TOF)**: m/z calculated for $C_{17}H_{21}N_3O_8Na^+$ 418.1196, found 418.1226.

Complex 2/32.

A solution of 3-*O*-[4-(3-formyl-4hydroxybenzyl)-triazol-1-yl]methyl-D-glucopyranose **2/31** (0.154 g, 0.39 mmol), 1,2-diaminobenzene (0.027 g, 0.25 mmol), and $UO_2(OAc)_2$ 2 H_2O (0.087 g, 0.20 mmol) in MeOH (4 ml) was stirred for 2 days. The complex was precipitated by slow addition of excess diethyl ether to the reaction mixture. After filtration, compound **2/32** was isolated as an orange solid (0.164 g, yield 74%).

^{1}H NMR (300 MHz, methanol-*d*$_4$) δ (ppm) = 9.57 (s, 2H), 7.96 (d, 2H, *J* = 3.00 Hz), 7.79-7.56 (m, 8H), 7.13 (d, 2H, *J* = 8.40 Hz), 5.60 (s, 4H), 5.06 (d, 1H, *J* = 3.90 Hz), 4.60 (s, 4H), 4.46 (d, 1H, J = 7.50 Hz), 3.79-3.59 (m, 8H), 3.45-3.27 (m, overlapped with the solvent signal). **^{13}C NMR** (300 MHz, DMSO-*d*$_6$) δ (ppm) = 171.4, 168.3, 148.4, 147.7, 147.5, 138.0, 137.5, 130.8, 125.9, 125.6, 125.0, 122.9, 122.2, 98.6, 94.1, 87.1, 84.1, 78.4, 76.4, 73.9, 73.8, 71.6, 71.5, 67.5, 62.8, 54.1. **HRMS (ESI-TOF)**: m/z calculated for $C_{40}H_{44}N_8O_{16}NaU^+$ 1153.3281, found 1153.3301.

5-bromomethyl-2-hydroxybenzaldehyde.[58]

2-hydroxybenzaldehyde (5 ml, 47.7 mmol) and formaldehyde 37% solution in water (3.6 ml, 48.3 mmol) were stirred overnight in 48% hydrogen bromide in water (48 ml). The off white solid formed was filter off, washed with water and redissolved in diethyl ether. The organic solution was dried over anhydrous sodium sulphate and the solvent removed under vacuum to afford a pinkish solid. After recrystallization from *n*-hexane, the product was isolated as white solid (2.284 g, yield = 22%).

^{1}H NMR (200 MHz, $CDCl_3$) δ (ppm) = 11.07 (s, 1H), 9.89 (s, 1H), 7.60-7.55 (m, 2H), 6.99 (d, 1H, *J* = 8.43 Hz), 4.51 (s, 2H). mp. 97-100 °C.

2,3,4,6-Tetra-*O*-acetyl-β-D-galactopyranosyl-(1→4)-1,2,3,6-tetra-*O*-acetyl-β-D-glucopyranose (2/36).

β-D-Lactose (5.032 g, 14.0 mmol) was suspended in acetic anhydride (16 ml). Dry pyridine (16 ml) was added and the mixture was stirred until the solid was completely dissolved. The reaction flask was cooled down with an ice bath and MeOH (30 ml) was slowly added. The crude reaction was diluted with ethyl acetate (200 ml) and the organic layer was washed twice with 6*N* HCl, once with saturated $NaHCO_3$ and finally with brine. The solution was dried over anhydrous sodium sulfate and the solvent removed under vacuum to afford the product as a white foamy solid (8.61 g, yield = 91%). Tlc analysis (cyclohexane:ethyl acetate, 1:1) revealed a single product with Rf = 0.2.

^{1}H NMR (200 MHz, $CDCl_3$) δ (ppm) = 6.26 (d, 1H, *J* = 3.62 Hz), 5.70-4.93 (m, 5H), 4.51-4.43 (m, 2H), 4.16-3.77 (m, 6H), 2.19-1.97 (m, 24H).

2,3,4,6-tetra-*O*-acetyl-β-D-galactopyranosyl-(1→4)-2,3,6-tri-*O*-acetyl-α-D-glucopyranosyl bromide (2/37).

Lactose octaacetate **2/36** (2.5 g, 3.68 mmol) was dissolved in dichloromethane (60 ml). The flask was cooled in an ice bath and 33% HBr in acetic acid (25 ml) was slowly added. The solution was stirred at room temperature until tlc (cyclohexane:ethyl acetate, 1:1) showed complete conversion of the starting material into a single product with Rf = 0.5 (2h). Ice-cold water was added to the flask and the aqueous layer was extracted three times with dichloromethane. The combined organic fractions were dried over anhydrous sodium sulfate and the solvent was removed under vacuum. The product was quantitatively recovered as a yellowish waxy solid.

^{1}H NMR (200 MHz, $CDCl_3$) δ (ppm) = 6.72-6.61 (m, 1H), 5.57-4.11 (m, 13H), 2.16-2.02 (m, 21H).

2,3,4,6-tetra-*O*-acetyl-β-D-galactopyranosyl-(1→4)-2,3,6-tri-*O*-acetyl-1-methyl-α-D-glucopyranoside (2/38).

Bromide **2/37** (2.57 g, 3.67 mmol) and silver(I)oxide (0.95 g, 4.10 mmol) were placed in a flask and dried under vacuum and anhydrous methanol (25 ml) was added in argon atmosphere. After adding CH_2Cl_2 (20 ml), the suspension was stirred overnight at room temperature. The tlc (cyclohexane:ethyl acetate, 1:1) shows that a single product is present (Rf = 0.3). The solid was filtered off using a celite pad and the solvent was removed under vacuum to afford 2.24 g of the product as a colorless waxy solid (yield = 94%).

^{1}H NMR (200 MHz, $CDCl_3$) δ (ppm) = 5.35-4.84 (m, 5H), 4.52-4.36 (m, 3H), 4.14-4.07 (m, 3H), 3.90-3.47 (m, 6H), 2.15-1.96 (m, 21H).

Methyl β-D-galactopyranosyl-(1→4)-β-D-glucopyranoside (2/39, LacβOMe).[61]

The acetylated LacβOMe **2/38** (2.20 g, 3.38 mmol) was dissolved in methanol (25 ml). Sodium methoxide 30% wt in methanol (20 µl) was added and the solution was stirred overnight at room temperature. The precipitate was filtered and recovered as a white solid (0.915 g, yield = 76%).
^{1}H NMR (300 MHz, D_2O) δ (ppm) = 4.31-4.24 (m, 2H), 3.87-3.77 (m, 2H), 3.67-3.42 (m, 12H), 3.18-3.13 (m, 1H). **^{13}C NMR** (300 MHz, D_2O) δ (ppm) =104.4, 104.2, 79.6, 76.7, 76.1, 75.7, 74.1, 73.8, 72.3, 69.8, 62.3, 61.3, 58.5. **ESI-MS**: m/z = 379.14 $[M+Na]^+$.

Complex 2/42.

A solution of **2/41** (70 mg, $1.42\cdot10^{-4}$ mol), 1,2-diaminobenzene (7.7 mg, $7.12\cdot10^{-5}$ mol), and $UO_2(OAc)_2$ 2 H_2O (30.3 mg, $7.14\cdot10^{-5}$ mol) in MeOH (13 ml) was stirred until tlc (ethyl acetate:methanol, 8:2) showed almost complete conversion of the starting materials. The product was precipitated by slow addition of excess diethyl ether to the reaction mixture. After filtration, compound **2/42** was isolated as an pale orange solid (71 mg, yield 38%).
^{1}H NMR (300 MHz, DMSO-*d_6*) δ (ppm) = 9.55 (s, 2H), 7.76-7.72 (m, 4H), 7.59-7.52 (m, 4H), 6.93 (d, 2H, *J* = 8.40 Hz), 5.25 (d, 2H, *J* = 6.00 Hz), 5.06 (s, 2H), 4.74 (s, 2H), 4.71 (s, 4H), 4.61-4.59 (m, 2H), 4.47 (d, 2H, *J* = 4.50 Hz), 4.21-4.17 (m, 4H), 3.97-3.79 (m, 6H), 3.59-3.09 (m, overlapped with the solvent signal). **^{13}C NMR** (300 MHz, DMSO-*d_6*) δ (ppm) = 170.8, 168.3, 148.6, 139.1, 137.6, 130.7, 127.9, 125.5, 122.6, 122.2, 105.8, 84.9, 82.7, 81.0, 78.3, 77.3, 75.1, 74.8, 72.4, 70.0, 66.7, 62.6, 33.7. **HRMS (ESI-TOF)**: m/z calculated for $C_{46}H_{58}N_2O_{24}NaS_2U^+$ 1347.3227, found 1347.3264.

4-(1-adamantyl)-phenol (2/45).[62]

Phenol (1.0 g, 10.7 mmol) was dissolved in trifluoroacetic acid and 1-adamantanol **2/44** (1.62 g, 10.7 mmol) was added. A solid immediately started to form and the reaction was further stirred for 2 h. Water (20 ml) was added and the solid was filtered and washed with several portions of water. Recrystallization from ethyl alcohol afforded 2.17 g of the product as white crystals (yield = 90%).
^{1}H NMR (MHz, $CDCl_3$) δ (ppm) = 7.23 (d, 2H, *J* = 8.82 Hz), 6.78 (d, 2H, *J* = 8.79 Hz), 2.12 (s, 3H), 1.87-1.75 (m, 12H). **GC-MS (+)**: m/z = 228 $[M]^+$, 100%. mp. 181-183 °C

2-hydroxy-4-(1-adamantyl)-benzaldehyde (2/46).[63]

In a dry flask, 4-(1-adamantyl)-phenol **2/45** (2.17 g, 9.5 mmol) was dissolved in anhydrous tetrahydrofuran. Anhydrous magnesium chloride (2.04 g, 21.4 mmol) and triethylamine (3.0 ml, 21.6 mmol) were added and the mixture was stirred at room temperature for 20 minutes, after which time paraformaldehyde (1.65 g, 55 mmol) was added and the suspension was refluxed for 3h. After cooling down to room temperature, the bright yellow crude reaction was diluted with ethyl acetate and extracted three times with 1*N* HCl and washed twice with brine. The organic portion was dried over anhydrous sodium sulfate and the solvent removed under vacuum to give a pale yellow solid. Chromatographic treatment of the crude reaction (silica gel; *n*-hexane:ethyl acetate, 99:1) afforded 1.65 g of the product as a white solid (yield = 68%).

^{1}H NMR (200 MHz, $CDCl_3$) δ (ppm) = 10.86 (s, 1H), 9.89 (s, 1H), 7.60-7.48 (m, 2H), 6.95 (d, 1H, *J* = 8.72), 2.12 (s, 3H), 1.90-1.54 (m, 12H). **GC-MS (+)**: m/z = 256 $[M]^+$, 100%

Complex 2/47.

Aldehyde **2/46** (0.100 g, 0.39 mmol), 1,2-diaminobenzene (0.021 g, 0.19 mmol) and $UO_2(OAc)_2$ $2H_2O$ (0.099 g, 0.23 mmol) were dissolved in a mixture of methanol (2 ml) and chloroform (2 ml) and the solution was stirred overnight at room temperature. The crude reaction was concentrated under vacuum and dichloromethane was added. The organic layer was extracted three times with water, then dried over anhydrous sodium sulfate and the solvent was removed under reduced pressure. 78 mg of complex **2/47** were recovered as an orange solid (yield = 48%).

^{1}H NMR (300 MHz, DMSO-d_6) δ (ppm) = 9.59 (s, 2H), 7.71-7.48 (m, 8H), 6.87 (d, 2H, *J* = 8.70 Hz), 2.02-1.69 (m, 30H). **^{13}C NMR** (300 MHz, DMSO-d_6) δ (ppm) = 168.1, 167.2, 147.0, 139.4, 133.3, 131.8, 128.7, 123.6, 120.4, 120.3, 43.1, 36.4, 35.0, 28.6. **ESI-MS**: m/z = 875.4 $[M+Na]^+$. Elemental Analysis calculated for $C_{42}H_{50}N_2O_6U$ (**2/47** · 2MeOH): C = 55.02%; H = 5.50%; N = 3.06%, found: C = 54.97%; H = 5.70%; N = 2.87%. HPLC trace show a single peak (C_{18} column, MeOH, 0.2 ml/min).

2.7 References.

[1] V. Vallet, B. Schimmelpfennig, L. Maron, Ch. Teichteil, T. Leininger, O. Gropen, I. Grenthe, U. Wahlgren, *Chem. Phys.*, **1999**, *244*, 185-194.

[2] P. A. Vigato, S. Tamburini, *Coord. Chem. Rev.*, **2004**, *248*, 1717-2128.

[3] J. L. Sessler, P. J. Melfi, G. Dan Patos, *Coord. Chem. Rev.*, **2006**, *250*, 816-843.

[4] G. Bandoli, D. A. Clemente, U. Croatto, M. Vidali, P. A. Vigato, *J. Chem. Soc. D*, **1971**, 1330-1331.

[5] R. G. Pearson, *J. Am. Chem. Soc.*, **1963**, *85*, 3533-3539.

[6] A. Dalla Cort, L. Mandolini, C. Pasquini, L. Schiaffino, *New J. Chem.*, **2004**, *28*, 1198-1199.

[7] A. Ciogli, A. Dalla Cort, F. Gasparrini, L. Lunazzi, L. Mandolini, A. Mazzanti, C. Pasquini, M. Pierini, L. Schiaffino, F. Yafteh Mihan, *J. Org. Chem.*, **2008**, *73*, 6108-6118.

[8] V. van Axel Castelli, A. Dalla Cort, L. Mandolini, D. N. Reinhoudt, *J. Am. Chem. Soc.*, **1998**, *120*, 12688-12689.

[9] L. A. J. Chrisstoffels, F. de Jong, D.N. Reinhoudt, *Chem. Eur. J.*, **2000**, *6*, 1376-1385.

[10] A. R. van Doorn; R. Schaafstra, M. Bos, S. Harkema, J. van Eerden, W. Verboom, D.N. Reinhoudt, *J. Org. Chem.*, **1991**, *56*, 6083-6093.

[11] C. J. van Staveren, D. E. Fenton, D. N. Reinhoudt, J. van Eerden, S. Harkemal, *J. Am. Chem. Soc.*, **1987**, *109*, 3456-3458.

[12] A. Dalla Cort, L. Mandolini,L. Schiaffino, *Chem. Commun*. **2005**, 3867-3869.

[13] V. van Axel Castelli, A. Dalla Cort, L. Mandolini, D.N. Reinhoudt, L. Schiaffino, *Eur. J. Org. Chem.,* **2003**, 627-633.

[14] V. van Axel Castelli, R. Cacciapaglia, G. Chiosis, F. C. J. M. van Veggel, L. Mandolini, D. N. Reinhoudt, *Inorg. Chim. Acta*, **1996**, *246*, 181-193.

[15] D. M. Rudkevich, W. P. R. V. Stauthamer, W. Verboom, J. F. J. Engbersen, S. Harkema, D. N. Reinhoudt, *J. Am. Chem. Soc.*, *1992*, *114*, 9671-9673.

[16] D. M. Rudkevich, W. Verboom, Z. Brzozka, M. J. Palys, W. P. R. V. Stauthamer, G. J. van Humme, S. M. Franken, S. Harkema, J. F. J. Engbersen, D. N. Reinhoudt, *J. Am. Chem. Soc.*, **1994**, *116*, 4341-4351.

[17] M. Cametti, A. Dalla Cort, L. Mandolini, M. Nissinen, K. Rissanen, *New J. Chem.*, **2008**, *32*, 1113-1116.

[18] M.-L. Lehaire, R. Scopelliti, H. Piotrowski, K. Severin, *Angew. Chem. Int. Ed.*, **2002**, *41*, 1419-1422.

[19] J. M. Mahoney, A. M. Beatty, B. D. Smith, *J. Am. Chem. Soc.*, **2001**, *123*, 5847-5848.

[20] M. Cametti, M. Nissinen, A. Dalla Cort, L. Mandolini, K. Rissanen, *J. Am. Chem. Soc.*, **2005**, *127*, 3831-3837.

[21] (a) M. Cametti, M. Nissinen, A. Dalla Cort, L. Mandolini, K. Rissanen, *Chem. Commun.*, **2003**, 2420-2421. (b) M. Cametti, M. Nissinen, A. Dalla Cort, L. Mandolini, K. Rissanen, *J. Am. Chem. Soc.*, **2007**, *129*, 3641-3648.

[22] (a) W. Wróblewski, Z. Brzózka, D. M. Rudkevich, D. N. Reinhoudt, *Sens. Actuators, B*, **1996**, *37*, 151-155. (b) M. M. G. Antonisse, D. N. Reinhoudt, *Chem. Commun.*,**1998**, 443-448.

[23] M. M. G. Antonisse, B. H. M. Snellink-Rüel, I. Yigit, J. F. J. Engbersen, D. N. Reinhoudt, *J. Org. Chem.*, **1997**, *62*, 9034-9038.

[24] C. Jimenez-Jorquera, J. Orozco, A. Baldi, *Sensors*, **2010**, *10*, 61-83.

[25] W. Wróblewski, K. Wociechowski, A. Dybko, Z. Brzózka, R. J. M. Egberink, B. H. M. Snellink-Rüel, D. N. Reinhoudt, *Anal. Chim. Acta*, **2001**, *432*, 79-88.

[26] A. C. Ion, I. Ion, M. M. G. Antonisse, B. H. M. Snellink-Rüel, D. N. Reinhoudt, *Russ. J. Gen. Chem.*, **2001**, *71*, 181-184.

[27] M. Cametti, A. Dalla Cort, K. Bartik, *ChemPhysChem*, **2008**, *9*, 2168-2171.

[28] A. Dalla Cort, P. De Bernardin, L. Schiaffino, *Chirality*, **2009**, *21*, 104-109.

[29] K. Omura, *J. Org. Chem.*, **1992**, *57*, 306-312.

[30] A. M. Bernard, M. R. Ghiani, P. P. Piras, A. Rivoldini, *Synthesis*, **1984**, 287-289.

[31] B. Arezzini, M. Ferrali, E. Ferrari, C. Frassineti, S. Lazzari, G. Marverti, F. Spagnolo, M. Saladini, *Eur. J. Med. Chem.*, **2008**, *43*, 2549-2556.

[32] F. Amblard, J. H. Cho, R. F. Schinazi, *Chem. Rev.*, **2009**, *109*, 4207-4220.

[33] T. Ami, K. Fujimoto, *ChemBioChem*, **2008**, *9*, 2071-2074.

[34] (a) D. I. Rozkiewicz, D. Jańczewski, W. Verboom, B. J. Ravoo, Dr. D. N. Reinhoudt; *Angew. Chem. Int. Ed.*, **2006**, *45*, 5292-5296. (b) N. Balachander, C. N. Sukenik, *Langmuir*, **1990**, *6*, 1621-1627.

[35] (a) H. C. Kolb, M. G. Finn and K. B. Sharpless, *Angew. Chem. Int. Ed.,* **2001**, 40, 2004-2021. (b) John E. Moses and Adam D. Moorhouse; *Chem. Soc. Rev.*, **2007**, 36, 1249-1262.

[36] (a) K. B. Sharpless, R. Manetsch, *Expert Opin. Drug Disc.,* **2006**, *1*, 525-538. (b) C. W. Tornøe, C. Christensen, M. Meldal, *J. Org. Chem*., **2002**, 67, 3057-3064. (c) V. V. Rostovtsev, L. G. Green, V. V. Fokin, K. B. Sharpless, *Angew. Chem. Int. Ed*., **2002**, 41, 2596-2599.

[37] R. J. Kaufman, R. S. Sidhu, *J. Org. Chem.*, **1982**, *47*, 4941-4947.

[38] for a recent review on the topic, see A. Chanda, V. V. Fokin, *Chem. Rev.*, **2009**, *109*, 725-748 and the references cited therein.

[39] D. C. Rideout, R. Breslow, *J. Am. Chem. Soc.*, **1980**, *102*, 7817-7818.

[40] Y. Jung, R. A. Marcus, *J. Am. Chem. Soc.*, **2007**, *129*, 5492-5502.

[41] J. K.-H. Hui, Z. Yu, M. J. MacLachlan, *Angew. Chem.*, **2007**, *119*, 8126-8129.

[42] I. Erlund, *Nutrition Research*, **2004**, *24*, 851-874.

[43] K. C. Nicolaou, H. J. Mitchell, *Angew. Chem. Int. Ed.*, **2001**, *40*, 1576-1624.

[44] J. Alais, A. Maranduba, A. Veyrieres, *Tetrahedron Lett.*, **1983**, *24*, 2383-2386.

[45] (a) Y. Tsuda, M. Nishimura, T. Kobayashi, Y. Sato, K. Kanemitsu, *Chem. Pharm. Bull.*, **1991**, *39*, 2883-2887. (b) S. David, S. Hanessian, Tetrahedron, 1985, 41, 643-663.

[46] M. A. Nashed, L. Anderson, *Tetrahedron Lett.*, **1976**, *39*, 3503-3506.

[47] E. Bedini, G. Forte, I. Carvalho, M. Parrilli, A. Dalla Cort, *Carbohydrate Chemistry: Proven Synthetic Methods*, 2nd volume, CRC press, accepted.

[48] S. Valerio, A. Iadonisi, M. Adinolfi, A. Ravidà, *J. Org. Chem.*, **2007**, *72*, 6097-6106.

[49] L. A. Estroff, A. D. Hamilton, *Chem. Rev.*, **2004**, *104*, 1201-1217.

[50] K. J. C. van Bommel, G. A. Metselaar, W. Verboom, D. N. Reinhoudt, *J. Org. Chem.*, **2001**, *66*, 5405-5412.

[51] W. Saenger, J. Jacob, K. Gessler, T. Steiner, D. Hoffmann, H. Sanbe, K. Koizumi, S. M. Smith, T. Takaha, *Chem. Rev.,* **1998**, *98*, 1787-1802.

[52] A. Harada, *Acc. Chem. Res.*, **2001**, *34*, 456-464.

[53] (a) L. A. Godínez, L. Schwartz, C. M. Criss, A. E. Kaifer, *J. Phys. Chem. B*, **1997**, *101*, 3376-3380. (b) J. Carrazana, A. Jover, F. Meijide, V. H. Soto, J. Vázquez Tato, *J. Phys. Chem. B*, **2005**, *109*, 9719-9726. (c) D. Harries, D. C. Rau, V. A. Parsegian, *J. Am. Chem. Soc.*, **2005**, *127*, 2184-2190.

[54] G. R. Newkome, H. J. Kim, K. H. Choi, C. N. Moorefield, *Macromolecules*, **2004**, *37*, 6268-6274.

[55] M. Fathalla, A. Neuberger, S.-C. Li, R. Schmehl, U. Diebold, J. Jayawickramarajah, *J. Am. Chem. Soc.*, **2010**, *132*, 9966-9967.

[56] (a) V. H. Soto Tellini, A. Jover, J. Carrazana García, L. Galantini, F. Meijide, J. Vázquez Tato, *J. Am. Chem. Soc.*, **2006**, *128*, 5728-5734. (b) L. Galantini, A. Jover, C. Leggio, F. Meijide, N. V. Pavel, V. H. Soto Tellini, J. Vázquez Tato, C. Tortolini, *J. Phys. Chem. B*, **2008**, *112*, 8536-8541.

[57] M. Holzinger, L. Bouffier, R. Villalonga, S. Cosnier, *Biosensors and Bioelectronics*, **2009**, *24*, 1128-1134.

[58] A. Dalla Cort, L. Mandolini, C. Pasquini, L. Schiaffino, *Org. Biomol. Chem.*, **2006**, *4*, 4543-4546.

[59] A. Dalla Cort, G. Forte, L. Schiaffino, *J. Org. Chem.*, **2011**, *76*, 7569-7572.

[60] V. Ayala, A. Corma, M. Iglesias, J. A. Rincón, F. Sánchez, *J. Catal.*, **2004**, *224*, 170-177.

[61] F. Smith, J. W. Van Cleve, *J. Am. Chem. Soc.*, **1952**, *74*, 1912-1913.

[62] A. V. Stepakov, A. P. Molchanov, R. R. Kostikov, *Russ. J. Org. Chem.*, **2007**, *43*, 538-543.

[63] R. L. Mackman et al., *J. Med. Chem.*, **2001**, *44*, 2753-2771.

CHAPTER 3.

Anion binding properties of the water-soluble uranyl salophen derivative.

This chapter concerns the spectrophotometric investigation of the binding properties of compound 3/1, whose synthesis was described in the chapter 2. The main features of the UV-Vis spectroscopy, in the survey of the supramolecular association processes, are presented in the first paragraph. The major issues that have been addressed during the present study are also discussed. The second part deals with the optical properties of 3/1. The values of the binding constants with a series of inorganic anions, obtained from UV-Vis titration experiments in water, are reported together with considerations concerning the affinity pattern displayed by the receptor. Particular attention is directed to the binding with fluoride, cyanide and phosphate, and to the study of the affinity towards biologically relevant phosphates under physiological pH conditions.

3.1 The spectrophotometric study of the binding constants.

As mentioned in the previous chapter, the uranyl-salophen complex **3/1** displays a fair solubility in water, which allows to prepare solutions in the 10^{-5} M concentration range. This actually represents the major drawback in the study of its properties in solution since most of the techniques generally employed to this purpose require a higher host concentration and, therefore, are precluded to be used in this case. Accordingly we report here the investigation of the binding properties towards anionic species in aqueous solutions based exclusively on UV-Vis titration experiments.

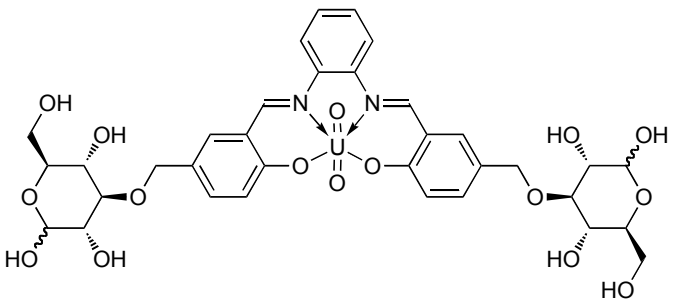

3/1

Along with NMR, UV-Vis spectroscopy is the most commonly employed technique for the study of binding phenomena in supramolecular systems.[1] With respect to the former, the choice of a proper chromophore in the UV-Vis light absorption experiments allows lower host concentrations to be applied and hence higher values of the binding constants can be determined. In a spectrophotometric titration experiment, the changes in the host absorption spectrum upon complexation are related to increasing concentration of the guest species, in a region where its absorption is negligible. Considering a 1:1 binding phenomenon taking place throughout the whole course of the titration experiment, the trend of the host absorbance variations depends on the equilibrium constant of the association process, at a certain temperature, according to the *binding isotherm equation* (**1**).

$$\Delta A_0 = \frac{\Delta A_\infty K[G]}{1 + K[G]} \qquad \textbf{(1)}$$

In the above reported equation, ΔA_0 is the difference between the absorbance of the system during the titration experiment and the initial absorbance of the host ($\Delta A_0 = A - A_0$), while ΔA_∞ is the difference between the absorbance of the saturated system[xii] and the initial absorbance of the host ($\Delta A_\infty = A_\infty - A_0$). The equation states that, in each point of the titration, the observed absorbance change from the initial one, is a fraction of the maximum one that depends on the association constant value, K, and on the concentration of the guest at the equilibrium, [G]. Clearly, increasing the concentration of the guest, the value of ΔA_0 will approximate that of ΔA_∞. Experimentally, the value of the binding constant can be obtained by fitting the trend of the experimental points in the A versus [G] plot with equations like 1. However, since the value of [G] is unknown, the total (analytical) guest concentration values can be used as initial parameters in the equation 1 and the binding constant value can be calculated with an iterative procedure. Otherwise equations that take into account the analytical concentrations of guest can be employed (see equation 2 below).[2]

In practical experiments, the initial concentration of the host $[H]_0$ depends on the absorption properties of the compound and should be chosen in order to have absorbance values within the 0-1 range. On the other hand, the explored guest concentration range should be varied

[xii] In theory at infinite guest concentration.

according to the estimated binding constant in such a way to collect as many experimental points as possible in the non-linear part of the binding isotherm hyperbola, which is the region where the probability of binding (p)[3] ranges between 0.2 and 0.8.[4] Where p is defined as follows:

$$p = \frac{[HG]}{[G]_0} \qquad [H]_0 \geq [G]_0$$

$$p = \frac{[HG]}{[H]_0} \qquad [H]_0 < [G]_0$$

Being the shape of the curve dependent on K and $[H]_0$ values, the proper guest concentration range should be adjusted in subsequent experiments with a trial-and-error type approach, starting from an estimated value for the binding constant. Two special cases deserve to be mentioned in this context. If the value of K is fairly low, with $[H]_0K < 10^{-2}$, different values of the initial host concentration do not affect the shape of the binding isotherm to an appreciable extend and thus reliable constant values can be obtained even with a poor accuracy on $[H]_0$. Instead, if the value of the binding constant is significantly high, with $[H]_0K > 100$, the non-linear portion of the isotherm is restricted to a small region around one equivalent of guest added and the curves generated by different K_{ass} values will be very close to each other. Thus the error on the binding constant value turns to be significantly high and, in this case, only a crude estimation of the lower limit for the K_{ass} value can be obtained.[5]

To perform the spectrophotometric titrations reported below in this chapter, the solutions of the host were filtered prior to carry on any experiment, in order to get rid of the light scattering phenomenon observable in the absorption spectrum of unfiltered solutions of **3**/**1**. Accordingly, the initial concentration of the host is less than the calculated one and therefore we were unable to determine the molar absorption coefficient for the receptor or the stoichiometry of the complexes with anions using the Job's method. As far as the values of the binding constants are concerned, those in the 10^2 M^{-1} range fall into the $[H]_0K_{ass} < 10^{-2}$ case and hence are reliable despite the uncertainty on $[H]_0$. On the contrary, the high binding constant values are only estimated to be greater than 10^4 M^{-1}, which is an acceptable lower limit under these conditions (see below).

3.2 Optical properties of 3/1 and the study of the association with anions.[xiii]

The UV-Vis absorption spectrum of compound **3/1** in water is reported in figure 3.1a and exhibits the same fine structure generally featured by analogous, non water soluble, uranyl-salophen complexes (Fig. 3.1b). In the region 280-550 nm, a monotonic increase in light absorption on lowering the wavelength and a shoulder around 350 nm are observed. Significant

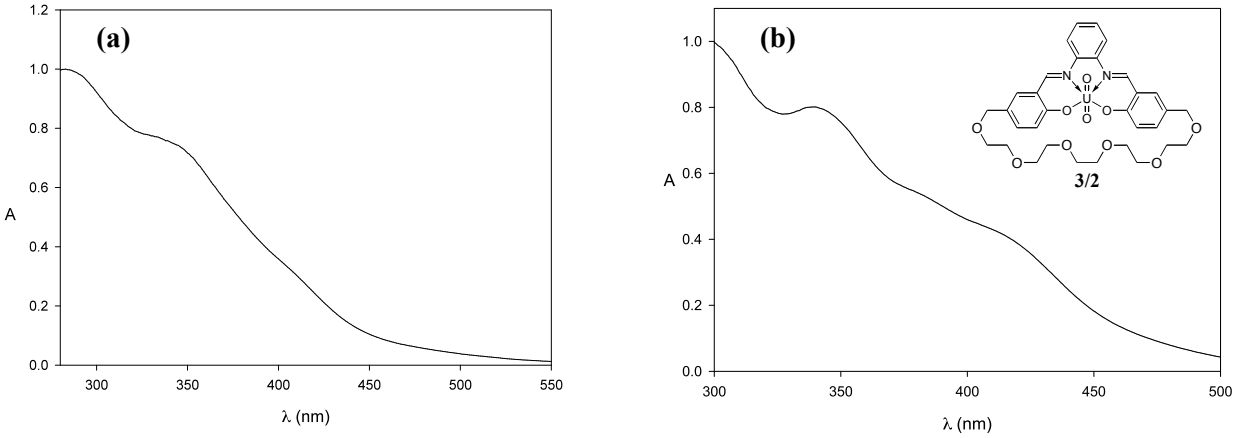

Figure 3.1 (*a*) Absorption spectrum of complex **3/1** ($4.7 \cdot 10^{-5}$ M) in water at 25 °C; (*b*) absorption spectrum of uranyl-salophen complex **3/2** ($5.0 \cdot 10^{-5}$ M) in $CHCl_3/CH_3CN$ 6:1 at 25 °C.

aggregation and dimerization phenomena, in some cases reported for this type of compounds,[6] can be ruled out within the range of concentrations explored during the titration experiments since the optical data points closely fit to the Lambert-Beer law at different wavelengths (Fig. 3.2). Moreover, from the inspection of figure 3.1a, it follows that 10^{-5} M concentration range for **3/1** is suitable to perform light absorption experiments since the requirement for the Lambert-Beer law is fulfilled (absorbance values below 1).

The UV-Vis spectrophotometric study of the binding properties of complex **3/1** towards inorganic anions was primarily carried out in unbuffered bidistilled water and a typical titration experiment is reported in figure 3.3. The addition of increasing amounts of sodium fluoride to a solution of **3/1** at 25 °C causes reproducible absorbance changes in the region 280-450 nm,

[xiii] Part of this chapter has been published in: A. Dalla Cort, G. Forte, L. Schiaffino, *J. Org. Chem.*, **2011**, *76*, 7569-7572.

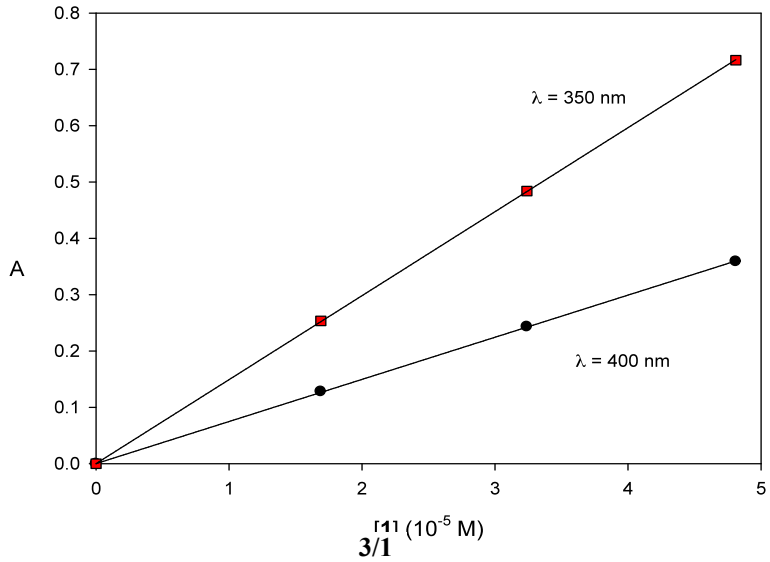

Figure 3.2 Absorption vs. concentration plots for compound **3/1** in water at 25 °C.

where the absorption of the added salt is negligible. Absorbance values at 330 nm fit to the binding isotherm described by equation 2,[7] where [*S*] is the total anion concentration in each point, *A* is the corresponding experimental absorbance, $[R]_0$ is the analytical concentration of the receptor and A_0 is the initial absorbance of the host.

Some general considerations can be drawn. First, the close adherence of the experimental data points to the binding isotherm described by the equation 2, together with the presence of

$$A = A_0 + \Delta A_\infty \frac{[R]_0 + K^{-1} + [S] - \sqrt{\left([R]_0 + K^{-1} + [S]\right)^2 - 4[S][R]_0}}{2[R]_0} \qquad \textbf{(2)}$$

sharp isosbestic points occurring during the course of the titrations, clearly suggests that the binding phenomenon is a 1:1 complexation. Second, the variations in the host absorption spectrum are rather small and the region around 330 nm seems to be the only one viable to carry on data analysis. In addition we tend to rule out any involvement of the sugar moieties in the binding process, at least with the small inorganic anions, as it can be confidently expected on the

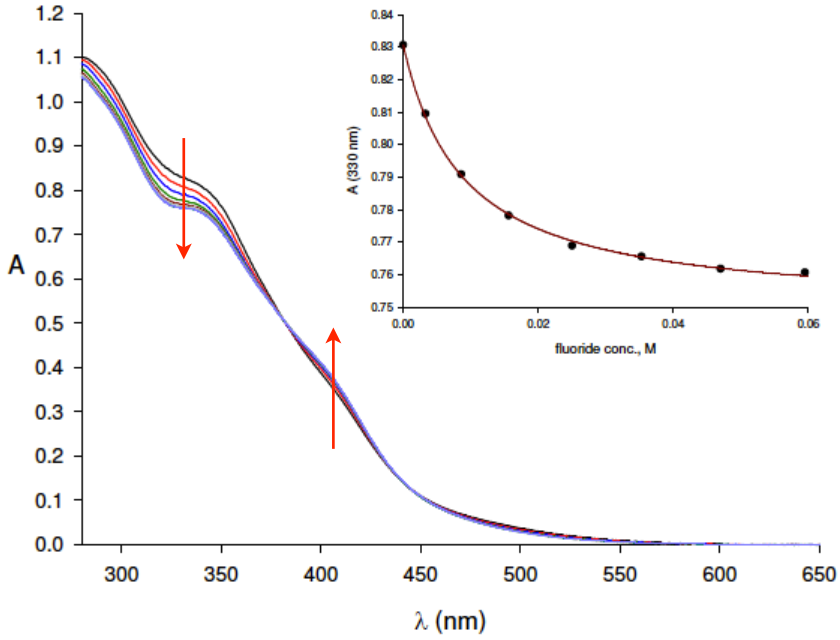

Figure 3.3 UV-Vis absorption spectra of complex **3/1** upon addition of increasing amounts of sodium fluoride, showing the two isosbestic points in the range 280-650 nm. The inset shows the titration plot at 330 nm of a $5.3 \cdot 10^{-5}$ M solution of **3/1** with fluoride at 25 °C in bidistilled water. The points are experimental, the curve is calculated using equation 2.

basis of the distance from the recognition site. An idea of the tridimensional location of the two glucose units with respect to the metal center in the complex **3/1** can be derived from the calculated structure[8] of the analogous zinc complex **3/3** and glycine in figure 3.4.[xiv]

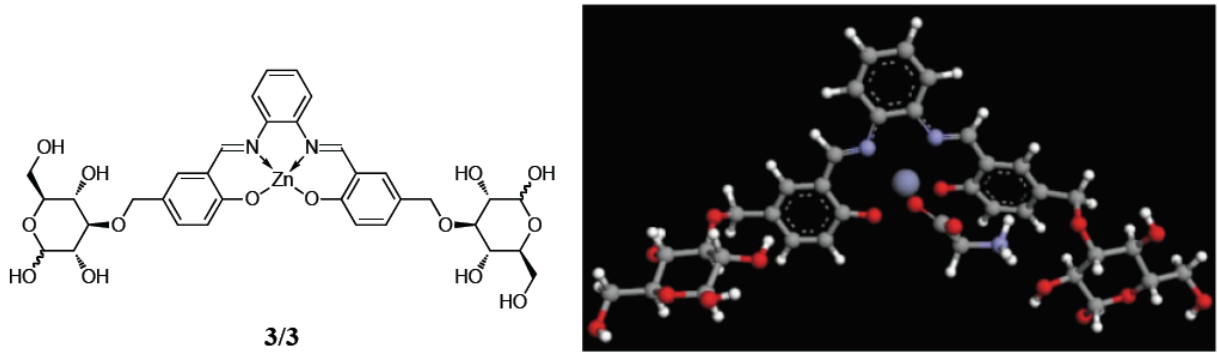

3/3

Figure 3.4 Structure of complex **3/3** (*right*) and ball and stick representation of the global minimum geometry of the **3/3**-glycine complex (*left*)

[xiv] It is essential to remind here that the structure of uranyl-salophen is bent rather than planar and that the coordination take place on the equatorial plane of the complex.

The association constant values obtained for **3/1** towards various inorganic anions in water (K_{ass}, M^{-1}) are reported in table 1. The first thing that catches the eye is the remarkable affinity between **3/1** and fluoride. This anion is very small, with the highest electronegativity value according to Pauling's scale, and it is effectively hydrated in water ($\Delta H° = -504$ KJ mol^{-1}). Despite the interest in the recognition of fluoride, few receptors have been hitherto reported to tightly bind to it in aqueous solutions. Indeed they generally work in organic solvent-water mixture and, as the water content increases, their affinity lowers to such an extend that the interaction, if survives, can be hardly detected.[9] Unfortunately, while it is possible to control the selectivity by tuning the binding site accessibility, it is much more difficult to raise the affinity of receptors. In particular cases, for example with spherical anions, additional binding motifs fail to give an effective benefit to the recognition process and the characteristics of the metal center become fundamental in tuning the affinity. Uranyl-salophen complexes show particularly high affinity values towards fluoride in organic solvents, even in competitive ones ($K_{ass} > 10^6$ M^{-1} in DMSO),[10] and this is due to the hard character of both the anion and the uranyl cation. We found that this interaction is maintained in aqueous environment and notably, although modest (K_{ass} = 115 M^{-1}), it is sufficiently strong to be detected in pure water with receptor **3/1**, decorated with glucose moieties.

Table 1 Association constants, K_{ass}, for the complexes formed between **3/1** and various anions in water at 25 °C.

Anion	K_{ass} (M^{-1})[a]
F^-	115 ± 6[b]
Cl^-	< 5
AcO^-	17 ± 4
SO_4^{2-}	< 5
CN^-	< 5[b]
NO_3^-	< 5
N_3^-	< 5
HPO_4^{2-}	480 ± 35[b]

[a]Errors are calculated as ±2σ. [b]Obtained in MOPS buffer at pH 7.5, see text.

Cyanide anion is a potentially interfering anion in the recognition of fluoride since the binding motifs that work for one usually are effective also for the other.[11] Actually, in organic solvents, uranyl-salophen complexes show a much lower affinity for cyanide than for fluoride (K_{ass} = 230 M^{-1} in DMSO),[10] as can be envisaged on the basis of the softer character of former. Therefore we expected the binding constant between **3/1** and cyanide in water to be barely detectable. Instead, titration experiments using aqueous solutions of NaCN led to puzzling results and the binding constant values obtained resulted to be in 10^4 M^{-1} range. Nevertheless the adherence of the experimental data points to the binding isotherm was poor at low cyanide concentration as if a simple 1:1 complexation model would not be a good assumption to describe the phenomenon. Cyanide is a basic anion (pK_a = 9.04) and it is involved in a protonation equilibrium in water, that increases hydroxide concentration. The affinity between **3/1** and hydroxide cannot be determined quantitatively using a 1:1 complexation model because titrations with NaOH show the presence of inflection points in the experimental data. However, even if such interaction is somewhat more complicated than a simple bimolecular association, it is strong enough to compete with other anions for the binding site on the receptor. It follows that the observed phenomenon can be in principle ascribed either to the exclusive OH^- binding or to a competitive process between OH^- and CN^-, which involves the simultaneous presence of multiple species in solution (Fig. 3.5). To shed light on such phenomenon, we investigated the

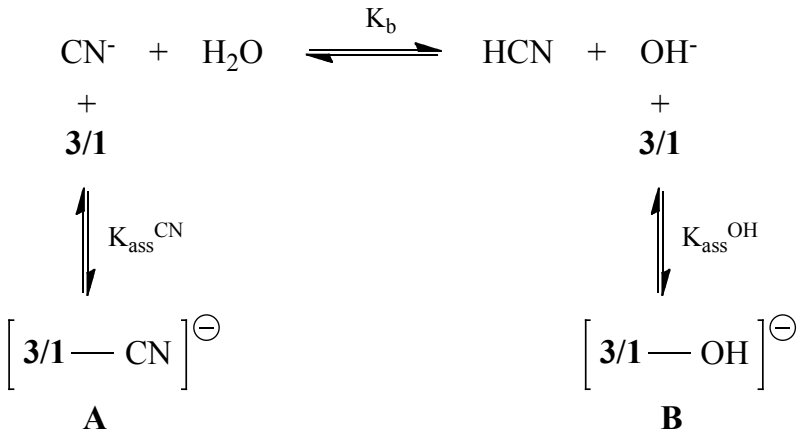

Figure 3.5 Species present in solution in the case of a competitive binding process between cyanide and hydroxide anions.

affinity in methanol between the cyanide ion and the receptor **3/5** (Fig 3.6), which is structurally related to **3/1** but showing higher solubility in organic solvents. Adding increasing amount of NaCN to the receptor **3/5** in anhydrous methanol, no absorption changes appeared in the

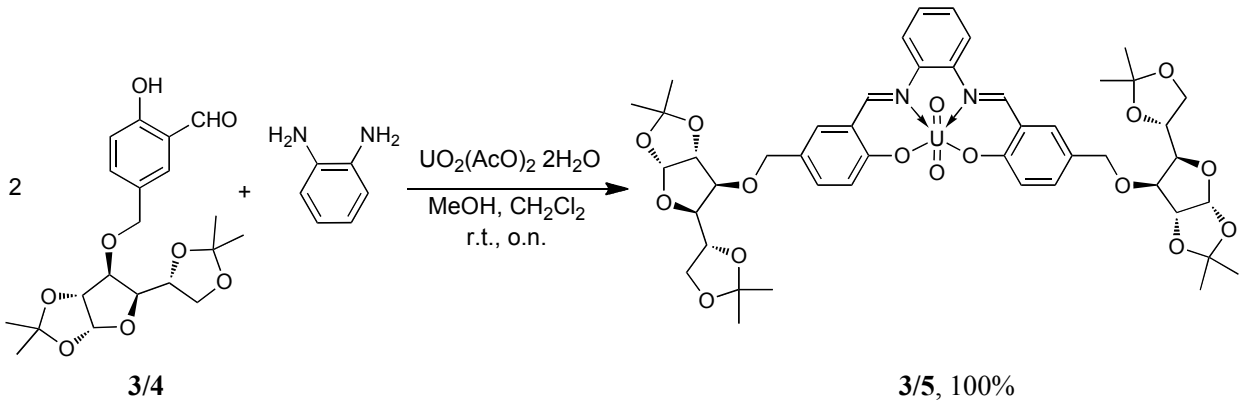

Figure 3.6 Synthesis of complex **3/5**.

spectrum, while performing the same experiment in wet methanol the association phenomenon was recovered and high binding constants could be calculated (Fig. 3.7). Likewise water, methanol is a protic solvent and it competes with anions for the binding site on the metal. Being its dielectric constant much lower than that of water, we argued that, if negligible affinity between uranyl moiety and cyanide can be detected in this solvent, a similar situation should likely occur in water as well. Therefore we are inclined to rule out any significant interaction between cyanide and **3/1** in water, ascribing the observed absorbance changes during the titration

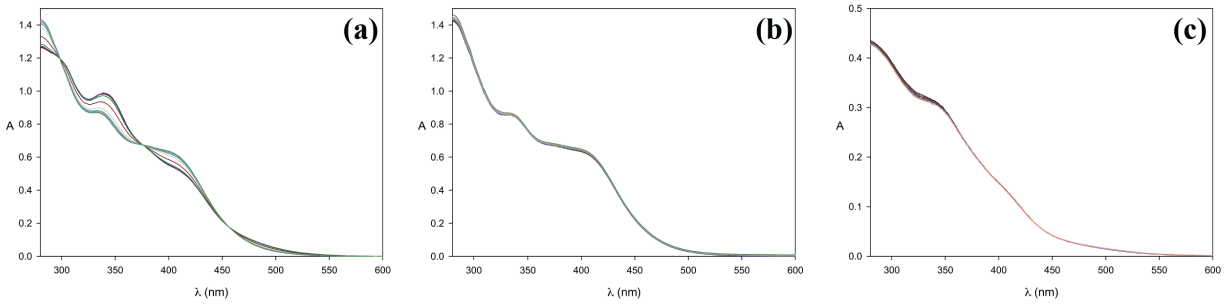

Figure 3.7 UV-Vis spectra of compound **3/5** with increasing amounts of NaCN in (*a*) wet and (*b*) anhydrous methanol. (*c*) UV-Vis spectra of compound **3/1** with increasing amounts of NaCN in 10 mM solution, pH 7.5.

solely to the presence of increasing amounts of OH^- ion in solution. The interference of hydroxide anion remains a common issue in the sensing of cyanide as water pollutant and controlled pH conditions are often required while performing the recognition. As mentioned in the first chapter, many colorimetric sensors for cyanide are based on the covalent recognition of the anion. The nucleophilic attack of CN^- on an electron deficient carbon atom generally causes a change in the conjugation in the receptor, giving rise to a change in color which can be naked-

eye detected. The pyrylium analogue **3/6**, which sense cyanide in aqueous solution at pH 9.5, is a recent example (Fig. 3.8). This pH value allows the CN^- not to be protonated at significant extend and, at the same time, avoids the sensor to undergo a hydroxide promoted bleaching process.[12]

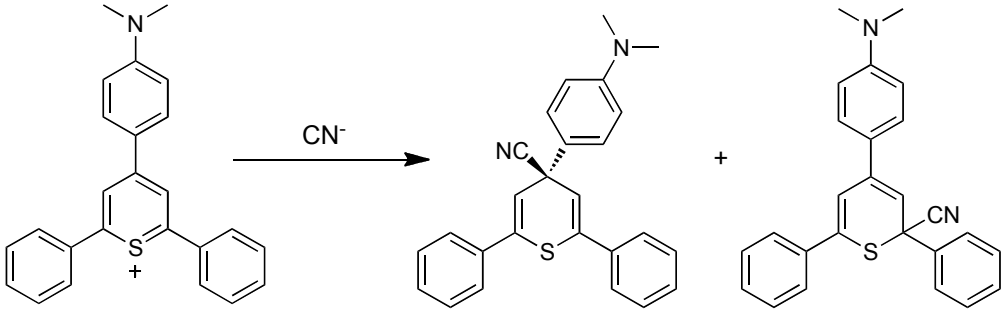

3/6, blue colorless

Figure 3.8 Proposed product formation in the recognition of cyanide ion performed by receptor **3/6**. The environment has to be basic to ensure the CN^- not to be fully protonated, but the pH must not raise over 9.5 to avoid the bleaching of the receptor.

Inspection of table 1 reveals that receptor **3/1** shows negligible affinity for all the oxoanions surveyed, with the only exception for hydrogen phosphate (HPO_4^{2-}, P_i) which, as a matter of fact, is the species displaying the strongest interaction with this receptor (K_{ass} = 480 M^{-1}). The apparent contradiction can actually be explained with an intra-complex hydrogen bond formation between the hydroxy group on the anion and one of the two "yl" oxygen atoms of the uranyl cation (Fig. 3.9). Indeed, the availability of these two oxygen atoms as hydrogen bond acceptors has been reported[13] and it is a frequently occurring binding motif described in uranyl protein complexes.[14] With the P_i, this second anchor point allows the formation of a six-membered cyclic adduct which, we suggest, accounts for the affinity increase (Fig. 3.9). In principle, a similar feature might occur also with fluoride, with a water molecule bridging the anion and the uranyl moiety. To date we cannot rule out such a binding arrangement. Experiments carried out in deuterium oxide did not provide any useful indication to shed light on this point.

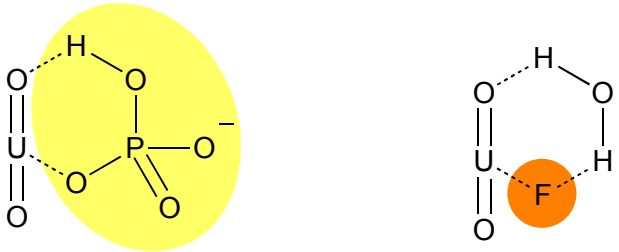

Figure 3.9 Proposed binding mode of HPO_4^{2-} to the uranyl cation showing the intra-complex hydrogen bond (*left*); hypothetic binding mode of fluoride with a water molecule acting as a bridge to the UO_2 unit (*right*).

Uranyl-salophen derivatives are actually known to effectively bind to the $H_2PO_4^-$ anion in organic solvents.[15] However any attempt to titrate **3/1** with $H_2PO_4^-$ in water led to the degradation of the receptor. Indeed, the acidity of the anion promotes the hydrolysis of the imine bonds of the salophen ligand and the absorbance band of the salicylaldehyde soon appears in the UV-vis spectrum (Fig. 3.10).

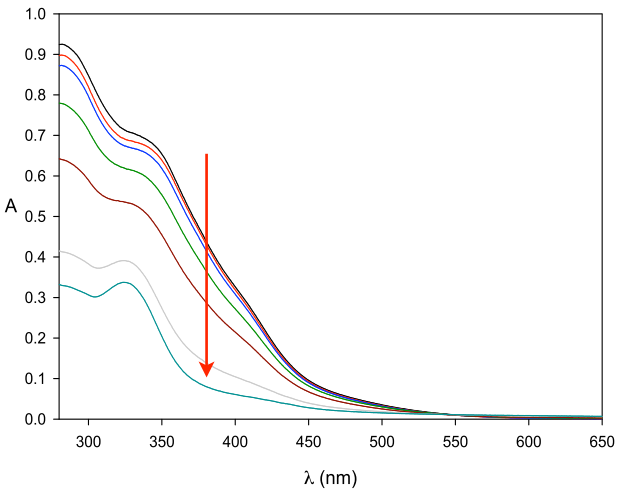

Figure 3.10 UV-Vis spectra of receptor **3/1** in the presence of increasing amounts of $H_2PO_4^-$.

Phosphates have a fundamental importance in biochemistry, and biomolecules bearing a phosphate moiety are ubiquitous in the living species. Many efforts have been made so far to create systems able to detect these species in biological samples, with diagnostic purposes. For example Anzenbacher and co-workers recently reported that tripodal receptors **3/7** and **3/8**, embedded in a

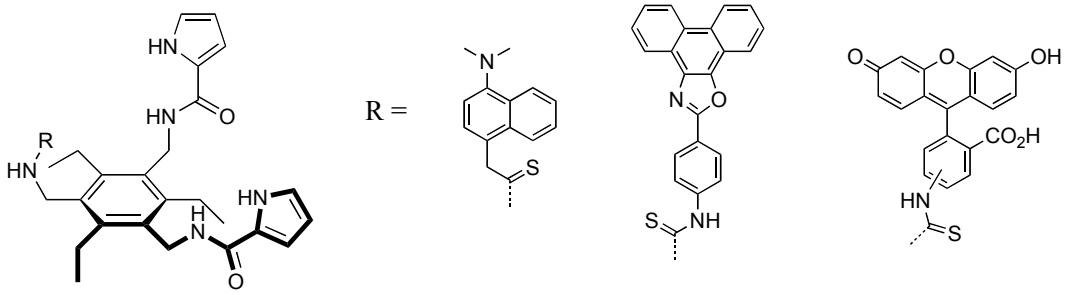

3/7

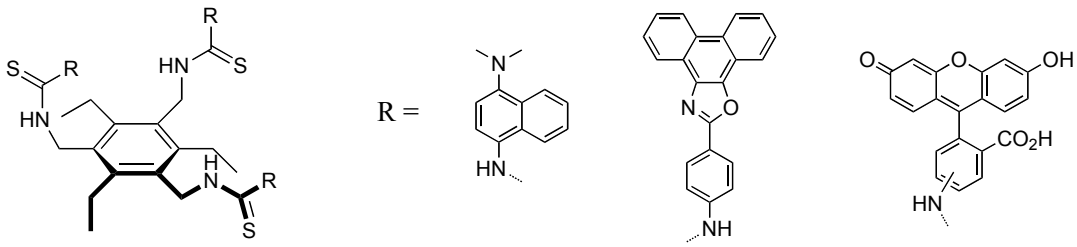

3/8

hydrophilic polyurethane matrix, are able to detect biological phosphates in blood serum, even though they are unable to bind to these species in water. Principal component analysis (PCA) demonstrates that films of **3/7** and **3/8** allow phosphate, pyrophosphate, AMP and ATP to be distinguished and, interestingly, the adenine moiety in AMP and ATP plays an important role in generating a unique response for these anions over inorganic phosphates in human serum analysis.[16]

Encouraged by the results obtained with HPO_4^{2-}, we decided to investigate the binding properties of **3/1** towards biologically relevant phosphates under physiological pH conditions. Given that the interaction between the receptor and sulfate is negligible (see table 1) and that no significant association occurs between uranyl-salophen derivatives and tertiary amines in organic solvents,[17] we chose the MOPS/NaOH system as a suitable non interfering buffer. Solutions of MOPS, 3-(N-morpholino)propanesulfonic acid (Fig. 3.11), up to 20 mM concentration are commonly used to buffer aqueous solutions around pH 7.5, reproducing the physiological pH values of blood serum and cytosol. To prove that MOPS does not sensibly associate to the receptor, the titration experiments with fluoride and hydrogen phosphate were repeated under buffered conditions, leading to binding constant values comparable to those obtained in pure water. We repeated the titration with cyanide as well and the low affinity detected represent a further confirmation that the interaction between the uranyl cation and the cyanide anion in water is sufficiently weak that cannot be determined under these conditions.

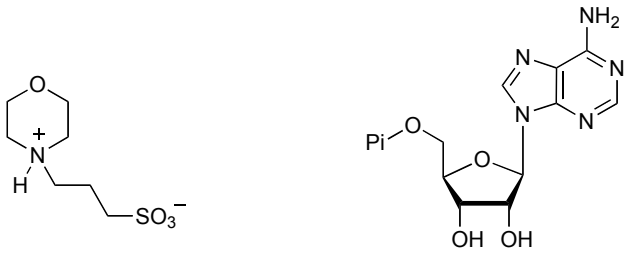

Figure 3.11 MOPS, acid form (*left*); general structure of adenosyl phosphates (*right*)

The association constants between receptor **3/1** and adenosyl phosphates in water at pH 7.5 (10 mM MOPS) are reported in table 2. The affinity for AMP^{2-} is about six times lower than that with HPO_4^{2-}. This is understandable since the intra-complex hydrogen bond that accounts for the affinity increase between the receptor and the hydrogen phosphate, as discussed above, cannot occur in the case of AMP which is in its dianionic form at pH 7.5. On the other hand, the value of the affinity constants towards ADP^{3-} and ATP^{4-} is sufficiently high that we can only provide a lower limit of 10^4 M^{-1}, due to the intrinsic limitation of the technique, as previously discussed (Fig. 3.12).[xv]

[xv] See above in the text.

Table 2 Association constants, K_{ass}, for the complexes formed between **3/1** and phosphate anions at pH 7.5 (MOPS, 10 mM). T = 25 °C.

Anion	K_{ass} (M^{-1})[a]
AMP^{2-}	83 ± 8
ADP^{3-}	> 10^4
ATP^{4-}	> 10^4
$P_2O_7^{4-}$	> 10^4

[a]Errors are calculated as ±2σ.

Even though also in this case no intra complex hydrogen bonding can form, the affinity is much higher with respect to the modest one displayed by AMP. Recently, the occurrence of a second anchor site in the complex between the zinc-salophen derivative **3/9** and adenosyl

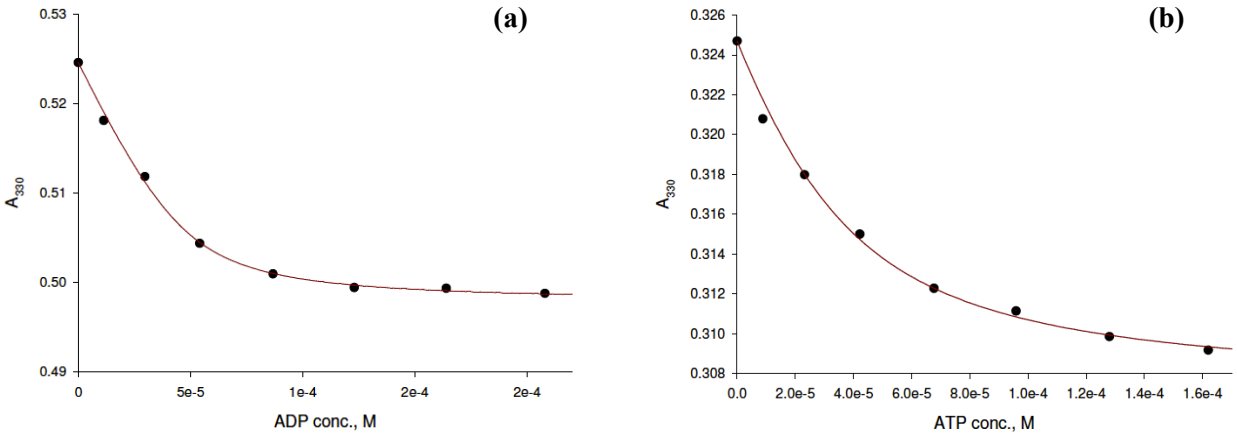

Figure 3.12 Titration plots at 330 nm of 10^{-5} M range solutions of **3/1** with (*a*) ADP^{3-} and (*b*) ATP^{4-} at 25 °C in 10 mM MOPS solution, pH 7.5. The points are experimental, the line is calculated using equation 2.

phosphates has been reported.[18] Phosphorus NMR shows that **3/9** binds to both organic and inorganic phosphates in ethanol, but only the interaction with the former lead to a quenching of the metal-complex fluorescence emission (Fig. 3.13). The observed selectivity towards adenosyl phosphates (ADP^{3-} > ATP^{4-} > AMP^{2-}) was correlated to the distance between the donor group

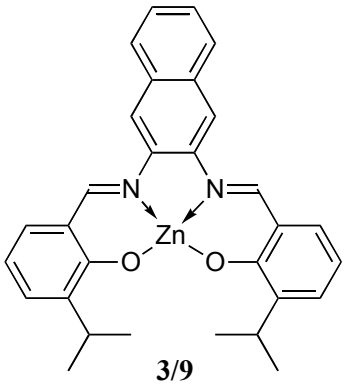

3/9

and the adenosine moiety that leads to the simultaneous occurrence of π–π stacking interactions between the adenine and the receptor. In the present case, the interaction between the adenine moiety and the aromatic skeleton of the salophen ligand can be ruled out because of the different coordination geometry of the uranyl cation with respect to the zinc. Moreover attempts to titrate

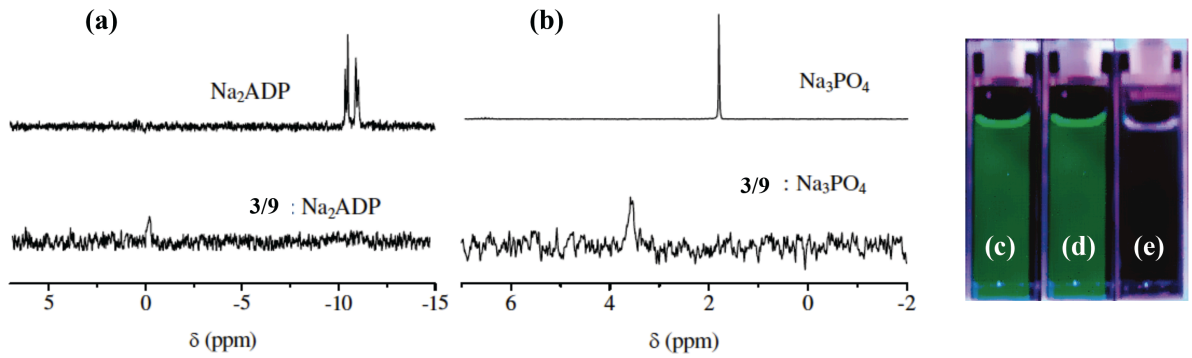

Figure 3.13 ^{31}P NMR spectra of ethanol-d_6 solution of (*a*) ADP^{3-} and (*b*) PO_4^{3-} in the absence (*above*) and with an equimolar amount of **3/9** (*below*). Emission of complex **3/9** under UV light (*c*), upon addition of (*d*) 1 equiv. of PO_4^{3-} and (*e*) 1 equiv. of ATP^{4-}.

receptor **3/1** with adenosine did not cause any spectral variation. We concluded, therefore, that the reason of the enhanced affinity of **3/1** for ADP and ATP over AMP must reside in the presence of the polyphosphate chain. This has been verified by titrating **3/1** with sodium pyrophosphate ($Na_4P_2O_7$, PP_i) and, as in the case of ADP and ATP, the value obtained for the binding constant can be only estimated to be higher than 10^4 M^{-1} (Fig. 3.14).

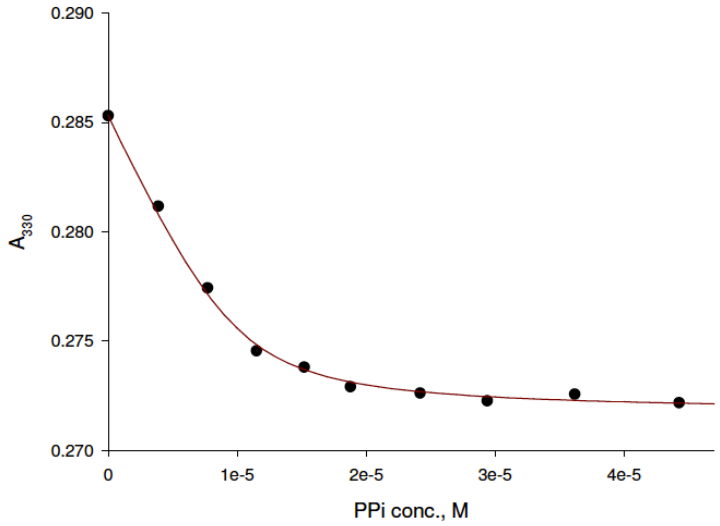

Figure 3.14 Titration plot at 330 nm of a $2.5 \cdot 10^{-5}$ M solution of **3/1** with PP_i at 25 °C in 10 mM MOPS solution, pH 7.5. The points are experimental, the line is calculated using equation 2.

3.3 Conclusion and future directions.

In this chapter the binding properties of the receptor **3/1** towards a series of inorganic anions in water have been described. Although not very high, the affinity towards fluoride is remarkable despite its high hydration energy and, to the best of our knowledge, it is one of the highest ever reported in pure water for a neutral receptor with no additional binding motifs.

The receptor displays a good selectivity toward ATP, ADP and PP*i* over AMP and P*i* under physiological pH conditions and the reason of such selectivity seems to be ascribable to the presence of the polyphosphate moiety. To date we do not know the binding mode of PP_i to the receptor and we are currently trying to grow crystals of the complex **3/1**·PP*i* in order to establish, at least in the solid state, the structural features that generate the affinity enhancement the polyphosphate group accounts for. It is noteworthy that good affinities towards polyphosphates, displayed by the mononuclear uranyl complex **3/1**, are generally reported for dinuclear metal complexes, such as bridged zinc derivatives.[19] By virtue of this characteristic, we believe that water soluble uranyl-salophen derivatives can constitute an interesting platform for a forthcoming design of biosensors.

3.4 Experimental section.

Complex 3/5.

Aldehyde **3/4** (0.197 g, 0.5 mmol), 1,2-diaminobenzene (0.028 g, 0.26 mmol) and $UO_2(OAc)_2$ $2H_2O$ (0.111 g, 0.26 mmol) were dissolved in a mixture of methanol (15 ml) and chloroform (5 ml) and the solution was stirred overnight at room temperature. The crude reaction was concentrated under vacuum and dichloromethane was added. The organic layer was extracted three times with water, then dried over anhydrous sodium sulfate and the solvent was removed under reduced pressure. Complex 3/3 was obtained as an orange solid with quantitative yield (0.291 g).

^{1}H NMR (300 MHz, methanol-d_4) δ (ppm) = 9.63(s, 2H), 7.82-7.61 (m, 8H), 7.19 (d, 2H, J = 8.70 Hz), 5.92 (d, 2H, J = 3.90 Hz), 4.79-4.64 (m, 8H), 4.42-4.38 (m, 2H), 4.20-3.95 (m, 8H), 1.50 (s, 3H), 1.41 (s, 3H), 1.39 (s, 3H), 1.35 (s, 3H); **^{13}C NMR** (300 MHz, $CDCl_3$) δ (ppm) = 170.9, 167.5, 148.2, 137.8, 136.5, 130.4, 128.5, 125.1, 122.1, 121.0, 112.9, 110.1, 106.7, 83.7, 82.5, 82.4, 74.1, 72.5, 67.9, 27.1, 27.0, 26.4, 25.6; **MS (ESI-TOF)**: m/z = 1151.37 $[M + Na]^+$; Elemental Analysis calculated for $C_{47}H_{58}N_2O_{17}U$ (**3/3** · MeOH): C = 48.62%; H = 5.04%; N = 2.41%, found: C = 48.63%; H = 5.60%; N = 2.47%.

Equilibrium measurements.

Titration experiments were carried out at 298 K by adding increasing amounts of the surveyed anion to a ~10^{-5} M solution of the uranyl-salophen complex. Sodium salt of all the anions were used. UV-vis spectra were recorded in the range 280-650 nm using a standard quartz cell (light path = 1 cm) on a double beam Perkin Elmer Lambda18 Spectrophotometer equipped with a Peltier temperature controller. Titration data were fitted to a standard binding isotherm for a 1:1 complexation and the association constants were calculated by non-linear least-square fitting of equation **2** to the data points.

MOPS buffer. 10 mM solutions were prepared by dissolving MOPS (acid form) in bidistilled water and by adjusting the pH to 7.5 with a 0.1 N sodium hydroxide solution.

Host and guests solutions. Solutions were prepared by dissolving the salts and the uranyl-salophen complex in bidistilled water or in a 10 mM MOPS solution at pH 7.5. The ATP and ADP were provided as ATP-H_2Na_2 and ADP-H_3 respectively, and the proper number of sodium hydroxide equivalents were added to their MOPS solutions to achieve the correct degree of protonation at pH 7.5.

3.5 References.

[1] K. A. Connors, *Binding Constants: The Measurement of Molecular Complex Stability*, Wiley-Interscience: New York, 1987.

[2] K. Hirose, *J. Incl. Phenom. Macrocycl. Chem.*, **2001**, *39*, 193-209.

[3] C. S. Wilcox, in *Frontiers in Supramolecular Organic Chemistry and Photochemistry*, ed. H.-J. Schneider and H. Dürr, VCH, Weinheim, 1991, pp. 123-144.

[4] G. Weber, in *Molecular Biophysics*, ed. B. Pullman and M. Weissbluth, Academic Press, New York, 1965, pp. 369-397.

[5] P. Thordarson, *Chem. Soc. Rev.*, **2011**, *40*, 1305-1323 and the references cited therein.

[6] K. Takao, Y. Ikeda, *Inorg. Chem.*, **2007**, *46*, 1550-1562.

[7] A. Dalla Cort, L. Mandolini, C. Pasquini, K. Rissanen, L. Russo, L. Schiaffino, *New J. Chem.*, **2007**, *31*, 1633-1638.

[8] A. Dalla Cort, P. De Bernardin, L. Schiaffino, *Chirality*, **2009**, *21*, 104-109.

[9] (a) S. Kubik, C. Reyheller, S. Stüwe, *J. Incl. Phenom. Macrocycl. Chem.*, **2005**, *52*, 137-187. (b) M. Cametti, K. Rissanen, *Chem. Commun.*, **2009**, 2809-2829. (c) S. Kubik, *Chem. Soc. Rev.*, **2010**, *39*, 3648-3663 and references cited therein. (d) Themed issue: *Chem. Soc. Rev.*, **2010**, *39*, 3581-4008. (e) P. Gale, *Chem. Commun.*, **2011**, *47*, 82-86.

[10] M. Cametti, A. Dalla Cort, L. Mandolini, M. Nissinen, K. Rissanen, *New J. Chem.*, **2008**, *32*, 1113-1116.

[11] T. W. Hudnall, F. P. Gabbaï, *J. Am. Chem. Soc.*, **2007**, *129*, 11978-11986.

[12] T. Abalos, S. Royo, R. Martínez-Máñez, F. Sancenón, J. Soto, A. M. Costero, S. Gil, M. Parra, *New J. Chem.*, **2009**, *33*, 1641-1645

[13] S. Fortier, T. W. Hayton, *Coord. Chem. Rev.*, **2010**, *254*, 197-214.

[14] J. D. Van. Horn, H. Huang, *Coord. Chem. Rev.*, **2006**, *250*, 765-775.

[15] D. M. Rudkevich, W. Verboom, Z. Brzozka, M. J. Palys, W. P. R. V. Stauthamer, G. J. Van Humme, S. M. Franken, S. Harkema, J. F. J. Engbersen, D. N. Reinhoudt, *J. Am. Chem. Soc.*, **1994**, *116*, 4341-4351.

[16] G. V. Zyryanov, M. A. Palacios, P. Anzenbacher, *Angew. Chem. Int. Ed.*, **2007**, *46*, 7849-7852.

[17] V. van Axel Castelli, A. Dalla Cort, L. Mandolini, D. N. Reinhoudt, L. Schiaffino, *Eur. J. Org. Chem.*, **2003**, 627-633.

[18] M. Cano, L. Rodríguez, J. C. Lima, F. Pina, A. Dalla Cort, C. Pasquini, L. Schiaffino, *Inorg. Chem.*, **2009**, *48*, 6229-6235.

[19] (a) L. Tang, Y. Li, H. Zhang, Z. Guo, J. Qian, *Tetrahedron Lett.*, **2009**, *50*, 6844-6847. (b) G. Ambrosi, M Formica, V. Fusi, L. Giorgi, A. Guerri, E. Macedi, M. Micheloni, P. Paoli, R. Pontellini, P. Rossi, *Inorg. Chem.*, **2009**, *48*, 5901-5912. (c) S. Khatua, S. H. Choi, J. Lee, K. Kim, Y. Do, D. G. Churchill, *Inorg. Chem.*, **2009**, *48*, 2993-2999.

CHAPTER 4

Single-molecule experiments: construction of rotaxanes to monitor the polymerase activity.

Stochastic sensing with nanopores allows the detection of analytes in solution at the single-molecule level. It basically relies on the perturbation of ion-current caused by the flow of particles through a physical constraint. In this technique, the use of proteins which form channels across a lipid membrane is particularly appealing as they provide identical pores for every experiment. Moreover they can be obtained in large quantities through gene expression in bacteria colonies and they can be engineered to virtually achieve whatever degree of affinity and selectivity towards the targeted substrates. Being the technique highly versatile, almost reagent-less and quite cheap, it is rapidly gaining much interest in polyanionic biological molecules sensing and in human genome sequencing. The research reported here lies within this framework and was performed during a six months stay in the group of Prof. Ghadiri at The Scripps Research Institute in La Jolla, San Diego, CA. The introduction to this chapter is mainly directed at giving an overview on the major characteristics of the stochastic sensing with nanopores, followed by examples of applications in detecting chemical species in aqueous solutions. Particular attention is directed to the nanopores formed by the toxin alpha-hemolysin across a lipid bilayer. The last part focuses on the nucleobase recognition in ssDNA with engineered versions of this protein and introduces to the preliminary experiments aimed at monitoring the polymerase activity on a circular ssDNA at the single-molecule level.

4.1 Stochastic sensing of molecules using nanopore devices.

Stochastic sensors likely represent the state-of-the-art among the modern sensory devices, especially because they allow for the recognition of chemical species at the single-molecule level. They belong to the general class of resistive pulse sensors,[1] such as the Coulter counter,[2,xvi] which measure the ionic current modulated as a result of particles flow through a constrained geometry.[3] With respect to the other methods of detection, electric measurements are fast, do not require high concentration of analytes and can be easily compatible with electronic and computational devices. In the simplest view of the apparatus, two chambers containing a saline

[xvi] The Coulter counter is a device used to count and size cells, microorganisms, and other small particles.

solution are separated by a membrane or a thin polymeric film (Fig. 4.1). Upon the application of a potential, a small aperture allows for the flow of a steady current, the magnitude of which also depends on the size of the pore. The random transit of particles through it, driven by the applied

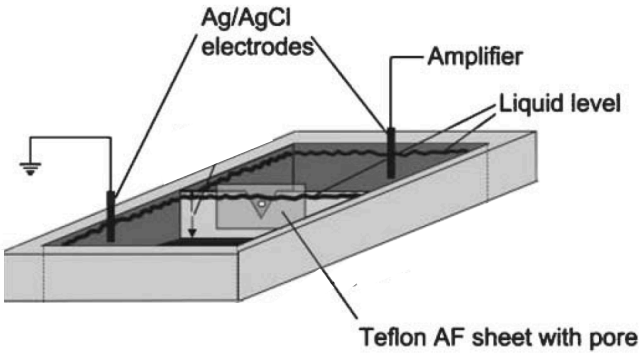

Figure 4.1 Schematic representation of the apparatus.

voltage (if they are charged) or by a concentration gradient, causes a partial clogging of the aperture and a transient reduction in current may be recorded. The optimal response of the device occurs when the pore size is comparable with that of the analytes to be surveyed. In these cases, each chemical species causes a characteristic current blockage (Fig. 4.2). There is, in principle, no limit for the minimum detectable particle size and the ultimate frontier in resistive pulse sensing concerns the miniaturization of the apertures to the nanometer scale. These, which may be naturally occurring or artificially fabricated, allow for the transit of a single molecule at a time and are called precisely stochastic sensors. The identification of chemical species in solution is based on the magnitude of the current blockages and on the mean dwell time of the particles inside the pore. As mentioned, these parameters act as fingerprints as they are unique for each type of analyte in solution. Furthermore the concentration of the surveyed analyte can be inferred by the frequency of the current blockages. Therefore, such devices are able, in principle, to discriminate different species in complex solutions without the selectivity generally required for the classic chemo and biosensors. Although each conductance modulation event is random, statistical

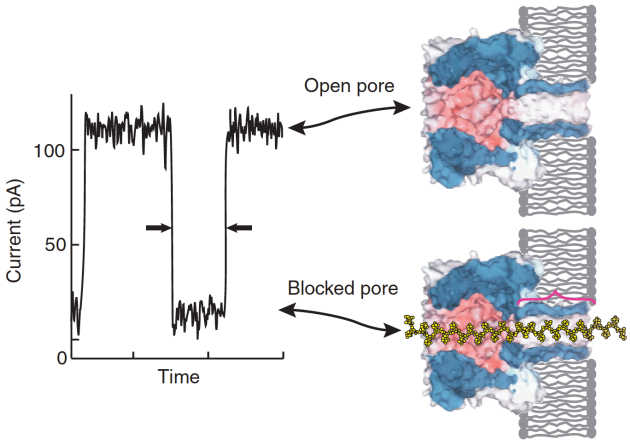

Figure 4.2 Transient current blockage occurring when a single stranded DNA string translocates through the transmembrane stem of an ion channel (α-hemolysin).

analysis of the magnitude, duration, and frequency of a series of events can yield a wealth of informations about the solution of interest, allowing the rapid simultaneous detection of multiple analytes by a single sensor. However, the detection of single species may sometimes require customized devices and the challenge is to tailor them with minor modifications in order to perform a wide range of analysis using the same sensory platform.

In the recents years, a growing interest towards nanopores and nanotubes as single-molecule sensors has developed. Even though this approach is not limited to biological systems (i.e. the nature of the pores can be either biological or artificial), the techniques used to measure the current flowing through the channels are strictly related to those used in patch clamp electrophysiology[4] and ion channel incorporation in lipid bilayer[5], employed in biology to measure the conductance of cell membranes.

As the potentialities and the applications of solid-state, synthetic, nanopores are in continuous growth, always new materials and techniques are used in this field. Some examples hitherto reported include the milling of silicon nitride (Si_3N_4) membranes, in which a bowl shaped cavity has previously been made. The etching can be performed either by a beam of accelerated argon ions (Fig. 4.3)[6] or by an electron beam in the case of silicon membranes,[7] stopping the process at the first sign of a pore formation, while accelerated heavy ions have been used to mill holes in films of polymeric materials.[8] It is also clear that the use of metal foils, instead of polymers, allows chemical modifications of the support surface nearby the pore, with the possibility to introduce specific binding sites for the surveyed analytes.[9]

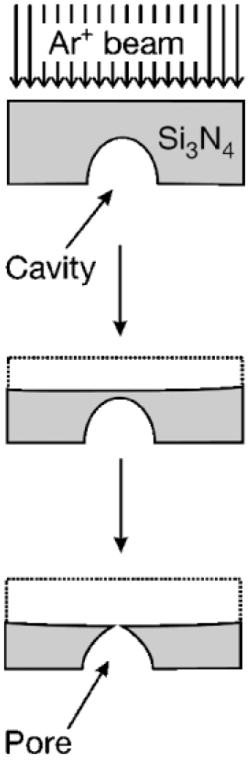

Figure 4.3 Schematic representation of a nanopore milling on a solid membrane of silicon nitride using a beam of accelerated Ar ions as etchant.

Sensing using proteins that form pores and ion channels across lipid membranes has its roots back in 1970, when Hladky and Haydon first observed a current flowing through a single ion-channel, formed by the peptide antibiotic gramicidin in a planar lipid bilayer.[10] The subsequent reports concerning the modulation of single ion-channel current, performed by molecules (channel blockers) that reversibly bind to the lumen of the pore, together with the huge growth in genetic engineering, constitute the basis of the stochastic sensing with biological channels.[11]

Protein pores have the advantage to allow for selective transport of matter. For example, the protein aquaporin is able to selectively transport water molecules across membranes, while excluding all the others.[12] For the size selective transport, the pore is required to be just slightly larger than the largest targeted particle, while charged amino acid residues projecting towards the channel lumen allow the opposite sign charged species to be selectively transported. The use of biological pores is especially appealing because their conductivity can be modulated by external stimuli and, in addition, they are available to be engineered to meet precise requirements, such as higher selectivity, affinity or conductivity. From this point of view, stochastic sensing with protein pores does not attempt to mimic the molecular devices found in nature, rather this approach is inspired by nature both in the use of protein pores and in the design of binding sites for analytes.

Channels, indeed, may be gated, meaning that their conductivity can be modulated by stimuli such as the voltage applied (voltage-gated) or the binding of ligands like ions and neurotransmitters (ligand-gated).[13]

The primary structure in a protein is determined by its genetic sequence and the folding process is driven by thermodynamics, resulting in identical structure for every copy of the protein. From engineering perspective, alterations in the genetic code lead to mutant proteins, where amino acid residues can be individually changed. The manipulated gene sequence can be subsequently cloned in a plasmid and expressed by bacterial colonies (e.g. *E. coli*). This approach allows to cheaply obtain large quantities of the desired protein.

To date, the exotoxin α-hemolysin is unquestionably the pore-forming protein most widely investigated and exploited in stochastic sensing experiments, largely due to the pioneering work of Bayley and co-workers on this subject. In figure 4.4 a schematic representation of the two states (bound and unbound) of α-hemolysin embedded in a lipid membrane is depicted. For a simple equilibrium, the analysis of the ion current trace can provide useful kinetic informations. Indeed $\tau_{off} = 1/k_{off}$, where τ_{off} is the mean dwell time of the analyte and k_{off} is the dissociation rate constant, and $\tau_{on} = 1/k_{on}[A]$, where τ_{on} is the mean time between binding events, k_{on} is the association rate constant and [A] is the analyte concentration.

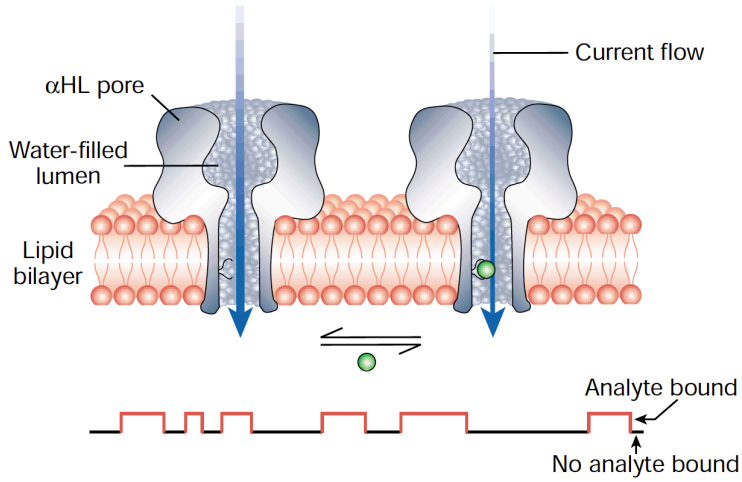

Figure 4.4 Schematic representation of the two states of the α-hemolysin (*above*). The ion current trace corresponding to the bound and unbound analyte, depicted as a green sphere (*below*). The frequency of the binding events and the characteristic residual current allow to identify the analyte and determine its concentration, even though the kinetic details of the binding process are unknown.

4.2 Lipid bilayers. Folding *method and issues.*

As mentioned, a biological pore is constituted by a protein which forms a channel across a lipid membrane. In stochastic sensing experiments, a lipid bilayer is formed over an aperture in a solid support (e.g. PTFE). The technique employed is referred to as *folding* method, as the bilayer is formed from two monolayers that fold over the hole, and was first described by Montal and Mueller in 1972.[14] The procedure here reported is a modification of the original one and applies for Teflon sheets used as membrane during the experiments in this work.[15] The procedure is schematically depicted in figure 4.5. A solution of hexadecane in hexanes (1:9) is dropped on the Teflon sheet in order to form a thick film over the hole, serving as a holder for the lipid monolayers to form the bilayer. After adding the saline buffer in both the two chambers of the cell, a pentane solution of the lipid is carefully placed on the surface of the solution, allowing a monolayer to form on the top of the aqueous phase after the solvent evaporation. Part of the solution is then removed with a syringe, allowing the monolayer to stand below the hole in the Teflon. Subsequent careful restoring of the initial volume of the solution, in both the two

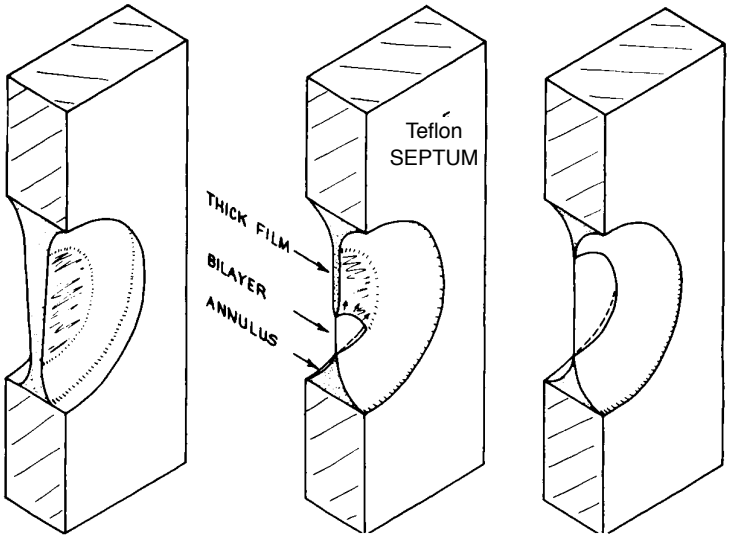

Figure 4.5 Lipid bilayer formation from monolayers. A thick film of hexadecane is formed over the hole in the Teflon septum (*left*). As the lipid monolayer reaches the aperture, it starts to fold over the hexadecane film (*middle*). When the monolayer on both sides is folded, a bilayer is set; the Plateau–Gibbs border is depicted as the annulus at the junction with the Teflon septum (*right*).

chambers of the cell, causes the monolayers to fold over the aperture, thus forming a bilayer. As mentioned, this is not directly in contact with the Teflon sheet, but it floats on a layer of hexadecane called *Plateau-Gibbs border*.[16] The presence of a non-polar solvent ensures the stability in the bilayer assembly process. The situation that would occur if attempting to form a bilayer without hydrophilic solvents is depicted in figure 4.6.

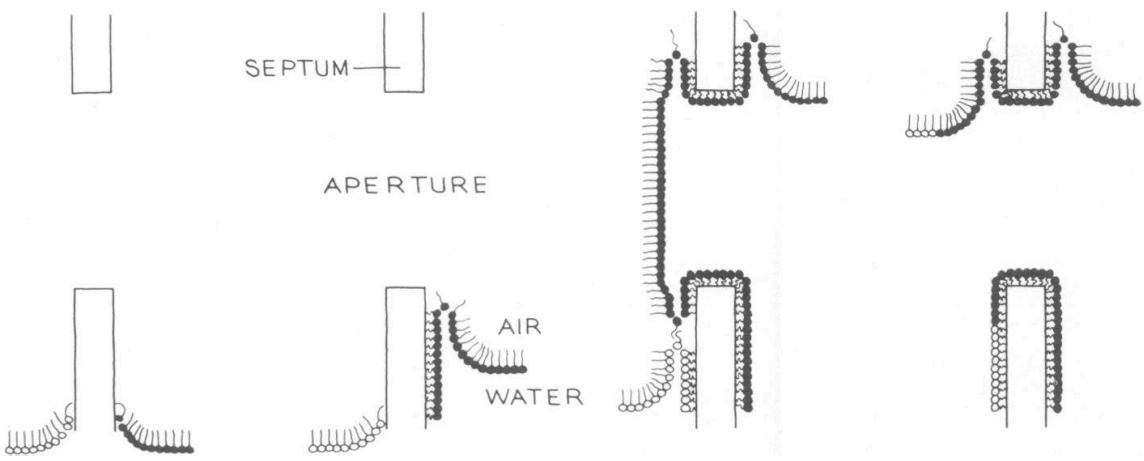

Figure 4.6 The sketches show what happens if attempting to form bilayers from monolayers in the absence of an alkane or other non-polar solvents. The raising of the left-hand water level "peels off" the monolayer on the right aqueous phase shown here protruding through the aperture (third and fourth frames).

The formation of a stable bilayer is crucial to have a steady current flowing through the nanopore for the duration of the experiment. Therefore, some parameters must be often checked, such as the correct amount of lipid to use, which depends on the quality of the lipid itself [xvii] and on the actual hole size in the Teflon sheet. Unfortunately free standing lipid membranes are very delicate and breakages or current leaking occur quite often, requiring vibration isolation tables and low acoustic environments.[xviii] Moreover, special solution handling is needed to avoid accidental mechanical breakages, and it must be kept in mind that the bilayer could be reformed only a limited number of times during a single experiment. Large, microscale apertures are one of the reasons for the frequent bilayer ruptures.[17] Nanoscale holes (10 nm to 1 μm) not only can help solving this issue, but it also allows only a single pore to insert the bilayer, thereby facilitating the manufacturability of stochastic devices. Some examples of promising platforms are milled apertures in silicon-based materials[18] and glass and fused-quartz nanopore membranes, GNM and QNM (Fig. 4.7) respectively.[19]

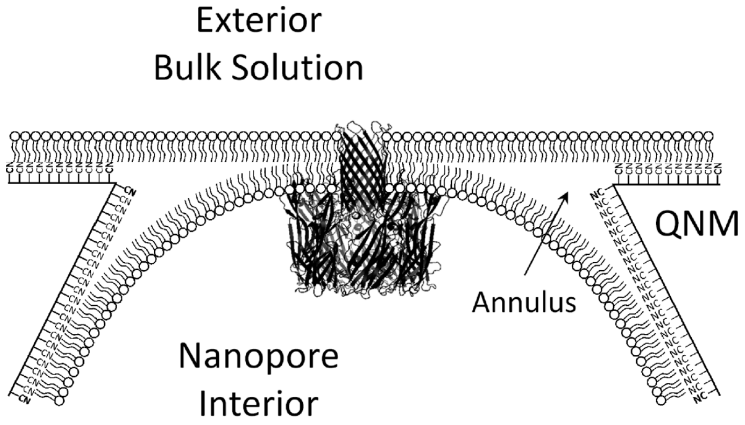

Figure 4.7 Cross-sectional schematic (not drawn to scale) of an α-HL pore embedded in a bilayer suspended across the orifice of a QNM.

It is worth also mentioning that stochastic sensors which exploit lipid bilayers incorporating single protein pores have been designed with an approach different from the one here reported.[20] Good results were obtained with bilayers standing on solid supports,[21] which require to be perfectly sealed to reduce leakage currents, and with bilayers supported on porous materials, such as gold coated polycarbonate membranes[22] and bacterial *S layers*.[23,xix]

[xvii] Many lipids are air or light sensitive and may partially degrade after a certain period of time.

[xviii] Also preventing any external noise to the current readout.

[xix] S layers are porous, two dimensional crystals of a single protein that envelope many bacteria.

4.3 Alpha-hemolysin as a suitable and versatile pore for stochastic sensing of molecules.

Wild-type *Staphylococcus Aureus* α-hemolysin (α-HL) is a homo-heptameric protein which forms transmembrane pores.[24] Its crystal structure shows a mushroom-shaped assembly in which the seven monomers are arranged around a central axis. In the assembled pore, the extra-membraneous domains form a hollow structure with a 2.6 nm aperture leading to a slightly wider vestibule. The transmembrane lumen is a β-barrel channel, with two antiparallel strands contributed by each subunit, approximately 10 nm long, with a diameter of 1.5 nm at the narrowest point (Fig. 4.8 and 4.9).[25] The α-HL pore is particularly stable and allows to operate at temperatures approaching the boiling point of water,[26] thus paving the way for experiments which involve thermophilic enzymes. Furthermore, in stochastic sensing, the pore can be endowed with proper recognition sites by site-directed mutagenesis or targeted chemical modifications.[27]

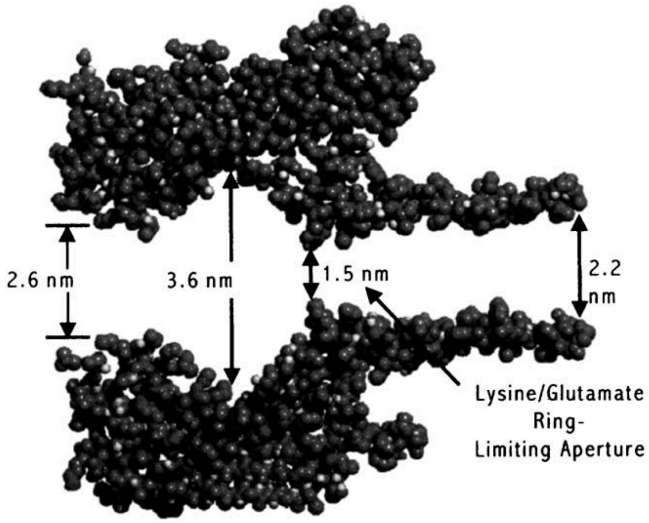

Figure 4.8 Cross-section of a space-filling model of α-hemolysin. The narrow channel on the right is the transmembrane hydrophobic β-barrel, while the large portion on the left is the "mushroom cap" of the protein protruding towards the aqueous solution.

Up to now, pores derived from the α-HL have been employed for different purposes, demonstrating how highly versatile this approach can be in a wide range of application in the stochastic sensing field.

The detection of divalent metal ions has been achieved with an engineered version of α-HL pores.[28] Good results were obtained replacing residues, with side chain projecting into the lumen, with four histidines to form a mutant subunit (4H). This was used to form a heteromeric pore, comprising six wild-type subunits and a mutant one (WT_64H_1), which contains a divalent metal ion binding site resembling that of carbonic anhydrase. Single-channel recording showed that WT_64H_1 reveals nanomolar concentrations of Zn(II) ion. Further studies demonstrated that mixture of M(II) ions can be analyzed under these conditions, since the anchor site is non specific and M(II) species can bind to it. But, being the binding mutually exclusive, only one M(II) cation is bound, giving a characteristic blockage signature (Fig. 4.10a).

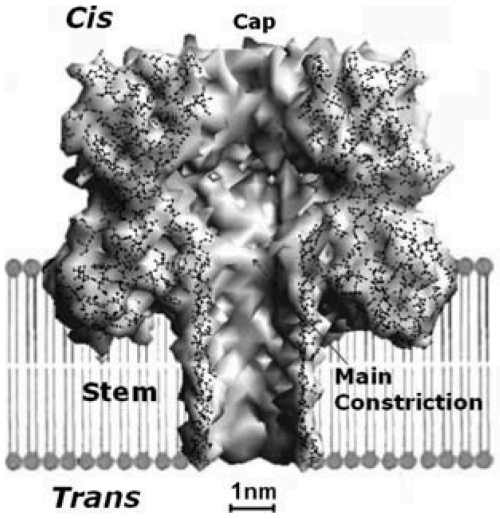

Figure 4.9 Pictorial representation of α-HL (cross section) forming a pore across a lipid bilayer. The conventional labels cis and trans are shown.

Small organic molecules can be detected using modified versions of α-HL.[29] For instance, the recognition of nitroaromatic compounds, such as TNT, has been achieved with a pore modified by site-directed mutagenesis.[30] Host-guest chemistry can be performed inside the pore by placing molecular adapters, such as cyclodextrins[31] and cyclic peptides[32] (Fig. 4.10b).

α-HL mutants also allow the stochastic sensing of biological macromolecules. However, bulky molecules, such as proteins, cannot fit inside the pore and a coupling between an external binding event and changes in current is required. This has been accomplished, for example, by covalently tethering a PEG strand inside the lumen of the protein.[33] The recognition arises from the changes in current related to the PEG motion when streptavidin or an antibody captures a biotin moiety attached to the end of the polymer (Fig. 4.10c).[34]

Since the inside diameter of the α-HL pore is barely as large as the diameter of a single nucleic acid strand, RNA and ssDNA can translocate through it. The analysis of the resulting transient partial current blockages provides informations about the length of the strands and their base composition.[35]

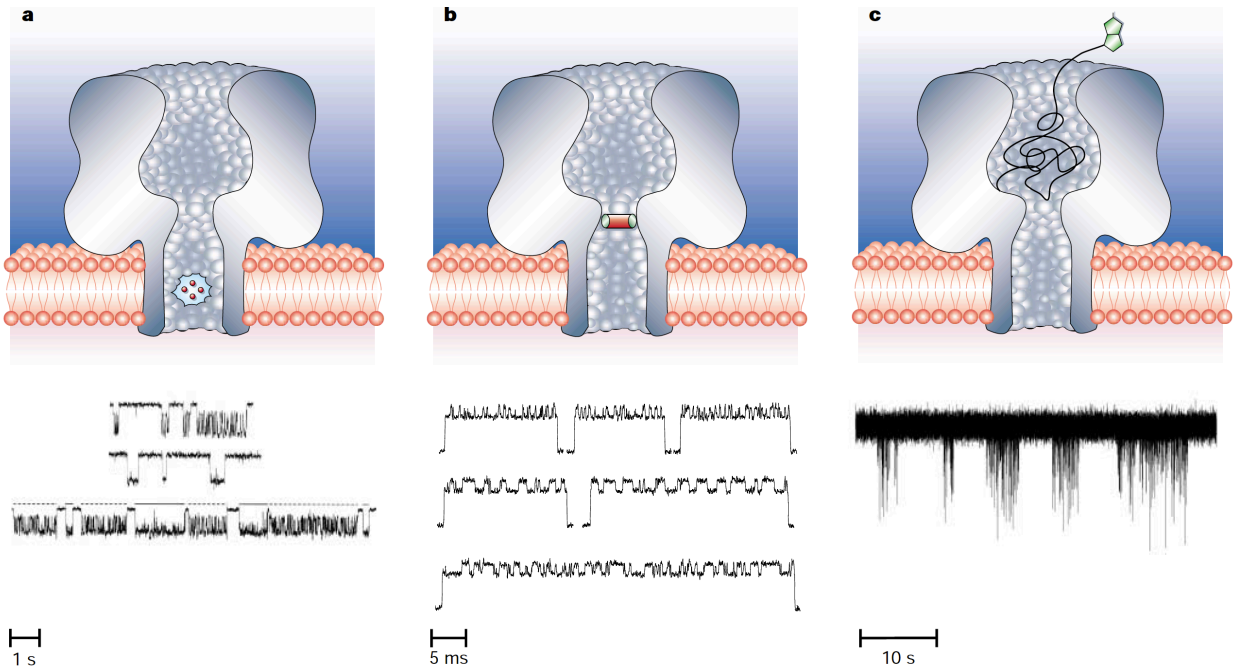

Figure 4.10 Detection of various analytes by stochastic sensing with α-HL. (*a*) $WT_6 4H_1$ mutant. The four histidines on one of the seven subunits project into the transmembrane stem and bind to divalent metal cations with different kinetics, giving different extents of channel block. Upper current trace, Zn^{2+}; middle trace, Co^{2+}; lower trace, mixture of Zn^{2+} (0.23 μM) and Co^{2+} (4.7 μM). (*b*) β-cyclodextrin is non-covalently lodged in the lumen of the pore. Upper current trace, promethazine; middle trace, imipramine; lower trace, mixture of promethazine and imipramine (both 100 μM). (*c*) A biotin-ended poly(ethylene glycol) chain is attached inside the pore. The current trace shows the motion of the polymer chain as a response to the binding of a mutant streptavidin (14.5 nM) of weakened affinity.

Bayley and his group investigated both the voltage dependency of the ssDNA translocation frequency through an α-HL channel and how to increase it with the use of site-directed mutagenesis.[36] The same authors recently highlighted some of the features of the interaction between the protein and nucleobases in ssDNA.[37] Moreover, single-molecule experiments with different α-HL versions allowed to study the processive replication of a ssDNA, using Phi29 polymerase,[38] and to detect sequence-specific duplex formation.[39]

Remarkably, single-channel current recordings show that α-HL mutants can discriminate single nucleotide or single base pair differences between otherwise identical DNA hairpin molecules[40] and recognize single nucleotides in an immobilized ssDNA[41] (Fig. 4.11).

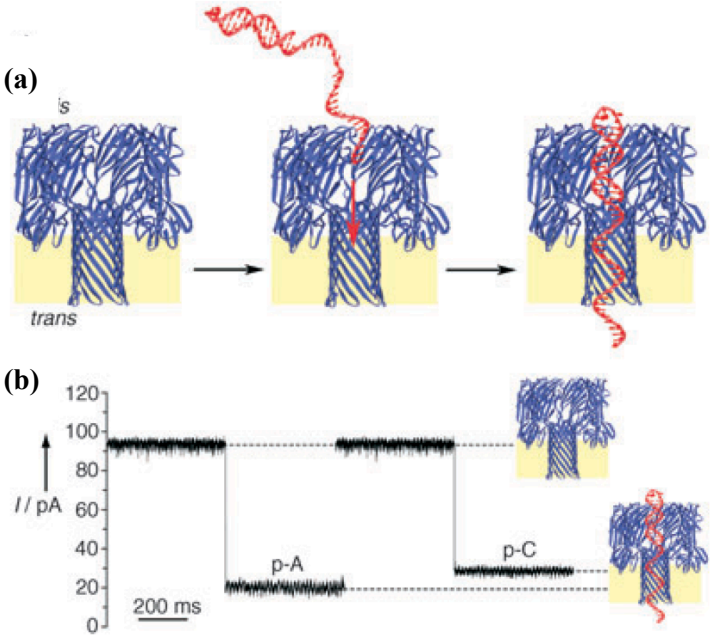

Figure 4.11 Immobilized ssDNA inside α-HL. (*a*) Schematic formation of single α-HL·DNA pseudorotaxane threading a ssDNA, capped with a hairpin, through the pore upon the application of a potential. (*b*) Perturbation in ion current caused by the capture of poly-d(A) (p-A) and poly-d(C) (p-C) single strands (170 mV, symmetrical salt conditions, 500 mM KCl).

Considering that stochastic sensing with nanopores does not require the analyte to be labeled, and that genetic engineering could virtually afford any type of pore mutants, Bayley pointed out that low cost genome sequencing may be likely achieved with the use of nanopore sensing at single molecule level (Fig. 4.12).[42]

Indeed, the potential of this approach is developing at an impressive rate towards single nucleobase detection and the continuous identification of nucleotide phosphate, by means of a cyclodextrin covalently linked in the lumen of α-HL, was recently reported.[43]

Human genome sequencing is an extremely coveted target. In 2004 the NIH set the challenge to reduce the total cost of sequencing within ten years: the $1000 genome. The task is quite discouraging as a diploid human genome contains 6000 million bases but,

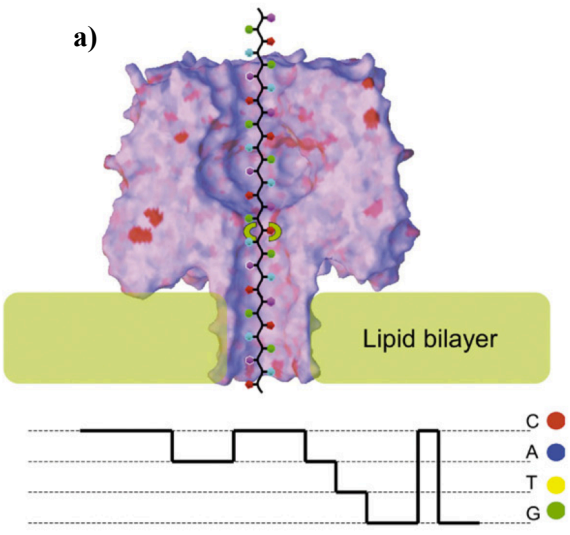

Figure 4.12 Representation of ideal real-time nanopore DNA sequencing.

at that price, many people could afford to have their genomes sequenced and personalized medicine would become a reality.[44] While the hitherto reported sequencing methods require the use of costly enzymes, fluorescently labeled molecules, state-of-the-art imaging equipment, and high-capacity data storage devices,[45] nanopore DNA sequencing would be "reagent-free" and employ a cheap electric readout.

At the moment, the real-time monitoring of a ssDNA thread, translocating through a single nanopore, is still far to be fully accomplished. Indeed there are small differences in current perturbation between purine and pyrimidine deoxyribonucleotides and, under the influence of an electric field, the DNA translocation through a nanopore is too fast to allow base identification by standard single channel recording.[46]

In 2004, the Ghadiri group reported the formation of a single rotaxane using α-HL as wheel and a properly designed DNA-PEG^{phos} thread as axle, where PEG^{phos} is a biotin-terminated polyethylene glycol phosphate strand and the DNA is conceived to form a terminal hairpin.[47] The rotaxane was formed by capping the biotinylated end with streptavidin, after threading the DNA-PEG^{phos} through the pore (Fig. 4.13). By virtue of its distinct backbone charge distribution and steric demand, the PEG^{phos} segment can give rise to characteristic ion current levels correlated with its relative position within the pore and can be used to probe the DNA strand motion. Using this feature, they were able to monitor the base-by-base activity of different DNA polymerases at the single-molecule level.[48] Recently, they also reported a real-time monitoring of single nucleotide incorporation by KF(exo$^-$) polymerase.[49] The axle of the rotaxane, blocked by a dsDNA segment, can be moved within the pore by the application of a potential (Fig. 4.14). Upon application of positive potential, the double strand section clogs the pore (Fig. 4.15a, state A), causing a decrease of ion

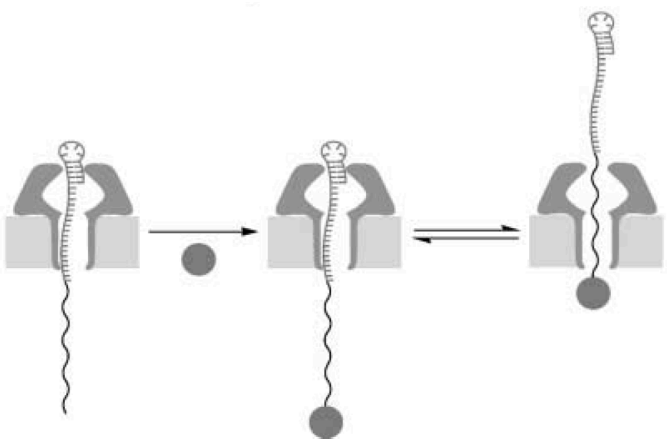

Figure 4.13 α-HL·DNA-PEG^{phos} rotaxane formation. Streptavidin is depicted as a gray solid circle.

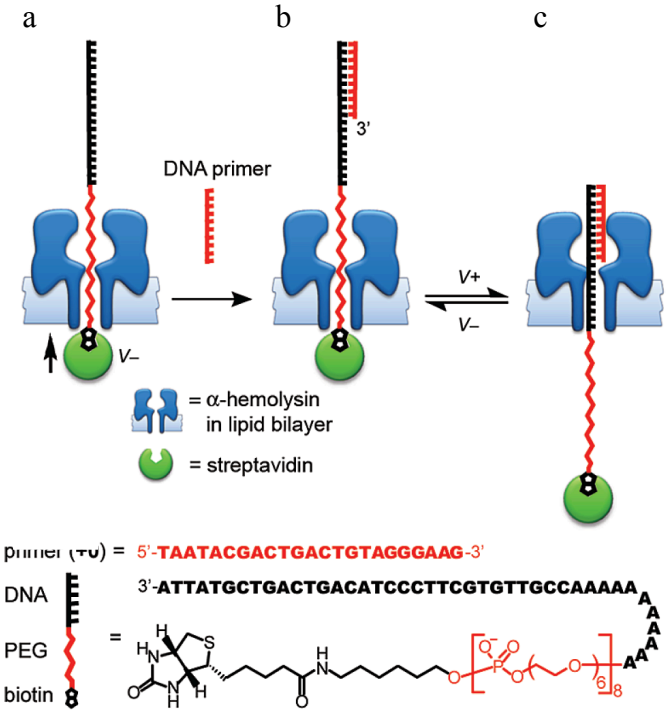

Figure 4.14 Formation of the rotaxane (*above*). The strand is electrophoretically driven into the pore in the *trans* side to form a pseudorotaxane (a), which can be stopped after hybridization with a primer. The thread moves as a consequence of the voltage applied (b and c). Primer and thread sequences (*below*).

current flow. By further increasing the potential, the double strand can enter the lumen of the pore until it reaches the entrance of the transmembrane channel (Fig. 4.15a, state B). The authors stressed that there are multiple and increasingly higher energetic structures in progressing from configuration A to B and a broad plateau zone in the current-voltage (*I-V*) curve is associated to this process (Fig. 4.15b). Since DNA polymerases recognize and bind to the 3' segment of a DNA primer-template duplex, which in state B is shielded within the protein, a transition to state C (Fig. 4.15a) is required to incorporate nucleotides (Fig. 4.16a). Working at positive potential, they succeed in slowing down the polymerase activity and in monitoring in real-time the polymerization process (Fig. 4.16b).

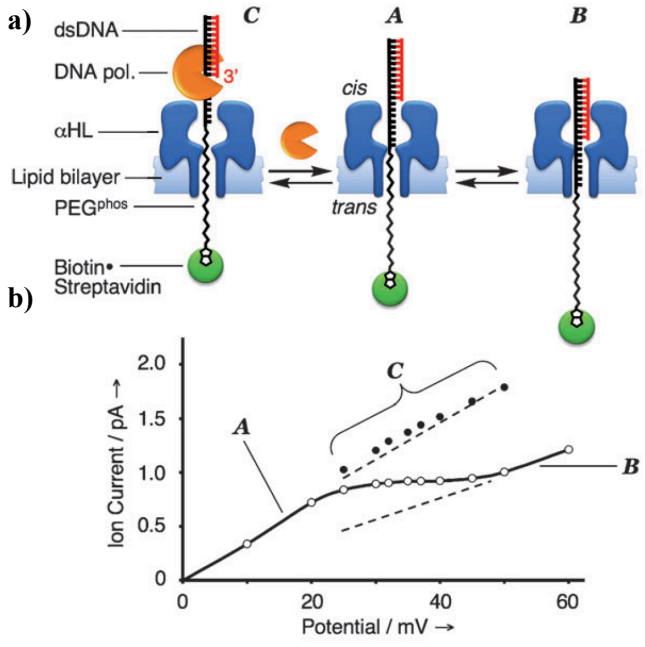

Figure 4.15 (*a*) The two limit configurations A and B adopted by the rotaxane. The configuration B is forced under high positive potential, otherwise the systems rests in the A state. The rotaxane adopts configuration C upon DNA polymerase binding. (*b*) The *I-V* curve of the rotaxane displays a deflection in the region corresponding to intermediate configurations between A and B. Lower potential results in the current associated to state A, while higher potential in that associated to state B. The solid circles represent ion-current levels of the rotaxane in the KF(exo⁻) bound configuration C under various applied potentials.

4.4 Results and discussion.

The work from Ghadiri highlights the possibility to harness the polymerase activity, under particular conditions, and to detect single base incorporation with single-channel current recordings.

A further step towards nanopore real-time DNA sequencing is the continuous readout of the same base sequence, i.e. recording the current signal for a certain DNA strand in a single experiment. This could be accomplished by monitoring the activity of a polymerase performing a rolling circle DNA amplification on a circular template.

Rolling circle DNA amplification (RCA)[50] consists in the synthesis of a single strand of DNA, containing n-copies of the sequence of a circular DNA template, performed by a polymerase, starting from a primer (Fig. 4.17).[xx] The beginning of a preliminary study on the monitoring of such reaction by single-channel recording is reported here. With this idea in mind, the design of a new rotaxane was carried on. A circular ssDNA, instead of the linear primer (see above in the text), has to be hybridized with the thread containing the PEG^{phos} segment. In this new configuration (Fig. 4.18), the circle is the template for a polymerization reaction starting at the 3' end of the thread, which act as a primer in this case. At the first stage, the RCA reaction, in the presence of polymerase and 4dNTPs in the cis chamber, would be signaled by the PEG

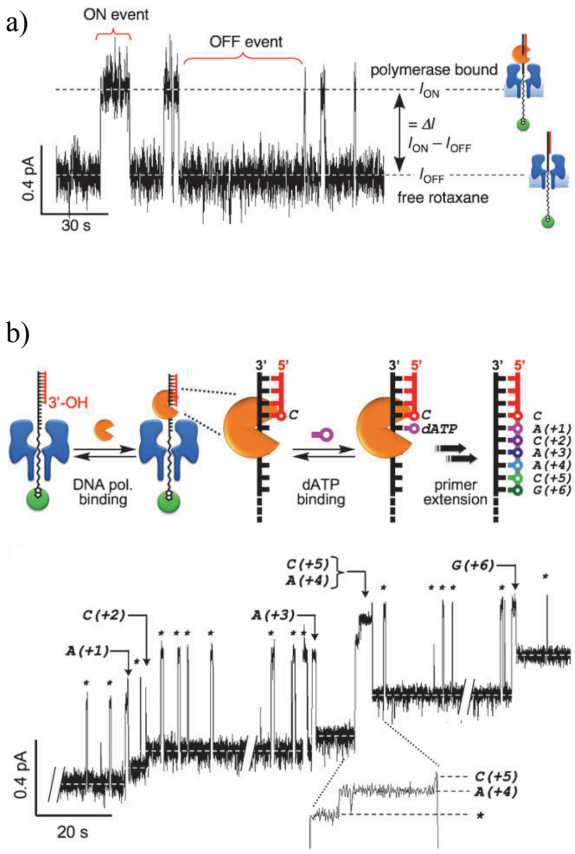

Figure 4.16 KF (exo$^-$) polymerase binding events to the rotaxane highlighted by the two states in the ion current trace recorded at +35 mV (*a*). Real-time monitoring of dNTP incorporation by the polymerase. Spikes in the current trace represent polymerase binding events, while the steps indicate single nucleotide incorporation. Two dNTPs (+4 and +5) are incorporated processively (*b*).

[xx] The length of the produced strand depends on the processivity of the polymerase used.

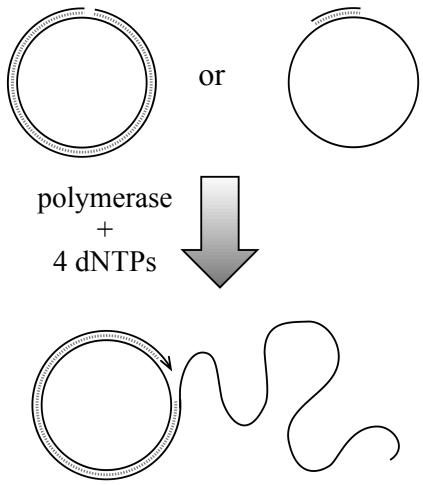

Figure 4.17 Schematic representation of the rolling circle amplification reaction.

moving and eventually translocating out of the pore. In order to assess the polymerase activity on such a system, three circular ssDNA, bearing a 28 bases sequence, complementary to the 3' end of the thread in figure 4.14 (thread 1), were designed. 58 and 75 bases-long circular ssDNA (c58 and c75 respectively) were prepared starting from the corresponding linear strands by enzymatic ligation. The phosphorilation at the 5' terminus with T4 polynucleotide kinase was carried on in the presence of ATP and the subsequent ligation with T4 DNA ligase in high dilution conditions to minimize the formation of linear oligomers. A small oligonucleotide (20 bases-long) was used to bridge the 3'- and the 5'-end together (Fig. 4.19). The final purification of the circles was performed with PAGE, PolyAcrylamide Gel Electrophoresis, under denaturing conditions (i.e. heating the samples in the presence of urea, before loading the gel).

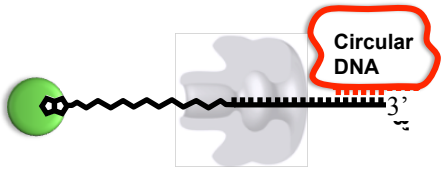

Figure 4.18 Configuration of the rotaxane for RCA reaction monitoring.

Several attempts to prepare a 169 bases-long circular ssDNA (c169) failed to give a pure product. In this case two strands, 84 and 85 bases long, were used, and the phosphorilation/templation/ligation was performed twice, with purification of the intermediate 169 bases-long linear strand (l-169). Invariably, after final purification of the circle, PAGE checking showed two bands close to each other, one of the two having a gel shift comparable to that of the l-169 (Fig. 4.20). Unfortunately, any attempts to get rid of the impurity by further PAGE purification or by reaction with different types of exonuclease failed to afford the pure circle.

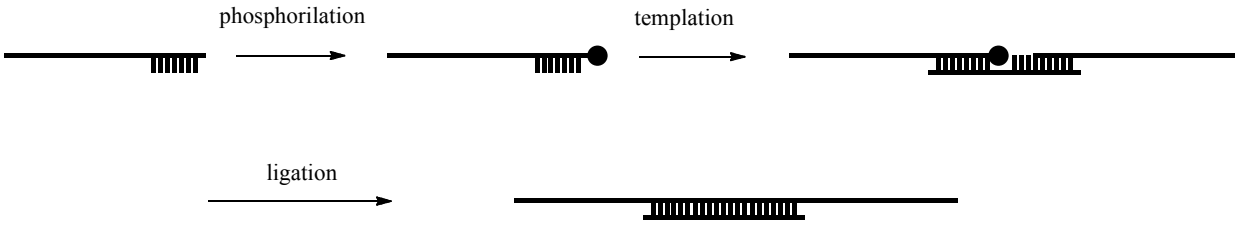

Figure 4.19 Schematic representation of the sequence of transformations required to obtain a circular ssDNA, starting from a linear strand. The bridge is eventually removed after PAGE purification under denaturing conditions.

4.5 Conclusions.

This part of the thesis basically deals with a different aspect of detecting anionic species in water, with respect to what discussed in the previous chapters. Two circular single stranded DNA have been synthesized using tandem enzymatic reactions. Attempts to purify a third, quite large circle unfortunately failed to afford a product sufficiently pure to be used in single-molecule experiments.

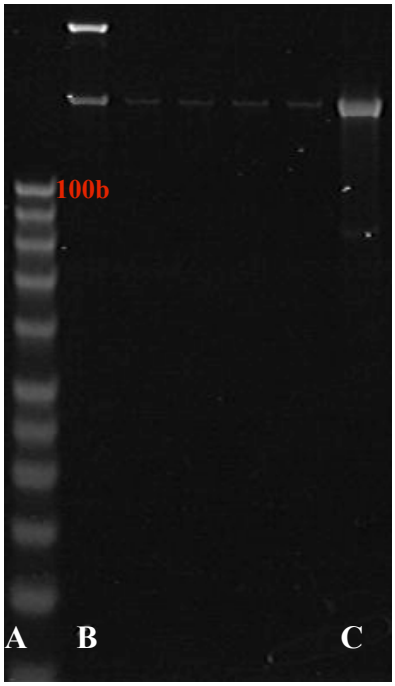

Figure 4.20 c169 PAGE. (*A*) DNA MW marker; (*B*) c169 after purification; (*C*) l-169.

The circles c58 and c75 were used for subsequent nanopore rotaxane formation. As confirmed by the *I-V* curve shape, rotaxanes can be formed through a single α-HL pore, using thread 1 and the circles c58 and c75. Several attempts to perform the RCA reaction were made by adding a solution of 4 dNTPs and *Bst* (*Bacillus stearothermophilus*) polymerase, large fragment, at the *cis* side of the rotaxane. Although slight changes in the ion-current trace were detected in few cases, the results of these experiments are not reported here because they are not sufficient to provide any irrefutable evidence of the polymerase activity on the circle.

4.6 Experimental section.

DNA purification. Polyacrylamide gel was prepared from TBE buffer solution of acrylamide containing 6M urea. Tetramethylethylenediamine (TEMED) and ammonium persulfate (APS) were added, as polymerization initiators, before pouring the solution between two glass plates. DNA samples were heat-denatured at 90 °C for 10 min in the loading buffer (containing 9M urea) and then loaded into the wells on the gel. DNA was extracted from the gel by electro-elution and finally precipitated from ethanol at 4 °C, in the presence of sodium acetate. ***Electro-elution of DNA***. The gel was thoroughly crushed and placed in a plastic tube endowed with a porous membrane. The DNA was electrophoretically eluted in TE buffer, which the membrane

was in contact with (Fig. 4.21). The solution containing DNA was concentrated under reduced pressure. ***Ethanol precipitation protocol***. 1/10 volume of 3M sodium acetate was added to the concentrated solution of DNA, followed by 3 x volume of absolute ethanol. The tube was left overnight at 4 °C, then centrifuged at low temperature for 30 min and the supernatant was discarded. Buffer was added to prepare stock solutions of DNA.

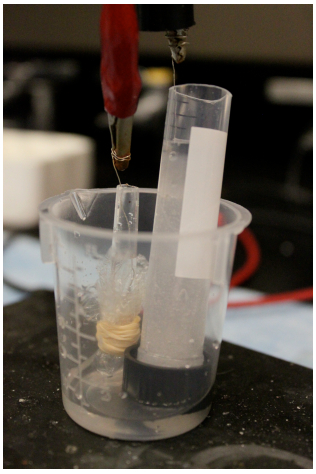

Figure 4.21 Apparatus for the electrophoretic elution of DNA. Positive pole is on the left (red) and negative one (black) is in contact the crushed gel (*right*).

General route to DNA ligation. DNA strands were custom made by e-Oligos (Hawthorne, NY) and purified by polyacrylamide gel electrophoresis, under denaturing conditions, prior to use. Enzymatic reactions were performed according to New England Biolabs Inc. protocols reported on the web. Purified ssDNA was treated with T4 polynucleotide kinase in T4 DNA ligase buffer and incubate at 37 °C for 2h. The reaction was diluted to ~2 μM, T4 DNA ligase and template were subsequently added, followed by the incubation at 16 °C for 4 days. Circular ssDNA was purified by electrophoresis on polyacrylamide gel under denaturing conditions and the final purity was checked on analytical gel (SYBR GOLD staining). Circular ssDNA stock solutions were prepared with tris buffer and the final concentration was obtained from the absorbance value at 260 nm. Note that this procedure was repeated two times for the 169 bases-long cDNA, starting from 84 and 85 bases-long linear ssDNA.

Instrumentation for single-channel current recording. Single-channel experiments with the α-HL were carried out in the delrin made cell shown in figure 4.22. Two hollow vessels are obtained inside the body of the cell and they are separated by a 25 μm thick Teflon sheet with a prefabricated aperture, whose diameter is around 100 μm. To prevent any mechanical and electrical interference, the measuring apparatus (electrodes are shown in figure 4.23) is sealed in a Faraday cage while the experiment is running, and stands on a vibration reduction platform. Electrodes are connected to an amperometer, which is controlled by a computer, and the output signal is converted into sound by the amplifier and the events that cause a change in current are easily revealed by a pitch change in the constant noise.

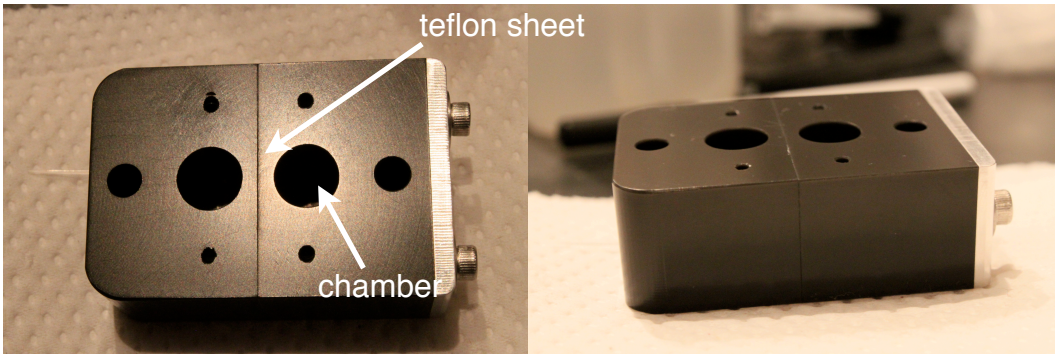

Figure 4.22 Top (*left*) and side view (*right*) of the cell used in the nanopore experiments. The black body of the cell is made in polyoxymethylene, POM (delrin).

Buffer solutions. Two buffer solutions, differing in KCl concentration, were used during the nanopore experiments both in symmetric and asymmetric salt conditions. 150 mM KCl, 25 mM tris·HCl, 4.5 mM solution at pH 7.5 and 500 mM KCl, 25 mM tris·HCl, 4.5 mM solution at pH 7.5 were prepared by dissolving the tris free base and the other salts in milli-Q water and adjusting the pH value with a HCl solution.

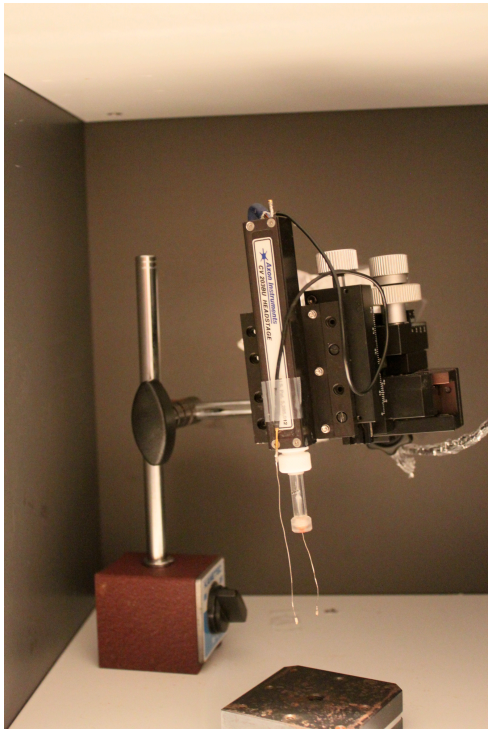

Figure 4.23 Electrodes used for single channel measurements.

Single-channel insertion in the bilayer. The lipid bilayer was set up as previously reported. The Teflon membrane in the cell was soaked with ~5 µl of a 1:9 solution of hexadecane in hexanes. Buffer was added in both the two vessels of the cell and a solution of 1,2-diphytanoyl-*sn*-glycero-3-phosphocholine in *n*-pentane (10 mg/ml) was gently dropped on the surface of the aqueous solution. After the solvent was evaporated, bilayers were formed with the folding technique previously described (see above in the text). A solution of α-HL_WT was added in the *cis* chamber and a positive potential of 50 mV was applied. The insertion of a protein is revealed by a current which starts flowing through the pore. A characteristic value of current is associated to a single channel of a given protein, under certain salt conditions and potential applied.

General procedure to form rotaxanes. Conventionally, the working electrode is the *trans* chamber of the cell, while the reference is in the *cis* one. A solution of streptavidin-capped

biotin-terminated linear ssDNA (thread) is added at the *trans* side of the pore and a negative potential is applied. After an efficient capture, potential is brought to -50 mV and the desired circular ssDNA is added in the *cis* chamber. After ~30 min, potential was slowly returned to 0 mV and the formation of a rotaxane was assessed by the the shape of the recorded *I-V* curve.

4.7 References.

[1] H. Bayley, C. R. Martin, *Chem. Rev.*, **2000**, *100*, 2575-2594.

[2] W. H. Coulter, *US Patent*, #2,656,508, 1953.

[3] J. Schmidt, *J. Mater. Chem.*, **2005**, *15*, 831-840.

[4] *Single-channel recording*, ed. B. Sakmann and E. Neher, Plenum Press, New York, 1995.

[5] *Ion channel reconstitution*, ed. C. Miller, Plenum Press, New York, 1986.

[6] (a) J. Li, D. Stein, C. McMullan, D. Branton, M. J. Aziz, J. A. Golovchenko, *Nature*, **2001**, *412*, 166-169. (b) J. Li, M. Gershow, D. Stein, E. Brandin, J. Golovchenko, *Nat. Mater.*, **2003**, *2*, 611-615.

[7] A. J. Storm, J. H. Chen, X. S. Ling, H. W. Zandbergen, C. Dekker, *Nat. Mater.*, **2003**, *2*, 537-540.

[8] A. Mara, Z. Siwy, C. Trautmann, J. Wan and F. Kamme, *Nano Lett.*, **2004**, *4*, 3, 497-501.

[9] J. C. Hulteen, K. B. Jirage, C. R. Martin, *J. Am. Chem. Soc.*, **1998**, *120*, 6603-6605.

[10] S. B. Hladky, D. A. Haydon, *Nature*, **1970**, *225*, 451-453.

[11] H. Bayley, O. Braha, L.-Q. Gu, *Adv. Mater.*, **2000**, *12*, 139-142.

[12] A. Burykin, A. Warshel, *Biophys. J.*, **2003**, *85*, 3696-3706.

[13] B. Trivedi, R. H. Kramer, *Neuron*, **1998**, *21*, 895-906.

[14] M. Montal, P. Mueller, *Proc. Natl. Acad. Sci. USA*, **1972**, *69*, 3561-3566.

[15] M.C. Peterman, J. M. Ziebarth, O. Braha, H. Bayley, H. A. Fishman, D. M. Bloom, *Biomedical Microdevices*, **2002**, *4*, 231-236.

[16] S. H. White, D. C. Petersen, S. Simon, M. Yafuso, *Biophys. J.*, **1976**, *16*, 481-489.

[17] R. Hirn, T. M. Bayerl, J. O. Rädler, E. Sackmann, *Faraday Disc.*, **1998**, *111*, 17-30.

[18] C. Schmidt, M. Mayer, H. Voegel, *Angew. Chem. Int. Ed.*, **2000**, *39*, 3137-3140.

[19] A. E. P. Schibel, E. C. Heider, J. M. Harris, H. S. White, *J. Am. Chem. Soc.*, **2011**, *113*, 7810-7815.

[20] L. X. Tiefenauer, A. Studer, *Biointerphases*, **2008**, *3*, 74-79.

[21] (a) E. Sackmann, *Science*, **1996**, *271*, 43-48. (b) E. Sackmann, M. Tanaka, *Trends Biotechnol.*, **2000**, *18*, 58-64. (c) D. J. McGillivray, G. Valincius, F. Heinrich, J. W. F. Robertson, D. J. Vanderah, W. Febo-Ayala, I. Ignatjev, M. Lösche, J. J. Kasianowicz, *Biophys. J.*, **2009**, 96, 1547-1553.

[22] (a) K. B. Jirage, J. C. Hulteen, C. R. Martin, *Science*, **1997**, *278*, 655-658. (b) G. Favero, L. Campanella, S. Cavallo, A. D'Annibale, M. Perella, E. Mattei, T. Ferri, *J. Am. Chem. Soc.*, **2005**, *127*, 8103-8111.

[23] (a) B. Schuster, D. Pum, O. Braha, H. Bayley, U. B. Sleytr, *Biochim. Biophys. Acta*, **1998**, *1370*, 280-288. (b) B. Schuster, D. Pum, M. Sára, O. Braha, H. Bayley, U. B. Sleytr, *Langmuir*, **2001**, *17*, 499-503. (c) H. M. Keizer, M. Andersson, C. Chase, W. P. Laratta, J. B. Proemsey, J. Tabb, J. R. Long, R. S. Duran, *Colloid. Surface B*, **2008**, *65*, 178-185.

[24] E. Gouaux, *J. Struct. Biol.*, **1998**, *121*, 110-122.

[25] L. Song, M. R. Hobaugh, C. Shustak, S. Cheley, H. Bayley, J. E. Gouaux, *Science*, **1996**, *274*, 1859-1865.

[26] X. Kang, L.-Q. Gu, S. Cheley, H. Bayley, *Angew. Chem. Int. Ed.*, **2005**, *44*, 1495-1499.

[27] H. Bayley, P. S. Cremer, *Nature*, **2001**, *413*, 226-230.

[28] (a) O. Braha, B. Walker, S. Cheley, J. J. Kasianowicz, L. Song, J. E. Gouaux, H. Bayley, *Chem. Biol.*, **1997**, *4*, 497-505. (b) O. Braha, L.-Q. Gu, L. Zhou, X. Lu, S. Cheley, H. Bayley, *Nat. Biotechnol.*, **2000**, *18*, 1005-1007.

[29] C. R. Martin, Z. S. Siwy, *Science*, **2007**, *317*, 331-332.

[30] X. Guan, L.-Q. Gu, S. Cheley, O. Braha, H. Bayley, *ChemBioChem*, **2005**, *6*, 1875-1881.

[31] (a) L.-Q. Gu, O. Braha, S. Conlan, S. Cheley, H. Bayley, *Nature*, **1999**, *398*, 686-690. (b) L.-Q. Gu, S. Cheley, H. Bayley, *Science*, **2001**, *291*, 636-640. (c) Y. Astier, O. Braha, H. Bayley, *J. Am. Chem. Soc.*, **2006**, *128*, 1705-1710.

[32] J. Sanchez-Quesada, M. R. Ghadiri, H. Bayley, O. Braha, *J. Am. Chem. Soc.*, **2000**, *122*, 11757-11766.

[33] S. Howorka, L. Movileanu, X. Lu, M. Magnon, S. Cheley, O. Braha, H. Bayley, *J. Am. Chem Soc.*, **2000**, *122*, 2411-2416.

[34] L. Movileanu, S. Howorka, O. Braha, H. Bayley, *Nat. Biotechnol.*, **2000**, *18*, 1091-1095.

[35] (a) J. J. Kasianowicz, E. Brandin, D. Branton, D. W. Deamer, *Proc. Natl. Acad. Sci. USA*, **1996**, *93*, 13770-13773. (b) A. Meller, L. Nivon, E. Brandin, J. Golovchenko, D. Branton, *Proc. Natl. Acad. Sci. USA*, **2000**, *97*,1079-1084. (c) S. E. Henrickson, M. Misakian, B. Robertson, J. J. Kasianowicz, *Phys. Rev. Lett.*, **2000**, *85*, 3057-3060.

[36] G. Maglia, M. R. Restrepo, E. Mikhailova, H. Bayley, *Proc. Natl. Acad. Sci. USA*, **2008**, *105*, 19720-19725.

[37] D. Stoddart, A. J. Heron, E. Mikhailova, G. Maglia, H. Bayley, *Proc. Natl. Acad. Sci. USA*, **2009**, *106*, 7702-7707.

[38] K. R. Lieberman, G. M. Cherf, M. J. Doody, F. Olasagasti, Y. Kolodji, M. Akeson, *J. Am. Chem. Soc.*, **2010**, *132*, 17961-17972.

[39] (a) S. Howorka, S. Cheley, H. Bayley, *Nat. Biotechnol*, **2001**, *19*, 636-639. (b) S. Howorka, L. Movileanu, O. Braha, H. Bayley, *Proc. Natl. Acad. Sci. USA*, **2001**, *98*, 12996-13001.

[40] W. Vercoutere, S. Winters-Hilt, D. Deamer, D. Haussler, M. Akeson, *Nat. Biotechnol.*, **2001**, *19*, 248-252.

[41] N. Ashkenasy, J. Sánchez-Quesada, H. Bayley, M. R. Ghadiri, *Angew. Chem. Int. Ed.*, **2005**, *44*, 1401-1404.

[42] H. Bayley, *Curr. Opin. Chem. Biol.*, **2006**, *10*, 628-637.

[43] J. Clarke, H.-C. Wu, L. Jayasinghe, A. Patel, S. Reid, H. Bayley, *Nat. Nanotechnol.*, **2009**, *4*, 265-270.

[44] (a) J. A. Schloss, *Nat. Biotechnol.*, **2008**, *26*, 1113-1115. (b) A. Kahvejian, J. Quackenbush, J. F. Thompson, *Nat. Biotechnol.*, **2008**, *26*, 1125-1133.

[45] (a) E. R. Mardis, *Annu. Rev. Genomics Hum. Genet.*, **2008**, *9*, 387-402. (b) J. Shendure, H. Ji, *Nat. Biotechnol.*, **2008**, *26*, 1135-1145.

[46] Brenton *et al.*, *Nat. Biotechnol.*, **2008**, *26*, 1146-1152.

[47] J. Sánchez-Quesada, A. Saghatelian, S. Cheley, H. Bayley, M. R. Ghadiri, *Angew. Chem. Int. Ed.*, **2004**, *43*, 3063-3067.

[48] S. L. Cockroft, J. Chu, M. Amorin, M. R. Ghadiri, *J. Am. Chem. Soc.*, **2008**, *130*, 818-820.

[49] J. Chu, M. González-López, S. L. Cockroft, M. Amorin, M. R. Ghadiri, *Angew. Chem. Int. Ed.*, **2010**, *49*, 10106-10109.

[50] D. Liu, S. L. Daubendiek. M. A. Zillman, K. Ryan, E. T. Kool, *J. Am. Chem. Soc.*, **1996**, *118*, 1587-1594.